Department of Engineering Cybernetics

Model Based Optimisation of Pacing Strategy in Time Trial Cycling

Author:
Sigurd Synnesønn Digre

June, 2023

Preface

A thesis submitted to the Department of Engineering Cybernetics at the Norwegian University of Science and Technology in Trondheim in partial fulfillment of the requirements for the degree of Master of Science in Cybernetics and Robotics.

Acknowledgements

The author would like to give thanks to the supervisors of this project, Anders Lyngvi Fougner, Johannes Tjønnås and Kristian Gaustad Hanssen.

Executive Summary

The objective of this project is to find optimal pacing strategies for time trial cycling. A pacing strategy, in this context, is based on power output levels measured on an ergometer. The thesis aims to model the energy expenditure of the human body, and set constraints on the system related to these dynamics. Physical tests on the bicycle involves one subject with limited experience cycling. Test protocols are conducted in order to determine parameters describing physical performance of the individual. Using an optimisation framework in MATLAB, a pacing strategy is developed for a certain time trial track. The tests and time trial attempts are all conducted through the use of the training software Zwift, which simulates a cycling environment. The project conducts two iterations of estimating the parameters, and verifying a pacing strategy.

The thesis produced a pacing strategy which proved to have a better time performance than a comparative strategy, set at the same power output throughout the entire time trial. However, results also indicated that the experimental routines of determining physiological parameters could have been more carefully designed and scrutinized. The method of formulating the final pacing strategy also proved an ineffectiveness within the implemented optimal program.

List of Figures

1 Input/Output System . . . 3
2 Forces on Bicycle . . . 5
4 Factors in Human Performance . . . 11
5 Relative Contribution if Energy Sources . . . 14
6 Intensity Domains and Power-Duration Curve . . . 14
7 Track Discretization . . . 23
9 Mono-exponential recovery; Contour-plot . . . 38
10 Mono-exponential recovery; 3D-plot . . . 38
11 Terms of Aerobic and Anaerobic Activation . . . 39
12 3D-plot with hyperbolic tangent expressions . . . 41
13 Contour-plot with hyperbolic tangent expressions . . . 41
14 Steady state velocity . . . 45
19 Bologna TT (Zwift) . . . 56
20 Bologna TT (Simplified) . . . 56
21 Bologna TT (Simplified, lower level) . . . 57
22 Simple track optimised . . . 57
23 Optimal power trajectory 1 . . . 59
24 Optimal power trajectory 2 . . . 59
25 Optimal power trajectory 3 . . . 60
26 Arrangement of Experimental Equipment . . . 63
27 First All-out test . . . 65
28 Bologna TT Test - Velocity and Power . . . 67
29 Bologna TT Test - Cadence and Heart Rate . . . 67
30 Bologna TT Test - Remaining Anaerobic Work Capacity (Values from all-out test) 68
31 Bologna TT Test - Remaining Anaerobic Work Capacity Values from Golden Cheetah 69
32 Second All-out test . . . 71
33 Optimal power trajectory 4 . . . 72
34 Simulated responses of Optimal power trajectory 4 . . . 73
35 Pacing Strategy Compared to Actual Power Output 1 . . . 74
36 Simulated Remaining Anaerobic Capacity Guided Attempt 1 . . . 75
37 Simulated Remaining Anaerobic Capacity Constant Attempt 1 . . . 75
38 RPE and Heart Rate Iteration 1 . . . 76
39 Third All-out test . . . 77

40 Optimal power trajectory 5 . . . 79
41 Initial Sprint Simulated . . . 80
42 Optimal Solution to First Ascent . . . 81
43 Recovery During Descent Simulated . . . 82
44 Optimal Power Trajectory of Short Sprint Problem . . . 83
45 Optimal Power Trajectory Iteration 2 Simulated . . . 83
46 Simulated Remaining Anaerobic Capacity Constant Attempt 2 . . . 84
47 Comparing Constant Attempt 2 with CP . . . 85
48 Pacing Strategy Compared to Actual Power Output 2 . . . 85
49 Simulated Remaining Anaerobic Capacity Guided Attempt 2 . . . 85
50 RPE and Heart Rate Iteration 2 . . . 86

List of Tables

1 C_DA for different positions, crank, range of air velocity and the blockage effect. . . . 8
2 Test Protocol Results . . . 87
3 Time Trial Results . . . 87
4 Time Schedule of Activities . . . 88

List of Abbreviations

AWC Anaerobic working capacity . . . 13

ATP Adenosine 5'-triphosphate . . . 13

CP Critical power . . . 1

LT Lactate threshold . . . 11

MPC Model predictive control . . . 98

3MT Three-minute all-out interval . . . 20

5MT Five-minute all-out interval . . . 66

12MT Twelve-minute all-out interval . . . 66

GET Gas exchange threshold . . . 13

IVP Initial value problem 23

TT Time trial 1

PCr Phosphocreatine 13

CRF Cardio Respiratory Fitness 9

CNS Central Nervous System 12

KKT Karush-Kuhn-Tucker 30

FTP Functional Threshold Power 15

RPE Rating of Perceived Exertion 12

NMPC Nonlinear Model Predictive Control 98

List of Variables

- α : Maximum power model parameter [1/s]
- α_c : Maximum cadence model parameter [rpm/J]
- ρ : Air density [kg/m^3]
- θ : Track inclination [rad]
- ϵ : Drive chain efficiency [unitless]
- A : Frontal cross sectional area of the bicycle and cyclist [m^2]
- A_{BSA} : Surface area of the body [m^2]
- AWC : Total anaerobic work capacity [J]
- C : Pedaling cadence [rpm]
- C_R : Coefficient of rolling resistance [unitless]
- C_D : Coefficient of drag [unitless]
- C_{max} : Maximum cadence [rpm]
- $C_{max,f}$: Maximum cadence of cyclist when w is fully depleted [rpm]
- CP : Critical power [W]
- g : Gravitational acceleration [m/s^2]
- I_w : Rotational inertia of wheels [$kg * m^2$]
- M : Total mass considering inertia of wheels [kg]
- m : Mass of cyclist and bicycle [kg]
- t : Time spent on track/segment [s]
- u : Control input power (of the cyclist) [W]
- R_w : Radius of wheels [m]
- v : State variable of velocity of center of mass of bicycle and cyclist [m/s]
- v_{ss} : Steady state velocity [m/s]
- w : State variable of remaining anaerobic work capacity [J]

Table of Contents

List of Figures iv

List of Tables v

List of Abbreviations vi

List of Variables vii

1 Introduction 1

1.1 Background and Motivation . . . 1

1.2 Problem Description . . . 2

1.3 Research Approach . . . 2

1.4 Scope and Limitations . . . 3

1.5 Structure of the Thesis . . . 4

2 Literature Review 4

2.1 Mechanical model . . . 4

2.1.1 Mathematical formulation . . . 5

2.1.2 Environmental and anthropometric parameters . . . 7

2.2 Physiological model . . . 9

2.2.1 Physiological factors involved in endurance performance . . . 9

2.2.2 Categories of metabolism . . . 13

2.2.3 "CP" concept . . . 13

2.2.4 Dynamics of Recovery and Expenditure of w . . . 16

2.2.5 Estimation of physiological parameters . . . 20

2.2.6 Maximum power generation . . . 22

2.3 State discretization . . . 23

2.3.1 Explicit Runge-Kutta methods . . . 26

2.3.2 Implicit Runge-Kutta methods . . . 27

2.4 Optimization . . . 28

2.4.1 Necessary conditions for a global minimum . . . 30

2.4.2 Optimisation algorithms . . . 33

3 Modeling the remaining anaerobic capacity 33

3.1 Linear model across entire domain . . . 33

3.2 Nonlinear recovery . . . 34

4 Design of the optimal program **41**

4.1 Problem hierarchy . . . 41
4.2 Dynamic models . . . 42
4.3 Nature of the problem . . . 46
4.4 Numerical integration . . . 48
4.5 Final Problem Formulation . . . 53
4.6 MATLAB framework . . . 54
4.7 Track selection . . . 55
4.8 Upper Level Strategy: Distributing Anaerobic Capacity . . . 57
4.9 Lower Level Tactics: Formulating an Optimal Power Trajectory . . . 61

5 Experimental Approach **62**

5.1 Experimental setup . . . 62
5.2 Test Protocols . . . 64
5.3 Verification of a pacing strategy . . . 66

6 Results **66**

6.1 Validation of W'-model . . . 66
6.2 Bologna TT Attempt 1 . . . 70
6.2.1 Physiological Parameters . . . 70
6.2.2 Optimisation . . . 71
6.2.3 Verification of a Pacing Strategy . . . 73
6.3 Bologna TT Attempt 2 . . . 77
6.3.1 Physiological Parameters . . . 77
6.3.2 Optimisation . . . 78
6.3.3 Verification of a Pacing Strategy . . . 84
6.4 Overview of Results . . . 86
6.4.1 Test Protocols for Physiological Parameters . . . 86
6.4.2 Time-Trial attempts . . . 87
6.4.3 Time Schedule of Tests and Attempts . . . 87

7 Discussion **88**

7.1 Results . . . 88
7.1.1 Bologna TT Attempt 1 . . . 88
7.1.2 Bologna TT Attempt 2 . . . 89
7.2 Mechanical Model . . . 90

7.3 Physiological Models . . . 90
7.3.1 The CP-model . . . 90
7.3.2 Model of Remaining Anaerobic Capacity . . . 91
7.3.3 Modeling maximum power generation . . . 92
7.4 Design of optimal program . . . 93
7.4.1 Optimisation hierarchy . . . 93
7.4.2 Iterations of the optimisation scheme . . . 93
7.4.3 The initial guess at a solution . . . 94
7.5 Experimental Execution . . . 95
7.5.1 Test protocols . . . 95
7.5.2 The Bologna Track . . . 96
7.6 Further Work . . . 97
7.6.1 Remodeling . . . 97
7.6.2 Alternative methods of optimisation . . . 98
7.6.3 Practical Implications . . . 98

8 Conclusion **99**

Bibliography **101**

Appendix **107**

A MATLAB code **107**
A.1 Parameters . . . 107
A.2 Upper level optimisation . . . 108
A.3 Upper level test . . . 111
A.4 Plot results from upper level . . . 112
A.5 Lower level optimisation . . . 114
A.6 Lower level test . . . 118
A.7 Plot results from lower level . . . 119
A.8 Sprint Problem . . . 121
A.9 Total optimisation iteration 1 . . . 124
A.10 Plot results from total optimisation iteration 1 . . . 127

1 Introduction

1.1 Background and Motivation

The act of using one's resources intermittently in order to optimize the activity towards some desired output is present in all sports. This is true, especially, in endurance sports, as this strategy is central to the nature of the competition itself. The models of the system involved in the activity could take many shapes and structures. One method of modeling human performance, is by measuring the power produced, and estimating the status of the available energy sources in the human body as a response to this. Due to differences in duration, movement pattern, and use of tools between sports, model requirements vary. One model might suit a situation of high intensity and simple movement patterns, while another fits the reality of a situation of longer duration, and a tool involved, like a bicycle. Cycling is especially suitable for such modeling of human performance, due to the relative ease of measuring power on an ergometer.

The power-duration relationship for human performance in endurance sports, can quite accurately be approximated in terms of two parameters, Critical power (CP) and work doable above CP, namely w. These parameters are subject dependent but constitute a static model. For an endurance sport competition with individual start like Time trial (TT) cycling, these parameters can be used to select a pacing strategy. For example, for a time-trial race on a completely flat track, an optimal pacing strategy would be to stay at peak power output at all times. This power level would naturally decrease throughout the run. During cycling TTs that are not completely flat, it could prove necessary to manage the finite amount of anaerobic capacity available across the track. This results in the need of a mathematical description of the physiological dynamics underlying power output during such an activity. Naturally, this concerns the high - to severe-intensity domains of exercise.

However, undulating terrain requires a more complex pacing strategy. For instance, in TT cycling, it is well known that it is beneficial to push harder on climbs and recover downhill. To find an optimal pacing strategy in this case, one has to intermittently use, and recharge the remaining anaerobic working capacity. Two dynamical models must be developed. A physiological model describing the "consumption" and "recharging" of w, and a mechanical model. The latter takes into account the external factors, such as the undulating terrain and rolling resistance. These models can then be used to find out how much more or less energy one should expend uphill and downhill. This could be classified as an optimal control minimum-time problem. Considering the problem in a simplified environment, where certain external factors are excluded, opens the door to producing a solution through the implementation of an optimal program. Looking at time-trial cycling, specifically, would limit the situation to an individual race, excluding the possibility of other riders affecting the situation. An eventual verification on an ergometer, using cycling software called Zwift [1], corresponds well with such simplifications. The environment being simulated within the software has a number of simplifications of the real world situation.

There have been numerous attempts at creating optimal pacing strategies in time-trial cycling. In [2] the effect of a variable gradient on TT cycling was explored. It compared a constant power output of 255 W with a power output varying with the gradient, averaging to 255 W, on the same, undulating time-trial course. The results were a reduction in trial time of 12 ± 8 s. In the thesis [3], the aim was do develop numerical pacing strategy optimization models and bioenergetic models for locomotive endurance sports and use these to assess objectives relevant in optimal pacing. These objectives include: Investigate the impact of hills, sharp course bends, ambient wind, and bioenergetic models on optimal pacing and assess the effect of optimal pacing strategies on performance. The results showed that athletes benefit from adapting their power output with respect not only to changing course gradients and ambient winds, but also to their own physiological and biomechanical abilities, course length, and obstacles such as course bends. The results of this thesis also showed that the computed optimal pacing strategies were more beneficial for performance than a constant power distribution. In [4], the physical system of the bicycle and the cyclist was modelled, as well as the fatigue and recovery of energy in the body. These models were used to analyze the power output of the cyclist, and a minimum-time optimal control problem was solved. Testing against a self-chosen pacing strategy for a number of athletes,

the result for one subject was a 3% reduction in trial time. In the experiment in question, the optimised pace was communicated to the subject in real time.

1.2 Problem Description

The goal of this project is to optimize a pacing strategy for time-trial cycling based on a mechanical, and a physiological model of a cyclist on an undulating track. After having solved the optimisation problem, the next step would be to demonstrate an improvement in time performance as a consequence of following the power instructions set by the pacing strategy. The performance would ultimately be verified in comparison to an attempt at the same time-trial track, but with a power strategy based on maintaining a constant power. Also, one needs to provide values for the parameters in the physiological model through test protocols, representing a subject's physiology. Verification of improvement in time performance and estimation of the physiological parameters is done through TT tests and test protocols in the software training platform Zwift ([1]), on an ergometer.

1.3 Research Approach

Firstly, a literature review was conducted in order to grasp the most essential principles governing relevant topics, and map the current consensus and findings that would help define the problem at hand. The physics behind a cyclist traversing a hill (inclined or declined) gives an equation of motion that is necessary to manipulate in order to simulate a real life situation corresponding to this scenario. Research conducted on the areas of interest with respect to these parameters is going to be included and explored, in order to accurately argue the numeric values and methods of determination for them as well. An additional literature review delving into the physiological principles governing human performance, and the resulting methods of modeling performance in different contexts, is going to be conducted. This also serves as motivation for following approaches, as well as a framework for the way of thinking about the distribution of energy in the context of cycling. The prospect of choosing different models describing different aspects of human performance, presents an opportunity of exploring and possibly synthesizing one's own model, drawing inspiration from already existing ones. This section of the review will also focus on the specific experimental estimation methods involved in determining physiological parameters needed in the resulting model.

Finally, mathematical methods necessary for completing the task of describing the system completely using dynamic equations, as well as formulating an optimal program, will have to be investigated. The simulation of a situation, however simple or complex, will have to rely upon some numeric integration method, which in turn affects optimisation design choices. The actual optimisation theory needed in order to formulate, implement and solve a problem is necessary as well. In particular, the underlying mathematical conditions that needs to be in place in order to get feasible solutions, and the constraints this may put on an eventual implementation method. This furthermore ties into design choices regarding what category of algorithm to utilise in solving the problem, and the type of framework used in order to implement constraints and optimization variables.

Stepping out of the theoretical domains of the approach, and into solving the problem defining the project, the underlying dynamics needs to be determined. In order to do this, the different possible models put forth will be analyzed in MATLAB, and their properties evaluated in relation to the demands of the optimisation problem. Furthermore, design of the optimal program will be explored and developed in the existing optimisation framework of MATLAB. Ultimately, an optimisation hierarchy is set up in this framework, distributing the energy available, and producing an optimal power trajectory capable of reaching the objective. By relying on a testing environment involving an ergometer (a smart trainer [5]) connected to Zwift with a computer, one subject intends to estimate relevant physiological parameters, and verify proposed optimal solutions to the problem.

1.4 Scope and Limitations

Due to all testing happening through simulation in the cycling software Zwift, the mechanical model proposed in this section has to approximate the model which this software is based on. As previously mentioned, limitations to the physical description is also key to unlocking a possible optimal solution to the problem. Because the code of the software is not open source, one has to make assumptions in order to develop the correct equations of motion. No mathematical method capable of producing a useful output is also capable of describing the entire physical reality of a situation. It is safe to assume, that in order for the Zwift software to have been developed, it too had to make assumptions and simplifications on the physical situation.

The model describing the power produced by humans, and the mechanics involving the bicycle and the rider, can be viewed as an input/output system. The input is power u, measured in Watt, produced by bodily processes $B(\cdot)$, which remains to be explored. This input power acts on a mechanical model $F(\cdot)$, which produces an output velocity v. Disturbances $H(\cdot)$ in the form of an inclination θ and air resistance (a function of velocity), results in an output velocity.

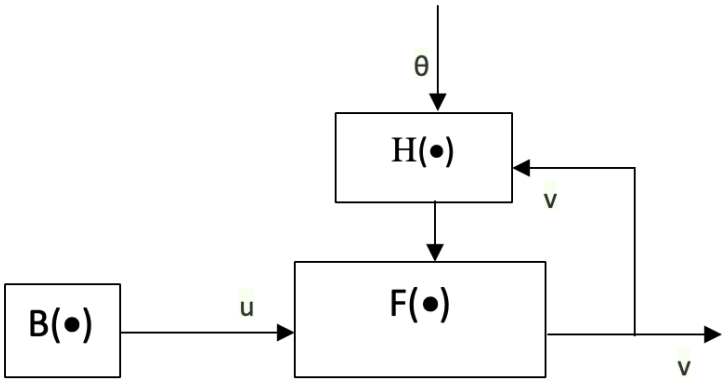

Figure 1: The system viewed as an input/output model

In order to solve the problem efficiently, some factors of disturbance would have to be left out. Turns in the track is one of these factors. It is entirely possible to include, but the inclusion of such dynamics presents some problematic changes to the situation. First of all, the overall complexity increases, with turns meaning the simulated situation having to consider three physical dimensions. But more importantly, turns in the track and considering all dimensions, puts some strange demands on the modeling of the system. The previously input/output model will be significantly challenged, as turns introduces the tilting of the bike, as well as the significant change in posture of the cyclist. Also, the entering and leaving of a turn must have some sort of dynamics, or else the system has to go in and out of states, or "modes" of turning. The latter would be highly possible to implement, but is considered outside the scope of this project.

Another factor which greatly affects the outdoor cycling situation, is wind. Gusts of wind and other weather phenomenons could greatly affect velocity through altering the expression of drag resistance. This is considered outside the scope of the project. So too is the notion of a varying temperature. This would in theory change with altitude and as a result of weather conditions. With a varying elevation during a time-trial, follows a varying air pressure (ρ), as well. This too, can be neglected, due to the minuscule contribution this has to the parameters of the system. A time-trial which is performed on a circular track with no inclination variations indoors, might be explained by a model neglecting all phenomenons of temperature dynamics, air pressure dynamics and wind, due to the steady-state conditions of these parameters in an indoor-setting. However, this will in turn result in a problem based on no inclination, which leaves this use case irrelevant for the problem described in Section 1.

One might argue that the problem of simply setting a pace for the rounds of a time trial in the indoor environment (setting bounds on how hard an athlete should pedal, measured in watt,

based on the length of the time trial) could be a relevant problem inside the scope of the project. However, this is not deemed as relevant as the varying inclination problem, seeing as this invites dynamics regarding both expenditure, and recovery of anaerobic capacity. Lastly, time-trials are also kept within approximately a 1-hour duration, making the dynamics of parameters like air pressure, temperature and wind fairly constant, except in the case of a sudden shift in weather conditions. Time-trials are planned often in such a way as to avoid them being conducted during big shifts in weather.

An important factor for velocity dynamics, affecting both power output, as well as air resistance, is the position which the cyclist takes on the bike. There are variants of standing positions, often generating a higher maximum power, and sitting positions, often gaining more velocity advantages going downhill, due to the frontal cross sectional area of the body taking up a smaller frame. Here, too, a "mode" of position could be introduced, shifting in a step-like manner, slightly changing both the power output potential and the drag resistance, could be introduced. However, due to time-trials being performed mostly in a time trial position when air resistance is high, and in a standing position during steep slopes and low velocity, the parameter deciding the air resistance on the rider and the bike as a consequence of the position (C_dA) is considered constant.

1.5 Structure of the Thesis

Each part of the thesis is ordered in such a way that it's preceding part builds the groundwork for it's guiding principles, and it's succeeding part brings forward it's findings toward reaching the objective. The parts involving modeling of remaining capacity, optimisation design and experimental approach makes up the overall approach of the project. In this manner, the structure of the thesis is as follows:

1. Literature Review
   (a) Mechanical Model
   (b) Physiological Model
2. Modeling the Remaining Anaerobic Capacity
3. Design of Optimal Program
4. Experimental Approach
5. Results
6. Discussion & Conclusion
7. Bibliography and Appendix

2 Literature Review

2.1 Mechanical model

In order to provide certainty of an optimal solution to an energy distribution problem in cycling, one has to describe the physical dynamics underlying the cycling itself. This will, in turn, enable the accurate mapping of the states of interest throughout the time trial. These states are the time spent along the track (t), the velocity at any given moment ($v(t)$), and the power going into the system of the bicycle, put out by the human on it (u). More specifically, it is the relation between the last two which is of most importance to derive, in order to see how this input power affects the output velocity. The equation of motion of the system is derived with the aforementioned simplifications in mind (Section 1).

2.1.1 Mathematical formulation

When making a physical model for the cyclist riding on a graded slope in two dimensions, one has to look at first principles. [6] includes an analytic overview of equations of motions for endurance sports, including cycling. The authors conclude that the instantaneous power P which is available to overcome friction and to increase the energy of the center of mass can simply be calculated from the propulsive force F and the velocity of the center of mass v.

$$P = F * v \tag{1}$$

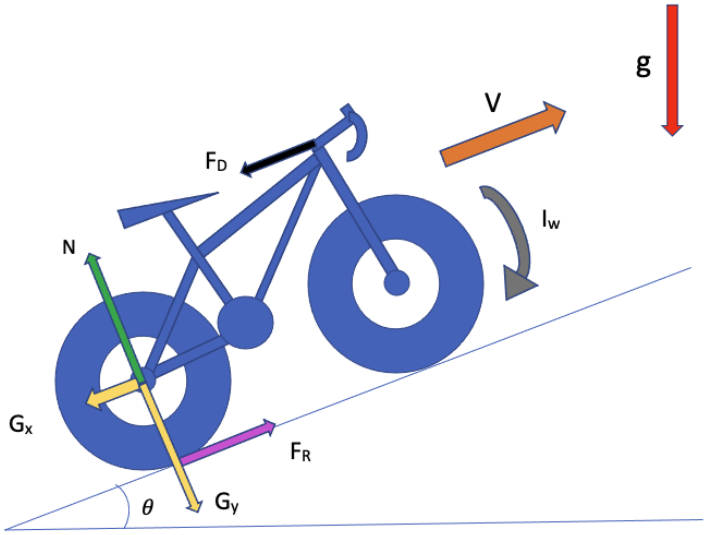

Figure 2: Figure partially based on illustration of forces acting on a bicycle in motion, [6]. The different forces acting on the system, along with the velocity (orange), gravitational acceleration (red) and rotational inertia of the wheels (gray). Gravity (yellow) is decomposed into the contributing vector in the direction of motion along the track, and the direction perpendicular to the track. The arrows in the illustration are placed according to visual simplification, rather than mathematical interpretation. The normal force (green), drag resistance (black) gravitational components (yellow), and the velocity vector (V) actually acts on the center of mass. The rolling resistance (purple) actually works on both wheels in the contact point between ground and the wheels.

Looking at a bicycle on a slope in 2D (Figure 2), the gravitational force decomposes into two vectors (G_x and G_y). They are given by the equations

$$G_x = mgsin\theta \tag{2}$$

$$G_y = mgcos\theta \tag{3}$$

where m is the total mass of the bicycle and cyclist, and g is the gravitational acceleration. The gravitational component acting on the system parallel to V is (2). Using (1) shows that the power to overcome this component is given by

$$P_g = mgvsin(\theta) \tag{4}$$

Total resistance is considered a sum of the rolling resistance due to energy losses as the wheels roll along the road, and the air resistance (or "drag") ([7]). The frictional force acting on the wheel is given by the coefficient of rolling resistance C_R and the normal force N ([8]).

$$F_R = C_R \times N \tag{5}$$

where N is given by

$$N = mgcos(\theta) \tag{6}$$

which gives the equation

$$F_R = C_R mgcos(\theta) \tag{7}$$

Combining (1) and (7) gives the power required for overcoming the rolling resistance

$$P_{RR} = C_R mgvcos(\theta) \tag{8}$$

The air resistance acting on the system results in a force given by the drag equation ([7])

$$F_D = \frac{1}{2}\rho C_D A v^2 \tag{9}$$

where ρ is the air density in kg/m^3, C_D is the drag coefficient (dimensionless, function of Reynold's number [9]) and A is the cross-sectional area of the cyclist, bicycle and wheels in m^2.

Combining (1) and (9)

$$P_D = \frac{1}{2}\rho C_D A v^3 \tag{10}$$

Combining (4), (8) and (10) gives the total expression for the required power output the cyclist has to have to maintain a steady velocity v

$$P_{tot} = C_R mgvcos(\theta) + mgvsin(\theta) + \frac{1}{2}\rho C_D A v^3 \tag{11}$$

While the wheels are spinning, the model of the system must take into account the rotational inertia of the wheels. The expression for the total mass is given by

$$M = m + 2\frac{I_w}{R_w^2} \tag{12}$$

where I_w is the rotational inertia, and R_w is the bike wheel radius. The equations of motion can be derived from (11) and (1), using Newton's second law of motion

$$\sum F = M * \frac{dv}{dt} = \frac{\epsilon u - P_{tot}}{v} = \frac{\epsilon u - C_R mgvcos(\theta) - mgvsin(\theta) - \frac{1}{2}\rho C_D A v^3}{v} \tag{13}$$

$$= \frac{\epsilon u}{v} - C_R mgcos(\theta) - mgsin(\theta) - \frac{1}{2}\rho C_D A v^2 \tag{14}$$

$$\rightarrow \frac{dv}{dt} = \frac{\epsilon u}{Mv} - \frac{m}{M} g[C_R cos(\theta) + sin(\theta)] - \frac{1}{2M}\rho C_D A v^2 \tag{15}$$

where ϵ is the drive chain efficiency (a coefficient describing the proportion of power directly transferred to the wheels, which will not be equal to 1, due to losses in the mechanical system of

the bicycle [6]), u is the power output of the system, and $\sum F$ is the sum of forces acting on the system. (15) is the same equation of motion for velocity as the one used in [4]. Concatenating the parameters, gives

$$\frac{dv}{dt} = a * \frac{u}{v} - b * sin(\theta) - c * cos(\theta) - d * v^2 \tag{16}$$

2.1.2 Environmental and anthropometric parameters

The parameters involved in the dynamic equation for velocity (16) needs to be determined. The gravitational acceleration constant is set to 9.81 m/s^2. [7] mentions that the rate of energy expenditure at a given speed, for level cycling, is directly proportional to the barometric pressure P_B [Torr], therefore decreasing with altitude. On the other hand, the maximal O_2 consumption of a given subject also decreases with altitude. The same article also mentions the mechanical power output as being directly proportional to air density. Neglecting air humidity, the density of dry air ρ is proportional to barometric pressure and temperature T [K]

$$\rho = \rho_0 \frac{P_B}{760} \frac{273}{T} \tag{17}$$

The standard air density for 20°C at sea level (ambient air pressure of 101.325 kPa), is set to 1.204 kg/m^3 [10]. Assuming that air humidity is outside the scope of the project, and that most tracks in the software Zwift take place at an elevation relatively close to sea level, this value is acceptable for the air density going forward. The road bike used in the Zwift software is called a 'TT Road Bike'. The weight of the bike, and radius of the wheels are not overtly given in the software. Therefore, these values has to be found through inspection online. The average weight of time-trial road bikes is set to 9.25 kg ([11]). The average radius of the wheels of these bikes is roughly 0.35 m (=28 inches), and the average weight of them is roughly 1.2 kg.

In [12], the coefficient of drag C_D was experimentally investigated. This coefficient is usually expressed through the product $C_D A$, where A is the frontal cross-sectional area of the cyclist, bike and wheels. The study includes a number of experiments (from other studies) conducted in wind tunnels to determine the value of $C_D A$ (Table 1). The different positions a cyclist can have on a bicycle were considered (upright, dropped and in time-trial position). The experiments varied in whether the crank was still or in motion, and they utilized different ranges of air flow velocities. The blockage effect (tunnel walls restricting the flow field around the cyclist, causing a local flow acceleration in certain areas) was either present and measured, not present and not measured, or present and not accounted for, in each article. [13] found that aerodynamic resistance accounts for over 90% of resistance a cyclist encounters on a flat surface, and [14] found that aerodynamic resistance accounted for between 56-96% of power depending on road gradient. This creates a circumstance where smaller, less powerful athletes can compete against larger stronger cyclists by optimising their interaction with the fluid medium (i.e. the air).

In road cycling in general, there are different positions the cyclist can take. The different positions results in different values for the drag coefficient, as the frontal cross section changes shape. Figure 3a shows the standing position, andFigure 3b shows the time-trial position.

(a) The cyclist standing while pedaling

(b) The cyclist sitting in a TT position

Article	Upright	Dropped	Time-trial	Crank	Vel. (m/s)	Blockage
1	-	0.28	-	Dynamic	1.5-18.5	-
2	0.32	0.26	-	Static	8.9–15.6	8%!
3	-	-	0.269	Dynamic	13.4	8%!
4	-	-	0.244	Static	13.9	-
5	0.358	0.307	0.269–0.240	Static	12.8	-
6	-	-	0.260	Static	15	$< 5.5\%$!
7	0.521–0.428	-	0.293–0.341	Dynamic	15	$< 5.5\%$!
8	0.318–0.282	0.289–0.275	0.235–0.223	Dynamic	13.9	$\simeq 2\%$!
9	-	-	0.296–0.226	Dynamic	11.1	$> 10\%$*
10	0.270	0.243	0.211	Static	10-20	$< 6\%$!
11	0.343	0.332–0.295	-	Dynamic	12.5	$< 9\%$*
12	-	-	0.251–0.214	Dynamic	18	$< 5\%$*

Table 1: $C_D A$ for different positions, crank, range of air velocity and the blockage effect. The superscripts * and ! refers to studies conducted in an open-jet and closed test section, respectively.

[15] developed a formula for estimating the surface area of the body based on height and weight.

$$A_{BSA} = 0.2025 h^{0.725} * m^{0.425} \tag{18}$$

In [16], the equation (18) is combined with a line of best fit-regression of world record data in time-trials, giving the equation for the cross-sectional area of the cyclist, bicycle and wheels (19), with a yaw-angle of 0°(frontal cross-sectional area). In terms of how well observed outcomes are replicated by this model of the cross-sectional area, the R^2 for this regression was 0.757. This is most likely due to the low number of cyclists involved in the data, because it only involved athletes on the elite level. The time-trial position was used during the experiments.

$$A = 0.1447 A_{BSA} + 0.1647 = 0.0276 h^{0.725} * m^{0.425} + 0.1647 \tag{19}$$

One subject is being slated to perform all tests and verification attempts of optimal pacing strategies in this project. This is executed using the Zwift software and an ergometer connected to the software. The height and weight of the subject is m = 84 kg and h = 1.87 meters. Assuming a time-trial position to be the one most frequently used during a time-trial ($C_D = 0.6$, [12]) (presumably the position used during segments where velocity is high, and therefore segments during when the term of air resistance in (16) contributes the most to resistance), and using the model for frontal cross-sectional area on a bicycle (19), results in the product $C_D A = 0.2182$. This coincides with the values found experimentally in Table 1, where values of $C_D A$ for time-trial position ranged from 0.211 to 0.296.

In [17], the determinants of the rolling resistance were shown to be wheel diameter, type of tire, inflation pressure, ground surface and the friction in the machinery of the bicycle itself. In experiments conducted in the study, a mean value of 0.0038 for the rolling friction coefficient was found for an asphalt pavement surface. [18] also investigated the influence of tyre pressure (P_r) and vertical load (F_v) on coefficient of rolling resistance, and concluded that these had a nonlinear relationship with C_R. Changes in magnitude of these had an important effect on competitive cycling performance. The results showed that an increase in P_r from 600 kPa to 900 kPa could yield an increase in velocity of 0.5 km/h. [19] investigated the probable values for rolling resistance on the different surfaces available in the Zwift software. For pavement (which is the normal surface for time trials), the value of rolling resistance was found to be $C_R = 0.004$. This was estimated for a typical road bike wheel.

Lastly, the drive chain efficiency ϵ is set to 1. This then assumes no losses in the drive chain of the bicycle in the software Zwift. Ultimately, the mechanical parameters of (16) can be concatenated into four new parameters, which for the values given in this section, becomes:

$$\begin{aligned} a &= \frac{1}{M} = 0.0105 \quad [1/kg] \\ b &= g * \frac{m}{M} = 9.5639 \quad [m/s^2] \\ c &= b * C_R = 0.0383 \quad [m/s^2] \\ d &= \frac{1}{2M} * C_d A * \rho = 0.0014 \quad [kg/m^2] \end{aligned} \tag{20}$$

2.2 Physiological model

2.2.1 Physiological factors involved in endurance performance

In order to analyze human performance within endurance sports, one has to be able to determine the physiological dynamics involved in making power output possible in humans. There are several ways of interpreting, and understanding human output of power and energy, and what is the most suitable method of understanding, depends on the desired outcome of the endeavour. If one is to model the human body in terms of its ability to sustain power output which lies in the high- to severe intensity domains, it is beneficial to look at the definitions of muscle fatigue, and the physiological parameters involved in this.

[20] defines fatigue as an exercise-induced progressive loss of the ability to sustain maximum power (energy exertion) over a desired duration of time. The author also calls it a dynamic process that leads to a drop in the required exercise intensity, which eventually leads to termination of exercise due to exhaustion. [21] ascribes a cycling TT to be 80-90% dependent of aerobic metabolism (oxygen-dependent energy expenditure in the body), while [22] ascribes the sum of the aerobic and the anaerobic work capacities to the total time performance in endurance sports. Factors involved in the aerobic metabolism are listed by the latter author as:

- $\dot{V}O_{2max}$
- Fractional utilization of $\dot{V}O_{2max}$
- Work economy

[23] defines $\dot{V}O_{2max}$ as the maximum amount of oxygen (in litres/min) a person can intake and argues that this individualized value does not change despite an increase in workload over a time period (as exclusion of the dot above the letter V is standard practice in non-science writing, the title of the article states this as VO_{2max}. However, these refer to the same variable, namely the maximal rate of change of the total volume of oxygen in the lungs). [23] also states that the World Health Organization considers this parameter to be the single best indicator of Cardio

Respiratory Fitness (CRF). Another name for CRF is aerobic fitness, or maximal aerobic power, which [24] defines as the ability to deliver oxygen to the muscles and to utilize it to generate energy during exercise. This depends on the pulmonary (related to the lungs), cardiovascular (related to the heart and blood vessels) and haematological components of oxygen delivery and the oxidative mechanisms of the exercising muscle.

Even though this variable is rated as a reliable parameter in determining aerobic fitness, it is also dependent upon direct measurement as this gives the most accurate estimation. There exists several indirect estimation methods that comes with a varying degree of uncertainty. The direct measurement method presents considerable equipment costs. The method also requires big practical interventions into the setup of the experimental environment. In the case of studying human performance in terms of oxygen uptake, a proposed dynamic model would either have to directly continuously measure the uptake, with the maximum possible value as some supporting parameter, or indirectly estimate it. The fractional utilization of the $\dot{V}O_{2max}$ refers to the bodily process of transferring the oxygen from the environment, all the way down to the mithocondria in the cells [22]. With this follows proposed mathematical models explaining the process, which in turn will have its own individualized parameters describing the properties of this utilization.

The final point, work economy, refers to the ratio between work output and oxygen cost to that output. [25] lists the causes for individual variation in this parameter as **(1)** anatomical traits, **(2)** mechanical skill, **(3)** neuromuscular skill and **(4)** storage of elastic energy. The nature of aerobic metabolism and fitness is therefore also shrouded by a number of factors difficult to determine and model. However, depending on the specific sport in question, and its corresponding movement pattern, by choosing a the right model describing performance, factors such as mechanical and neuromuscular skill can be suppressed as to their influence on what is being modelled.

When cycling on an ergometer (a stationary exercise bicycle measuring the amount of work done by pedalling), the measure of work can easily be recorded and used as a variable in mathematical models. However, the process of turning the metabolic energy cost having been spent, into the actual amount of work having been executed on the ergometer, includes some losses of energy along the way. Efficiency, as it is called, is defined as the ratio of work generated to the total metabolic energy cost [26]. In [26], re-analysis of data from five other, separate studies found that variation in gross efficiency explained 30% of the variation in power output during cycling time-trials. This shows the effect of work economy has on aerobic metabolism, as previously mentioned, and therefore also the power output. A problematic scenario, which can affect the reliability of a mathematical model, might be when a cyclist's pedaling technique results in a gross efficiency which creates a gap between the estimated physiological parameters in the model, and the power output seen on the ergometer. An example is a cyclist with a particularly "incorrect" or inefficient technique. However, the choice of the right model will help suppress this effect, as models which include parameters that are power-dependent will exclude power-dependent variability, which gross efficiency affects. In Figure 4, the system formulated in Figure 1 is expanded, giving a deeper insight into the bodily processes which govern human power output in cycling.

Figure 4 mentions ambient conditions as a factor involved in determining the final performance time during a time trial. The effect of ambient conditions on the mechanical model of the system is already covered, but other ambient factors including temperature, and pain perception, might affect the time performance as well. [28] argues that the perception of temperature is a non-negligible factor during endurance performance. The states that during steady-state exercise of 30-40 minutes, thermal perception ratings (subjects rating the perception of temperature) can be attributed to skin and ambient air temperatures, while the thermal discomfort ratings (subjects rating the subjective comfort of temperature) can be attributed to the skin blood flow and the sweating response. One study used menthol (a cooling compound acting on cutaneous thermoreceptors to induce perceptions of coolness) on the surface of the skin in the face under heat stress during exercise [29]. The results showed a significant increase in power output on an ergometer doing a cycling-protocol, compared with a control trial (placebo-controlled). [30] argues that the metabolic steady state core temperature for running (an endurance sport similar to cycling in many respects) is 38.4 °C.

Figure 4 also shows pacing strategy as a factor in total time performance in endurance sports.

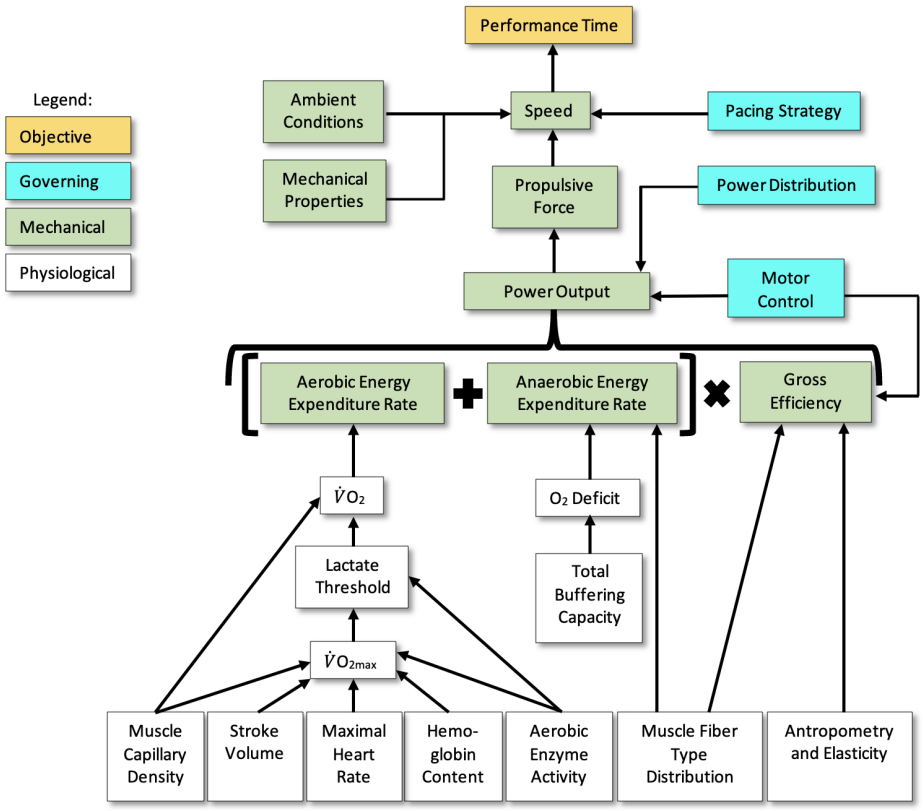

Figure 4: Factors involved in performance time in an endurance sport. Based on illustration from [3], which is based on the work of [27]. There are a number of physiological parameters (white boxes) affecting the energy expenditure rate in the body. Muscle capillary density (number of blood vessels per unit cross-sectional area), stroke volume of blood in the heart, maximal heart rate, and other factors affect the $\dot{V}O_{2max}$. This, in turn, affects the Lactate threshold (LT) and the variable $\dot{V}O_2$. The total buffering capacity refers to the chemical uptake of oxygen in the body, in turn affecting the oxygen deficit (when the body's need for oxygen exceeds it's intake). This deficit helps define the amount of anaerobic energy sources needed to sustain a certain physical activity. Gross efficiency ($\in [0, 1]$) then plays the role as a multiplier of the total energy expenditure rate. The energy expenditure rate then plays into the power output, which will have its own distribution across the time trial. The speed, ultimately, will also be affected by ambient conditions like temperature, surface, air density, humidity, wind and shape of the track. Mechanical properties, such as drive chain losses in the bicycle will also affect the resulting speed.

Having taken all other mechanical and physiological factors into consideration, a form of strategic energy distribution in the form of such a strategy, will help determine whether the cyclist is able to traverse a particularly steep hill when having already spent a lot of energy going through the earlier parts of the track. Throughout a professional cyclist's career, this kind of knowledge is automatically developed through exposing themselves to competition and time-trials. However, such an energy distribution also has an optimal solution, given that all other factors in Figure 4 are either included (explained and determined), or excluded (simplification leading to them being negligible) from the model of the total system.

In [31], a literature review was conducted which investigated recent nutritional findings and their influence on endurance sports. In this review, a technique called carbohydrate-mouth-rinse is discussed in relation to performance in endurance sports. The technique consists of rinsing the mouth with a carbohydrate solution every 5-10 minutes during for instance a 1-h cycling time-trial performance. [32] demonstrated time trial cycling performance improvements with glucose a mouth-rinse compared to placebo even in short term (one hour) exercise. The authors concluded that it was unlikely that carbohydrate ingestion exerts its beneficial effect through its contribution to energy expenditure as only about 10-20% of ingested carbohydrates is actually oxidized in the first hour of exercise, so "the explanation for this increased performance remains to be established".

The author of [31] mentions that some proposed a mechanism of action being that it modulates the central governor theory [33], a Central Nervous System (CNS)-established safe level of exertion during exercise to preserve an emergency reserve margin of energy storage. A later study [34] even showed that an intravenous infusion of glucose during a 1 h time trial, despite increases in plasma glucose for oxidation and evidence of increased glucose uptake into the tissues, had no effect on 1-h cycling time trial performance. This is important information going into a scenario of a time-trial, or another type of competition of this duration. These findings point towards nutritional tactics on the day of a competition having less of an impact on the performance time than previously assumed.

Lastly, all of the factors mentioned above, are ultimately affecting the performance time through what can be interpreted as a filter, in the form of subjective experience. Herein lies a vast number of sub-factors, which potentially contributes to reducing the power output. Some of these factors are experience level, pain tolerance, general mood of the day, external factors increasing the motivational pull to perform well, and a lot more. The experience level, meaning the amount of exposure the cyclist has had to situations of severe fatigue and mounting pressure related to a competition, certainly seems to affect the other factors which are mentioned. This creates a complex network of mutually dependent sub factors within the subjective realm of endurance sports. These sub-factors may not be captured correctly by a mathematical model, but there are ways of attempting to measure them. A way of measuring the experienced exertion of an activity, a scale was invented. The Borg Rating of Perceived Exertion (RPE) [35] is a scale of numbers ranging from 6 to 20. Numbers with no description lie in between the values associated with perception. The scale is 6: No exertion at all, 7, 7.5: Extremely light, 8, 9: Very light, 10, 11: Light, 12, 13: Somewhat hard, 14, 15: Hard (heavy), 16, 17: Very hard, 18, 19: Extremely hard, 20: Maximal exertion.

Exercise intensity may be measured using respiratory kinetics ($\dot{V}O_2$), velocity, lactate dynamics and power output. The heart rate during physical activity also plays a significant role in the intensity of the effort. It reflects the respiratory and circulatory responses to the energy requirements at any point in time. [36] proposed a method to determine the exercise intensity that coincides with the 4 mmol l^{-1} lactate exercise intensity. This so-called 'heart rate break-point' is based on the deflection point in the sigmoidal heart rate versus power output curve that results from a progressive incremental exercise test. However, [37] argues that this point is an artefact rather than a phenomenon. The authors states that when the duration of each exercise intensity is very short ($\leq$ 1min), the adaptation of the circulatory system to a certain work rate will be incomplete and heart rate will start to lag behind progressively. When heart rate is plotted as a function of velocity or work rate, a deflection point is automatically found. However, when the duration of each exercise intensity is longer, some adjustment of the cardiovascular system will take place and it is more difficult to find the deflection point.

The authors argues that heart rate monitoring is useful for identifying insufficient recovery between training sessions (over-training). Cardiac drift is also mentioned as a feature of heart rate monitoring. This is the phenomenon of heart rate increasing during exercise over time, for a constant work rate. This might occur due to fatigue, a decrease in the technical execution of the movement pattern, or subjective experience of the exercise. [37] also lists temperature and dehydration as causes that may increase the cardiac drift even further, indicating that heart rate recorded during training may not reflect muscular work alone.

Despite weaknesses of heart rate monitoring for measuring exercise intensity, the method is might still be useful in measuring performance. [37] lists the intensity zones of heart rate monitoring, whereby different physiological phenomenons acts as demarcations. **Zone 1** is the low heart rate zone, believed to result in a minimal training effect. **Zone 2** is at a slightly higher intensity, but still below the LT. **Zone 3** us situated around the LT, whereas **Zone 4** is above the LT. A zone 5 is sometimes added, marking maximum effort. The aforementioned indication that a higher heart rate than normal during a certain power output, might also aid in the programming of a training schedule. This phenomenon, along with the cardiac drift, may in combination with subjective experience, help to validate different models of physical performance.

2.2.2 Categories of metabolism

The definition, and borders of, the aerobic and anaerobic domains for metabolism also helps describe the situation. [38] defines aerobic exercise as endurance-type exercises in which a person's muscles move in a rhythmic and coordinated manner for a sustained period. These exercises require oxygen to generate energy. [38] defines anaerobic exercise as short, intense bursts of physical activity, which involves an increase in the absorption and transportation of oxygen. During anaerobic exercise, the body breaks down glucose stores in the absence of oxygen, leading to a buildup of lactic acid in the muscles.

[39] lists three ways of detecting the onset of anaerobic metabolism (starting from aerobic metabolism) during exercise:

- An increase in the lactate concentration in blood
- A decrease in arterial blood bicarbonate and pH
- An increase in the respiratory Gas exchange threshold (GET)

The GET is the ratio between the metabolic production of CO_2 and the uptake of O_2 in the human body [40]. Lactate concentration in the bloodstream reaches a threshold when it builds up faster than the body is able to remove it. This threshold represents the boundary between the moderate- and high-intensity domains in exercise. It can occur at around 80-90% $\dot{V}O_{2max}$ [41]. [42] investigates the relative contribution of the aerobic, and the anaerobic systems during maximal exercise. The author defines three distinct, yet integrated processes that operate together to satisfy the energy requirements of muscle:

- **Anaerobic lactic process** - Nonaerobic breakdown of carbohydrate to lactic acid through glycolysis
- **Anaerobic alactic process** - Splitting of stored phosphagens, Adenosine 5'-triphosphate (ATP) and Phosphocreatine (PCr)
- **Aerobic process** - Combustion of carbohydrates and fats in the presence of oxygen

ATP and its phosphate bonds are the basic components of energy exchange in many biological systems, including humans [43]. PCr is the byproduct of reversible interconversion of creatine, where large pools of it is created during creatine kinase, in order to achieve spatial and temporal buffering of ATP in the cells [44]. The author argues that the literature within the field of exercise physiology has undermined the aerobic component in high intensity exercise, and has too often deemed the two processes to be disjoint sets within the intensity domain. The author also argues that the current literature suggests that all physical activity derive some energy from each of the three processes, and in an overlapping fashion to the energy demands of the exercise, rather than sequentially.

2.2.3 "CP" concept

[45] introduced the hyperbolic relationship between constant power output and tolerable duration inside the "severe" intensity domain. The model consists of the parameters CP, and the Anaerobic working capacity (AWC). CP represents the theoretically maximal sustainable power output (in watt) associated with metabolic steady state. Above this threshold, $\dot{V}O_2$ and the lactate levels can not attain a steady state. The AWC is the full capacity of energy (in joules) that is usable, when above the CP. The hyperbolic relationship is formulated as:

$$P = \frac{AWC}{t_{lim}} + CP \tag{21}$$

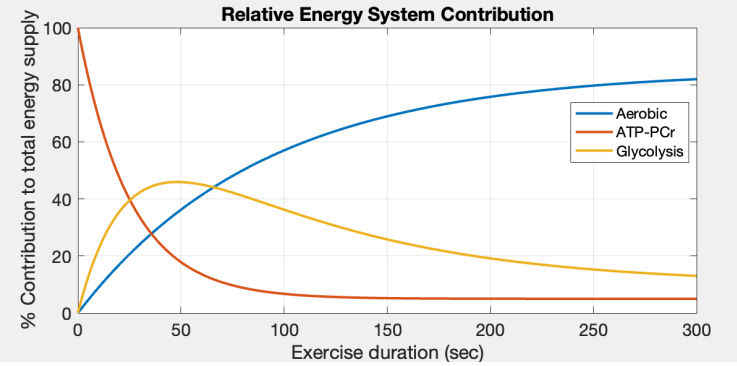

Figure 5: Relative energy contribution of anaerobic (ATP-PCr) and aerobic metabolism. Based on illustration from [42], page 737

where P is the power output level in the given endurance sport (in watt) and t_{lim} is the time to exhaustion (a point in time whose definition varies between experiments, but often relies on the same interpretation as the definition of fatigue in [20]). Reformulating (21), gives the basis for the most common model for expenditure of the anaerobic energy above CP:

$$AWC = (P - CP) * t_{lim} \tag{22}$$

This means that the total available anaerobic energy storage will be drained at t_{lim}, at a rate dependent on what level above CP the output power is. [46] defines AWC as the total work that can be performed above the CP using only stored energy sources within the active muscles (sources like adenosine triphosphate, phosphocreatine, glycogen and the oxygen bound to myoglobin). The same article also names other studies suggesting that the AWC is also associated with the accumulation of metabolites (which could be inorganic phosphate, H+, lactate and ammonia) and extracellular potassium K+ during fatiguing exercise. According to [41], CP occurs at a higher absolute value and relative intensity than the LT. Based on the work of [47], the illustration in Figure 6 shows the power-duration relationship, and the relative positioning of CP and AWC within this curve (where $W' = \text{AWC}$).

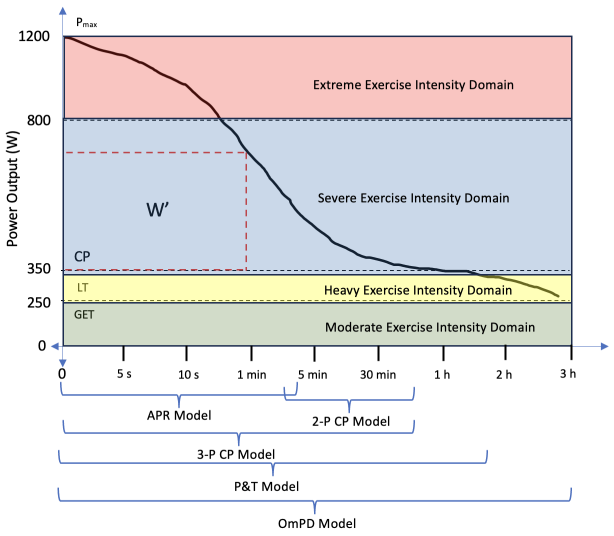

Figure 6: Power-duration curve with intensity domains of power output with arbitrary power levels. Different models of designed for a varying duration of exercise. 2-P CP model is uses the same relation shown in (21). The area under the curve and over the CP (= 350 W) is the AWC (W'). The LT and GET can be seen just below CP, at 250 W. Based on illustration in [47], page 306.

Figure 6 provides further information that the CP model is mostly applicable for physical activity ranging from a duration of 30 minutes to 1 hour. Also, the illustration shows how different models (nonlinear-2, nonlinear-3 etc.) for estimating CP bases its experiments on different parts of the power-duration curve. Both the time duration, and the intensity domain over which this model is applicable, corresponds well with the demands set on the mathematical modeling in the introduction of this project. In [48], attempts were made to better quantify the energy expenditure associated with heavy/severe exercise and the recovery of that exertion. The author concluded that anaerobic-type activity with multiple recoveries would result in a larger energy expenditure than equivalent work performed at a lower aerobic rate. This hints at a possible underlying non-linear dynamic in the expenditure and recovery of w.

[49] lists a number of assumptions implied in the CP - model, which in turn stimulates a discussion regarding the simplification these assumptions introduces, as well as possible extensions for the model. The assumptions are:

1. There are only two components to the energy supply system for human exercise, termed aerobic and anaerobic
2. The aerobic supply is unlimited in capacity, but is rate limited. This limiting parameter is the CP
3. The anaerobic supply conversely is not rate limited, but is capacity limited by the parameter AWC
4. Exhaustion, and by implication termination of exercise, occurs when all of AWC has been utilised
5. Aerobic power is available at its limiting rate CP the moment the exercise begins and remains so right up until the end of the exercise
6. The power domain over which the model applies is all of $CP < P < \infty$
7. The time domain over which the model applies is all of $0 < t < \infty$, and endurance at CP is infinitely long
8. The efficiency of transformation of metabolic energy to mechanical energy is constant across the whole power (and time) domain(s)
9. CP and AWC are constants, independent of P (and/or of t)

Even though the literature clearly indicates an existence of several sources of energy during high - to severe intensity exercise, one could categorise these into the two aforementioned larger sources, called anaerobic and aerobic. However, the transition of one to the other, as well as their relative contribution around the CP threshold, prompts awareness of the simplification underlying this assumption. The limitation of capacity with regards to the aerobic supply must also be brought into question, as this allows for a theoretically infinite endurance at the threshold CP. However, as has been already established, the model in question, and the activities relevant for the project, all deal with duration of exercise around 30 to 60 minutes. The literature suggests this could be an acceptable simplification of the physiological situation. One does not need to include the wear and tear of the body in order to model the fall in endurance over an even longer period of time. This would only become relevant for activities lasting several hours. Going forward, however, one does have to keep in mind the limitations of the parameter CP itself, seeing as it has been shown to be overestimated in its absolute value [50].

Authors of [51] also mentions another parameter often used in the discussion of performance metrics in cycling. The authors defines Functional Threshold Power (FTP) as the maximum average power sustained over a 1-hour period, which is estimated through 8- or 20-minute self-paced cycling protocols by subtracting 10 or 5% of the average power achieved after each respective cycling test. Although there is a lack of evidence demonstrating the utility of FTP testing for tailored exercise prescription aimed at improving cycling performance, FTP seems an important performance quality because maximum power sustained over 1 hour is predictive of time-trial

performance in elite cyclists. Despite the increasing use of FTP in practice, the energy systems and physiological qualities that contribute to FTP are incompletely understood. Also, the experimental routines and estimation methods used to determine the parameter varies between experiments and use cases.

In light of the list of critique in Figure 2.2.3, the concept of CP reveals its shortcomings. It might also render a new interpretation of the physiological phenomenon. Intra-day variations [20] and general uncertainty regarding the determination of the CP (as well as the parameter AWC) for athletes and non-trained cyclists, show that the concept might be better understood as an interval of threshold, demarcating the severe intensity from the heavy intensity power output domains, rather than a scalar value.

2.2.4 Dynamics of Recovery and Expenditure of w

In the framework of the CP model presented first in [45], the amount of remaining anaerobic capacity at each moment in time would be dependent upon the curve of the power output of the cyclist. A good portion above the threshold of CP, one could with certainty say that the cyclist is expending capacity. Inversely, a good portion below the threshold, the cyclist is recovering this lost capacity, in the form of energy. However, the exact dynamics underlying these changes are unknown. For the expenditure of capacity, there exists a proposed formula linear in power (or the difference between the output power and the CP), derived from the relation (22). Most models trying to describe either only the expenditure of the anaerobic capacity, or the total remaining anaerobic capacity (which includes recovery of the capacity), usually uses this formula for expenditure. For recovery, however, the situation is more ambiguous, which is reflected in the research done on this topic. Experiments performed in order to uncover the dynamics are often tailored to a specific application, and often performed at one or few levels of recovery power. [52] uses one single recovery power in experiments when attempting to fit the recovery of w to an exponential time-response. This range of recovery duration vary in time, making the data eligible to uncover the time response for this recovery. However, the power output is fixed to a certain level, making these experiments unable to describe the dynamics of w with respect to a varying power below CP.

[4] and [53] both take an optimal-control approach in order to minimise the duration of time trials. In these articles, the authors uses bi-conditional models for expenditure and recovery of w.

$$\begin{aligned} &\text{If } u \geq CP : \frac{dw}{dt} = -u + CP, \\ &\text{If } u < CP : \frac{dw}{dt} = -a * u - b + CP \end{aligned} \tag{23}$$

where a, b are individualised parameters, making recovery slightly slower than expenditure, for non-zero values of these parameters. [4] finds these experimentally, whereas [53] uses $a = 1, b = 0$, resulting in an equal rate of expenditure and recovery above and below CP. Both models based their system dynamics on (21), (22). However, research done on the topic of w recovery - and expenditure dynamics tells a slightly different story.

In [54], a literature review regarding the modeling of the recovery and expenditure of the w, several mathematical models are mentioned. In this review, [55] is mentioned as proposing a non-linear recovery model of w, after having investigated the topic specifically in cycling. The author describes a curvilinear relationship for the reconstitution (recovery) of w with respect to time, during above-CP exercise. It also suggests that neither recovery of $\dot{V}O_2$ or lactate concentration to their normal levels, correlates sufficiently with the w recovery. Given the small number of data points in each subjects' data, (n = 3), the authors does not attempt to formulate some kinetic characterization.

[54] also investigates the role of muscle glycogen in the kinetics of w. Test protocols were performed on an ergometer (**1.** a maximal incremental ramp test, **2.** a test involving four

constant load tests at different levels, determining the power-duration relationship, giving CP and w, and **3.** an above-CP exercise followed by a three-level constant power protocol) all involving rest-periods at 20 W power output. The last protocol had rest-periods of 2, 6 and 15 minutes. The results showed a 15% shortfall in w recovery during the 15 minute recovery.

The authors conclude that the recruitment patterns of muscle raise the possibility that a degree of fiber type dependent regional glycogen depletion may account for this. They conclude that there is a dissociation between decrease in muscle glycogen and the decrease in AWC. Evidence of unchanged concentration in intramuscular ATP [56] also supports the final conclusion on the topic of muscle glycogen in the article [55], which states that it is unlikely that AWC is simply reflecting a source of stored energy that is depleted during above-CP exercise. This argument is therefore pointing towards the highly physiologically simplified nature of the model of CP and AWC. This is an important note going forward, when implementing findings into reality.

[57] proposed an exponential response in time for the recovery of anaerobic work capacity. The authors used participants which were recreational athletes, but not highly trained. The participants were exposed to so-called 3 minute all-out tests on an ergometer, which will be described in detail later. These tests seek to estimate the subjects' CP and AWC based on a maximum effort for 3 minutes. The CP was estimated as the last 30 seconds of the test, and AWC was estimated as the power-time integral above the CP. In the next tests, the subjects performed trials of constant work rate to exhaustion in the severe intensity domain, as well as four intermittent exercise trials to exhaustion. The intermittent trials consisted of 60 seconds of work intervals at P_6 (the power output predicted to result in exhaustion in 6 minutes above CP) + 50% of the difference between P_6 and the subjects CP. In between the work intervals, there were 30 second recovery intervals at a predetermined intensity. Different levels of recovery power were used, in order to uncover the recovery dynamics with a varying power level. The four levels below were tried. P_{GET} is the power level associated with the GET (mentioned in 2.2.1).

1. Low intensity of recovery: 20 W
2. Moderate intensity of recovery: 90% of P_{GET}
3. Heavy intensity of recovery: GET + 50% of (CP - P_{GET})
4. Severe intensity of recovery: P_6 - 50% of (P_6 - CP)

The authors in [57] had already hypothesized an exact mathematical formulation for the recovery of the remaining anaerobic capacity w, consisting of an exponential function. In [58], the dynamic model of recovery of the anaerobic work capacity is derived from first principles. The authors conceptualize w in the framework of chemical kinetics. During bouts of recovery in which u is less than CP, the rate of change of w depends on the amount of w remaining (i.e. recovery slows as w approaches the initial w, which is denoted w_0) and the power output relative to CP.

$$\frac{dw}{dt} = \Big(1 - \frac{w}{w_0}\Big)(CP - P) \tag{24}$$

The first-order differential equation is solved using standard methods as follows

$$\begin{aligned} &D_{CP} = CP - P \\ &\int \frac{dw}{\Big(1 - \frac{w}{w_0}\Big)} = \int D_{CP} dt \end{aligned} \tag{25}$$

The integral is solved using the substitutions rule. Note also that P is considered constant with respect to time, such that D_{CP} is constant.

$$ln\Big(1 - \frac{w(t)}{w_0}\Big) = \frac{D_{CP}}{-w_0} t + const \tag{26}$$

Here, the authors state that for any time duration T that follows the expenditure of w, $w(t) = w(T)$, which by definition is less than w_0. They substitute these values into the equation, and solve algebraically for $w(t)$ to obtain the final solution:

$$w(t) = w_0 - (w_0 - w(T))e^{(-D_{CP}/w_0)(t-T)} \tag{27}$$

The authors of [57] also hypothesize some time constant taking up a spot in the mathematical expression for this recovery. This ultimately resulted in the hypothesized recovery dynamics taking the form:

$$w(t) = AWC - \int_0^t (w_{exp})e^{-\frac{t-l}{\tau_w}}\,dl \tag{28}$$

Here, w is the variable representing the remaining anaerobic energy, l is the variable of integration, w_{exp} is the spent anaerobic energy during the time above CP and τ_w is the time constant of the recovery of w. The results of the tests showed an inverse correlation with CP (higher CP leads to a shorter duration needed to recover from a bout of severe intensity measured in power). There was no linear correlation when recovery power exceeded CP. The results gave an expression for the time constant as a non-linear exponential response with respect to D_{CP}, which is the difference between the average recovery power for the entire exercise and CP, given by:

$$\tau_w = 546e^{-0.01D_{CP}} + 316 \tag{29}$$

Discussing the results of the findings, the authors of [57] attempts to explore the reasoning behind the correlations of τ_w and CP. The time constant was well fit by an exponential function for all power outputs below CP. The authors propose a likely explanation for this to be the presence of a smaller "oxidative reserve" with increasing recovery power output. In other words, the smaller the difference between the $\dot{V}O_2$ required to maintain the recovery power and the $\dot{V} =_2$ at CP, the smaller the capacity to reconstitute the w.

In the model formulation of the author in [57], D_{CP} is expressed as the average difference between input power u and CP throughout the whole activity. This means that (28) is mostly applicable for post-calculation with regards to the estimation of the remaining anaerobic capacity. The model also allows for a negative value for w, making it possible for the subject to draw more energy from their w stores than they did during the test protocols for determining CP. The same authors of [57], proposed in [58] proposed a bi-conditional model for w:

$$\begin{aligned} &\text{If } P > CP, w = w_0 - [(P - CP) * t], \\ &\text{If } P < CP, w = w_0 - w_{exp} * e^{\frac{-D_{CP}*t}{w_0}} \end{aligned} \tag{30}$$

where w_{exp} is the energy expended during some time interval. Like the model used in [4], (30) relies upon a non-continuous, conditional expression, shifting from one dynamic to another, depending on the power output being above or below the discrete line of CP. This makes use of the findings of an exponential time response of recovery, whose rate depends on the recovery power level, in [57].

[52] proposes a bi-exponential model of the recovery of w in the human body. The article describes the previously mentioned model for constant power output and tolerable duration [45] as a basis for contemporary models of w kinetics. Early work suggested that w is dependent upon levels of phosphocreatine, stored glycogen and oxygen within the muscle [59]. Today, w is believed to be at least partly dependent upon the accumulation of fatiguing metabolites such as adenosine diphosphate, inorganic phosphates and hydrogen ions ([60], [61], [62]).

Much like the previous models, [52] bases its arguments on theory proposing a depletion of w when the power output is above CP, and a reconstitution of w below CP. The author

goes on to list research showing the same dynamics for muscle PCr ([63], [64]). However, [55] showed that w recovers slower than PCr levels. The authors of [52] argues that both PCr and w reconstitution kinetics are slowed following repeated severe intensity efforts that culminate at the limit of tolerance, suggesting that w reconstitution processes are partially dependent upon PCr regeneration. They also cite the curvilinear tendency of w reconstitution found in [55], following observations of its recovery to 37%, 65% and 86& of baseline levels resulting from respective recovery durations of 2, 6, and 15 minutes. The model proposed by [57], here referred to as the mono-exponential model, is also mentioned.

The authors of [52] argues that the mono-exponential model has been suggested to underestimate w reconstitution in elite cyclists ([65]), and that it does not account for the slowing of w reconstitution with repeated maximal incremental exercise. Furthermore, large individual variations in τ_w were observed in both the modelling of τ_w in untrained cyclists ([57]) and for a modified τ_w model for elite cyclists [65]. Therefore, the critique of the authors of [52] centers around the argument of an individualized time constant of recovery of w. The authors propose a multi-exponential model, which also considers the body's ability to sustain the repeated severe-intensity bouts relevant for the scope of models for anaerobic metabolism. Their mathematical hypothesis proposes a sum of exponential terms, which seeks to describe the slowing of the recovery rate of w as the number of severe-intensity bouts during a longer activity increases. This coincides with the power curve of a typical TT.

In [52], 10 trained cyclists (who were all familiar with cycling, ergometers and had a relatively high $\dot{V}O_{2max}$) conducted 6-10 tests in a period of 3-4 weeks. The tests consisted of a warm up on low power levels and three intervals of ramps (a gradual increase in power output on the ergometer). In between the three ramps, there were two recovery intervals, which varied in their duration. Different combinations of durations for the recovery intervals (where an interval could have the duration 30 sec, 60 sec, 120 sec, 180 sec, and 240 sec) were used, in order to uncover the underlying dynamics of the time constant for w reconstitution.

The CP of the subjects was estimated using an unspecified test. This estimate was used and perfected through a series of other tests, consisting of ramps of 20 w/min (increasing the power output on the ergometer by 20 watt per minute). This was done until the point of exhaustion, which was decided to be the point where the cadence (frequency of the pedaling) fell below 60 rotations per minute. At that point, the previously estimated CP was used to set the power level down to $CP + 30W$ in order to fully empty the remaining anaerobic work capacity w. The point of empty w was set to when cadence dropped to below 50 repetitions per minute, upon which the subjects cycled all-out for 2 minutes. Knowledge of time to completion of this phase was withheld to minimise the likelihood of pacing.

The model proposed in [52], compared to the more widely accepted "mono-exponential" model proposed by [66], takes the form of the sum of two exponential terms. Restating the remaining anaerobic capacity $w(t)$ from [66] as the remaining percentage of the AWC, the models can be compared in the following fashion:

$$\begin{aligned}
&\text{Mono - Exponential: } \%w_{rec} = 100 * (1 - e^{-t/\tau_{mono}}) \\
&\text{Bi - Exponential: } \%w_{rec} = FC_{amp} * (1 - e^{-t/\tau_{FC}}) + SC_{amp} * (1 - e^{-t/\tau_{SC}}) \\
&\text{and where: } SC_{amp} = (100 - FC_{amp})
\end{aligned} \tag{31}$$

where τ_{mono}, τ_{FC} and τ_{SC} are the time-constants for the mono-exponential model, the fast component of recovery in the bi-exponential recovery model, and the slow component of the bi-exponential recovery model, respectively. Using the data from the test protocols previously mentioned, and fitting it to this model using nonlinear regression, the results showed that it the best fit was the bi-exponential model. The results also indicated that both the time-constants, and the amplitudes of the two recovery components varied markedly between individuals, despite similar training status. A further novel finding was that the slow component alone exhibited impaired w reconstitution kinetics following a repeated bout of exercise, the magnitude of which was related to measures of aerobic fitness. The authors also noted that the use of only 30s and 240 s recoveries

were found to be effective in determining w reconstitution kinetics when compared to using a wider range of recovery duration.

2.2.5 Estimation of physiological parameters

No matter what model one seeks to deploy, they all require individualized, estimated parameters which describes the current state of physical capacity. A number of these have been mentioned (CP, AWC, α, τ_w). However, practical considerations have to be made to determine the desired mathematical, and experimental complexity of a physiological model. In other words, one has to evaluate the needs of accuracy of the model, in light of the available time and resources allocated for experimental purposes.

[67] proposes a method of determination for CP and AWC called Three-minute all-out interval (3MT). The authors tests the hypothesis that the power output attained at the end of the cycling test would be equivalent to CP. The experimental method included ten subjects performing a test protocol designed to warm up the cyclist, and then expend all of the assumed available capacity (AWC) during a 3 minute bout of maximum effort. The entire test protocol included a warm-up at 100 watt for 5 minutes, followed by 5 minutes of rest. After the recovery, the subjects did 3 minutes of unloaded baseline pedaling at each subjects preferred cadence, followed by an all-out 3 minute effort. The resistance on the pedals during the 3-min effort was set using the linear mode of the ergometer so that the subjects would attain the power output halfway between $\dot{V}O_{2peak}$ and the GET (i.e. +50% Δ, with Δ being the magnitude of the interval between GET and $\dot{V}O_{2peak}$) on reaching their preferred cadence.

The last 30 seconds of the 3 minute effort is the crucial segment of the test. The average value of the power output measured on the ergometer is estimated to be the CP, whereas the area between the power curve and the line representing this newly determined parameter of critical power (above this line) is the AWC. The findings from [67] demonstrated that it is possible to determine CP and AWC using a single bout of all-out exercise. [4] used this 3MT test to estimate CP, AWC and the parameter involved in describing the maximum attainable output power, α. The latter parameter can be found throuht solving the equation $P_{max} = \alpha * AWC + CP$ where P_{max} is the maximum recorded power throughout the 3 minute effort, and the values of AWC and CP are found as explained previously.

However simple this all-out test seems to execute, it has been deemed to be a somewhat inaccurate measure of the CP and the AWC. [20] argues that the test has been shown to overestimate CP and AWC. More involved mathematical methods of determining these values have been used in studies, compared against the values from the parameters coming from the 3MT. [46] makes a note of the fact that different estimation methods of CP and w results in different times to exhaustion for a power output at exactly CP. Known models of estimating these two parameters are the Linear-P (linear power) model, Linear-TW (linear time-work), Nonlinear-2 (nonlinear 2-patameter model), Nonlinear-3 (nonlinear 3-parameter model) and the EXP (exponential model, only capable of estimatin CP, not AWC). [68] proposes that linear models of estimation underestimates CP. [69] found an inverse relationship between models reporting high critical power and a low w, and vice versa. The figure (Figure 6 [47]) visualises how these models relate to each other along the power-duration curve.

The Linear-TW model is given by

$$w_{lim} = AWC + (CP * t) \tag{32}$$

where w_{lim} = maximum amount of work able to be completed in an effort. The linear-P model is given by

$$P = \frac{w}{t} + CP \tag{33}$$

The Nonlinear-2 model is based on the hyperbolic relationship between t and P

$$t = \frac{AWC}{P - CP} \tag{34}$$

which can be seen to be the exact same as the hyperbolic relationship represented in [45]. The Nonlinear-3 model extends on the Nonlinear-2 model, by also including a parameter k for the maximal instantaneous power (P_{max}), in an attempt to more accurately estimate the CP

$$\begin{aligned} t &= \frac{AWC}{P - CP} + k \\ k &= -\frac{AWC}{P_{max} - CP} \\ \Rightarrow t &= \left(\frac{AWC}{P - CP} - \frac{AWC}{P_{max} - CP} \right) \end{aligned} \tag{35}$$

where t is the time to exhaustion, P is the power output, and P_{max} is the maximal instantaneous power. The exponential model is given by

$$P = CP + (P_{max} - CP) * e^{-\frac{t}{\tau}} \tag{36}$$

where τ is an undefined time constant. The findings in [46] showed that Nonlinear-3 resulted in the lowest estimated CP, and EXP the highest. The authors lists a number of studies having showed that Linear-P, Linear-TW, Nonlinear-2 and EXP models overpredict CP as a sustainable exercise intensity associated with metabolic steady state. The authors also lists a number of studies having shown that the same models overpredict the highest exercise intensity, where $\dot{V}O_2$ and blood lactate reach steady state. This has led investigators to evaluate the estimates of CP from the Nonlinear-3 model. The authors of [46] claim these investigations of several studies concluded that among the aforementioned models, the Nonlinear-3 is the most accurate one. According to [70], the AWC from the Nonlinear-3 model was a more accurate reflection of the total energetic reserve.

[71] attempted to validate the Nonlinear-3 model by using incremental tests, constant power trials to exhaustion and single-leg maximum instantaneous power measurements. The data from the tests was fitted to the Nonlinear-3 model (35) using nonlinear regression. The trials of constant power resulted in a time-to-exhaustion (T_{lim}) ranging from 20 minutes to 20 seconds, allowing for an accurate analysis of the power-duration curve. The curves from the Nonlinear-2 and the Nonlinear-3 model are superimposed for $T_{lim} \geq 2$ min, whereas they start to diverge when $T_{lim} \leq 2$ min. For the latter case, the Nonlinear-2 model starts to overestimate the output more the shorter T_{lim} is. The authors claim that a strength of the study is the fact that the subjects involved in the tests were allowed to increase their pedaling frequency at the highest power outputs, unlike other studies in which only the pedal torque was changed.

[72] investigates the bioenergetics of w, and compares four different models for estimating CP and AWC - Linear-P, Linear-TW, Nonlinear-2 and Nonlinear-3. The authors took the work of [46] further, by comparing the four models' ability to ascertain critical power and w in elite road cyclists, while making comparison to power output as respiratory compensation point (point in the increasing exercise intensity at which respiration starts compensating for the worsening metabolic acidosis, distinguished by an increase in the volume of air inhaled relative to CO_2 production, [73]), work rate (in $J * sec^{-1}$).

[72] assumes that W' encompasses an aerobic component between critical power and VO_{2max}, referred to as the VO_2 slow component (based on [74]). The author states that a contributing factor to the AWC would be an individual's ability to sustain VO_{2max} ([75]), as well as the buildup of fatigue-inducing metabolites ([55]). This makes it difficult to estimate, and also somewhat unlikely that it represents exactly the same physiological phenomena for each individual. Ultimately, the authors of [72] found that even though the Nonlinear-3 model, for instance, was shown (by [46]) to estimate the physiological parameters well, the use of CP in performance optimisation is questionable.

Lastly, whether one performs a host of tests in order to determine a time constant of recovery, undergo a single test in order to estimate CP and AWC or performs a time-trial attempt, a warm-up phase leading up to the bout is necessary. [76] reviewed different warm-up strategies for both short-term and long-term exercise and sports. The authors concluded that passively or actively elevating the temperature of the muscles used can markedly influence subsequent exercise performance via mechanisms such as increases in ATP turnover (ratio between ATP content and ATP production) and muscle cross-bridge cycling rate. Warming up could also lead to improvements in muscle fibre functionality and conduction velocity. The authors argue that athletes competing in sprint and sustained high-intensity events seem the most likely beneficiaries of elevations in body temperature due to increases in muscle glycogen availability and the rate of force development.

2.2.6 Maximum power generation

The last 100 m of a long race cannot be performed at the same power output which would have been possible if the athlete would perform these same 100 m completely fresh. In order for the state of the remaining anaerobic capacity to have an influence on the output power in the model, there has to be a maximum amount of power possible to generate at any time, dependent on this state. In other words, the main role of the state of w, is to limit the amount of power which is possible to attain at any moment. Therefore, an expression describing the interaction between this maximum level, and the state of w is needed.

[49], with [77] as an inspiration, proposes a feedback system which operates to limit the maximum power output achievable depending on the amount of anaerobic energy left.

$$P_{peak} = CP + \frac{w(P_{max} - CP)}{AWC} \tag{37}$$

In [4], this relation was expressed as

$$P_{peak} = \alpha * w + CP \tag{38}$$

where α was found experimentally for each individual subject that participated in the project. Looking at (37), it simply states that for a fully rested individual, the theoretical maximum power attainable would be available as output power. Inversely, a fully depleted w results in a maximum power generation equal to the threshold of CP. This relations stems from an assumption made in [4], that the peak power during a 3MT can be approximated as a linearly decreasing function of remaining anaerobic energy $w(t)$. The authors performed 3MT tests on six subjects, and the parameter α was estimated by the linear fit of the 3MT peak power data. The measure of fit (in this case an R^2) was estimated to one for all subjects conducting the full schedule of experiments.

The authors of [4] had assumed that subjects were free to choose their pedaling speed (cadence) for maximal power generation. However, they report that several studies ([78],[79],[80]) have shown through a series of short sprints, that cadence affects the maximum power generation ability of cyclists, regardless of their state of fatigue. At any given fatigue state, the maximum power is parabolic function of cadence as in,

$$P_{max} = 4P_{peak}\Big(\frac{C}{C_{mac}}\Big)\Big(1 - \frac{C}{C_{max}}\Big) \tag{39}$$

where P_{peak} denotes the peak of the parabola, C is the cyclist's cadence, and C_{max} is the cyclist's maximum cadence, which is reached when $P_{max} = 0$. Moreover, maximum cyclist cadence C_{max} also decreases with the state of fatigue [78], [80], and this relationship is linear as experimental results in [80] show. That is,

$$C_{max} = \alpha_c w + C_{max,f} \tag{40}$$

where α_c is a model parameter and $C_{max,f}$ is the maximum cadence of the cyclist when $w(t)$ is fully depleted. Using (38) in (39) results in

$$P_{max} = 4(\alpha w + CP)\Big(\frac{C}{C_{max}}\Big)\Big(1 - \frac{C}{C_{max}}\Big) \tag{41}$$

The authors of [4] also calibrated the relationship in (41) with data available from one of the subjects involved in the experiments.

2.3 State discretization

In order to simulate models proposed by the literature put forth so far, one has to be able to discretize their continuous representations. This allows for the system to be tested for different types of inputs (power output trajectories on the bike), as well as different shapes of the track (flat, undulating, etc.). One way to discretize states and inputs, is to imagine the track being sorted into segments, separated by points. In these points, states are updated. Each point also has a corresponding new input command, as well as a degree of inclination based on the position. This is visualised in Figure 7.

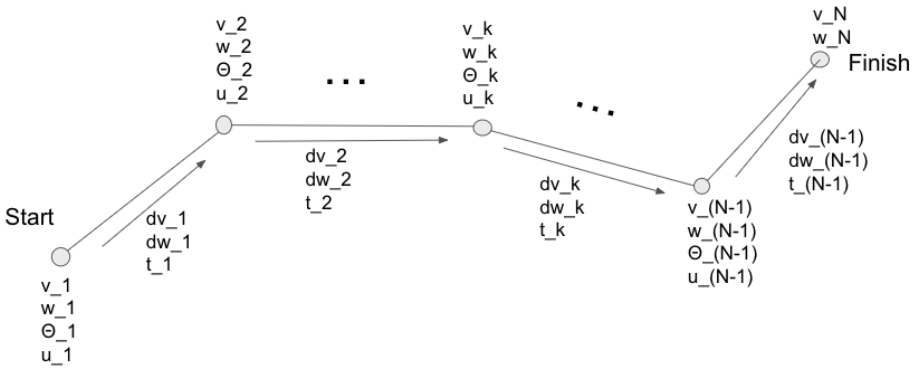

Figure 7: Discretization of track, with corresponding steps for the states t_k, v_k, w_k and their dynamics dv_k, dw_k, the control input power u, and the inclination θ_k

In order to calculate the states at the next point, one has to numerically solve the differential equations. Therefore, each point, and its corresponding states and inputs, results in a miniature Initial value problem (IVP). The tools normally used for this are called numerical integrators. [81] lists several such methods and their properties. The authors also points out the advantage of using such simulations of dynamic systems, in order to uncover potential errors in the model formulation, or implementation, prior to using it to solve a specific problem. All equations and mathematical principles of Section 2.3 are based on the work of [81].

In [81], the IVP can be stated as follows

$$\dot{\mathbf{y}} = \mathbf{f}(\mathbf{y}, t), \quad \mathbf{y}(t_0) = \mathbf{y_0} \tag{42}$$

where $\mathbf{y}$(t) is the exact solution of the system. The goal is to compute a numeric solution which approximates the exact solution with satisfactory accuracy. A time step h is used, and the numerical solution of the system is computed for $(t_0, t_1, ..., t_n, ..., t_N)$, where $t_{n+1} - t_n = h$. Denoting the numerical solution as $\mathbf{y}_n$, and the exact solution as $\mathbf{y}(t_n)$, one may analyze the accuracy of the computed solution. The local solution $\mathbf{y}_L(t_n; t)$, which is the exact solution at time t_n with initial condition $\mathbf{y}_n$, is given by

$$\dot{\mathbf{y}}_{\mathbf{L}}(t_n;t) = \mathbf{f}[\mathbf{y}_L(t_n;t)], \quad \mathbf{y}_L(t_n;t) = \mathbf{y}_n \tag{43}$$

One may express the deviation between the local solution of the next timestep $\mathbf{y}_L(t_n;t_{t+1})$, and the computed solution $\mathbf{y}_{n+1}$ as the local error introduced by the numerical scheme from time t_n to time t_{n+1}

$$\mathbf{e}_{n+1} = \mathbf{y}_{n+1} - \mathbf{y}_L(t_n;t_{n+1}) \tag{44}$$

The global error $\mathbf{E}_{n+1}$ is the error in the computed solution $\mathbf{y}_{n+1}$ relative to the exact solution $\mathbf{y}(t_{n+1})$ at time t_{n+1}. This means the total error as a result of computation from time t_0 to time t_{n+1}.

$$\mathbf{E}_{n+1} = \mathbf{y}_{n+1} - \mathbf{y}(t_{n+1}) \tag{45}$$

Any one-step numerical integration method, takes the form

$$\mathbf{y}_{n+1} = \mathbf{y}_n + h\phi(\mathbf{y}_n, t_n) \tag{46}$$

where $\phi(\cdot)$ is given by the particular numerical method used. The order of the method is given by

$$\mathbf{e}_{n+1} = O(h^{p+1}) \tag{47}$$

where the $O(\cdot)$ notation is based upon [82]. The function $\phi(\cdot)$ satisfies

$$\phi(x) = O[\psi(x)] \tag{48}$$

if there exists a constant $C > 0$ so that

$$|\phi(x)| \leq C|\psi(x)| \tag{49}$$

when x is close to zero.

[81] further states that the stability and performance of a one-step method for the numerical integration of the IVP (42) can be evaluated through the investigation of linearized system equations. The dynamics of this linearized system can to a large extent be described by the eigenvalues of its corresponding jacobian matrix. In order to analyze the performance of a one-step method, one can use these eigenvalues in the *stability function* of the method. The authors first establishes the mathematical background for this.

Suppose $\mathbf{y}^*(t)$ is a solution to the IVP

$$\dot{\mathbf{y}}^* = \mathbf{f}(\mathbf{y}^*, t), \quad \mathbf{y}^*(t_0) = \mathbf{y}^*_{\mathbf{0}} \tag{50}$$

Linearization of the system is expressed through the Taylor series:

$$\begin{aligned} \mathbf{y} &= \mathbf{y}^* + \Delta\mathbf{y}, \\ \dot{\mathbf{y}}^* + \Delta\dot{\mathbf{y}} &= \mathbf{f}(\mathbf{y}^*, t) + \left.\frac{\partial \mathbf{f}(\mathbf{y}, t)}{\partial \mathbf{y}}\right|_{\mathbf{y}=\mathbf{y}^*} \Delta\mathbf{y} \end{aligned} \tag{51}$$

The jacobian of this system is given by

$$\mathbf{J} = \left.\frac{\partial \mathbf{f}(\mathbf{y},t)}{\partial \mathbf{y}}\right|_{\mathbf{y}=\mathbf{y}^*} = \left\{ \left.\frac{\partial f_i(\mathbf{y},t)}{\partial y_j}\right|_{\mathbf{y}=\mathbf{y}^*} \right\} \tag{52}$$

This results in the linearization

$$\Delta\dot{\mathbf{y}} = \mathbf{J}\Delta\mathbf{y} \tag{53}$$

The solution of $\Delta\mathbf{y}(t)$ is expressed as the linear combination

$$\Delta\mathbf{y} = \sum_{i=1}^{d} q_i(t)\mathbf{m}_i \tag{54}$$

where $q_i(t)$ are solutions of the scalar differential equations

$$\dot{q}_i = \lambda_i q_i, \quad ,i? = 1, ..., d \tag{55}$$

where $\mathbf{q} = (q_1, ..., q_n)^T, \lambda_i$ are the eigenvalues of $\mathbf{J}$, and $\mathbf{m}_i$ are the eigenvalues of $\mathbf{J}$. Therefore, studying the eigenvalues of the jacobian $\mathbf{J}$ lets one evaluate the dynamics of the linearized system (53). Viewing the linearization as a one-step method, (54) may be expressed as

$$\Delta\mathbf{y}_{n+1} = \sum_{i=1}^{d} (q_i)_{n+1}\mathbf{m}_i \tag{56}$$

The *stability function* is defined as satisfying the numerical solution

$$(q_i)_{n+1} = R(h\lambda_i)(q_i)_0\mathbf{m}_i \tag{57}$$

The authors of [81] then concludes the mathematical reasoning; the numerical solution $\Delta\mathbf{y}_n$ of the linearized system (53) is stable if the magnitude of the stability function is less than or equal to unity for all the eigenvalues, that is, if

$$|R(h\lambda_I) \leq 1, \quad i = 1, ..., d \tag{58}$$

where h is the step.length and λ_i is an eigenvalue of $\mathbf{J}$. A simple example is the *linear test system*

$$\dot{y} = \lambda y \tag{59}$$

The numerical solution is

$$y_{n+1} = R(h\lambda)y_n \tag{60}$$

where $R(h\lambda)$ is the stability function for the given method. Therefore, the stability of this numerical integration scheme is ensured if the relation below is satisfied:

$$|y_{n+1}| \leq |y_n| \tag{61}$$

This is ensured if

$$|R(h\lambda)| \leq 1 \tag{62}$$

which, in turn, results in conditions put on the time-step h, and the eigenvalue λ for the numerical integration scheme to be stable.

2.3.1 Explicit Runge-Kutta methods

One of the simplest methods of numerical integration is the Euler's method:

$$\mathbf{y}_{n+1} = \mathbf{y}_n + h\mathbf{f}(\mathbf{y}_n, t_n) \tag{63}$$

The stability function, by the method of (57), gives the step-length criteria $h \leq -\frac{2}{\lambda}$. The order of the method is $p = 1$. Modifying the method to higher orders, by computing approximations of $\mathbf{f}$ over the interval, results in explicit Runge-Kutta methods. These methods computes $\mathbf{y}_{n+1}$ as a linear combination of these approximations [81]. The methods are said to have have σ stages, when they have σ number of approximations of the function derivative. A general Runge-Kutta method is expressed as

$$\begin{aligned}
\mathbf{k}_1 &= \mathbf{f}(\mathbf{y}_n, t_n), \\
\mathbf{k}_2 &= \mathbf{f}(\mathbf{y}_n + ha_{21}\mathbf{k}_1, t_n + c_2 h), \\
\mathbf{k}_3 &= \mathbf{f}(\mathbf{y}_n + h(a_{31}\mathbf{k}_1 + a_{32}\mathbf{k}_2), t_n + c_3 h), \\
&\vdots \\
\mathbf{k}_\sigma &= \mathbf{f}(\mathbf{y}_n + h(a_{\sigma 1}\mathbf{k}_1 + ... + a_{\sigma,\sigma-1}\mathbf{k}_{\sigma-1}), t_n + c_\sigma h), \\
\mathbf{y}_{n+1} &= \mathbf{y}_n + h(b_1\mathbf{k}_1 + ... + b_\sigma\mathbf{k}_\sigma)
\end{aligned} \tag{64}$$

where the interpolation parameters $c_i, i \in 2, ..., \sigma$ are in the range of $0 \leq c_i \leq 1$ and form an increasing sequence $0 \leq c_1 \leq ... \leq c_\sigma \leq 1$. The weighting parameters at stage i are denoted $a_{ij}, i \in 2, ..., \sigma, j \in 1, ..., i-1$, and satisfy the normalization condition

$$\sum_{j=1}^{i-1} a_{ij} = c_i \leq 1, \tag{65}$$

whereas the weighting parameters b_i of the solution $\mathbf{y}_{n+1}$ are required to satisfy the normalization condition

$$\sum_{i=1}^{\sigma} b_i = 1 \tag{66}$$

The stability function of the explicit Runge-Kutta methods can be derived looking at the same linear test system from (59) as an example. The authors of [81] formulates the general explicit method for this system, resulting in the form

$$\begin{aligned}
k_1 &= \lambda y, \\
&\vdots \\
k_\sigma &= \lambda[y_n + h(a_{\sigma 1}k_1 + ... + a_{\sigma,\sigma-1}k_{\sigma-1})], \\
y_{n+1} &= y_n + h(b_1 k_1 + ... + b_\sigma k_\sigma)
\end{aligned} \tag{67}$$

Writing this in vector notation (for $\kappa = (k_1, k_2, ..., k_\sigma)^T$ and $\mathbf{1} = (1, 1, ..., 1)^T$):

$$\begin{aligned} \kappa &= \lambda(\mathbf{1}y_n + h\mathbf{A}\kappa), \\ y_{n+1} &= y_n + h\mathbf{b}^T\kappa \end{aligned} \tag{68}$$

This gives the stability function for explicit Runge-Kutta methods

$$R_E(h\lambda) = det\left[\mathbf{I} - \lambda h\left(\mathbf{A} - \mathbf{1}\mathbf{b}^T\right)\right] \tag{69}$$

The stability function $R_E(h\lambda)$ is a polynomial in $h\lambda$ of order less than or equal σ, and $|R_E|$ will tend to infinity when $|\lambda|$ goes to infinity.

2.3.2 Implicit Runge-Kutta methods

When a system like (42) is integrated with an explicit Runge-Kutta method, the time step h cannot be selected so that $h|\lambda_{max}|$ is significantly larger than unity, where λ_{max} is the largest eigenvalue of the jacobian $\mathbf{J} = \partial\mathbf{f}(\mathbf{y}, t)/\partial\mathbf{y}$. For Euler's method, for instance, $h|\lambda_{max}|$ must be less than 2. As some systems have a large spread in eigenvalues, and the time-step of an explicit method must be chosen to ensure stability, very many time steps are required to compute the dynamics corresponding to the small eigenvalues. This results in problems with simulation time and accuracy. Such systems are referred to as stiff systems, and are difficult to solve with explicit methods. Stiff problems can be solved efficiently using implicit Runge-Kutta methods. The authors of [81] goes on to describe these methods. Such a method for the system $\dot{\mathbf{y}} = \mathbf{f}(\mathbf{y}, t)$, with σ stages, has the general form

$$\begin{aligned} \mathbf{k}_1 &= \mathbf{f}(\mathbf{y}_n + h(a_{11}\mathbf{k}_1 + ... + a_{1\sigma}\mathbf{k}_\sigma), t_n + c_1 h), \\ &\vdots \\ \mathbf{k}_\sigma &= \mathbf{f}(\mathbf{y}_n + h(a_{\sigma 1}\mathbf{k}_1 + ... + a_{\sigma\sigma}\mathbf{k}_\sigma), t_n + c_\sigma h), \\ \mathbf{y}_{n+1} &= \mathbf{y}_n + h(b_1\mathbf{k}_1 + ... + b_\sigma\mathbf{k}_\sigma) \end{aligned} \tag{70}$$

where the interpolation parameters $c_i, i \in 1, ..., \sigma$ are in the range $0 \leq c_1 \leq 1$. The weighting factors satisfy the normalization equation $\sum_{i=1}^{\sigma} b_i = 1$, and usually the weighting factors at each stage satisfy $\sum_{j=1}^{\sigma} a_{ij} = c_i$. The implicit Euler method becomes

$$\begin{aligned} \mathbf{k}_1 &= \mathbf{f}(\mathbf{y}_n + h\mathbf{k}_1, t_{n+1}), \\ \mathbf{y}_{n+1} &= \mathbf{y}_n + h\mathbf{k}_1 \end{aligned} \tag{71}$$

This method has the corresponding stability function $R(h\lambda) = \frac{1}{1-h\lambda}$, which results in the region of stability $|h\lambda| - 1 \geq 1$. Another method commonly known is the implicit mid-point rule. It is derived from the implicit Runge-Kutta method of order 2:

$$\mathbf{k}_1 = \mathbf{f}\left(\mathbf{y}_n + \frac{h}{2}\mathbf{k}_1, t_n + \frac{h}{2}\right) \tag{72}$$

Using $h\mathbf{k}_1 = \mathbf{y}_{n+1} - \mathbf{y}_n$ from (72) gives the scheme

$$\mathbf{y}_{n+1} = \mathbf{y}_n + h\mathbf{f}\left(\frac{\mathbf{y}_n + \mathbf{y}_{n+1}}{2}, t_n + \frac{h}{2}\right) \tag{73}$$

resulting in the stability function $R(h\lambda) = \frac{1+\frac{h\lambda}{2}}{1-\frac{h\lambda}{2}}$. Compared to other similar implicit Runge-Kutta methods (for instance the trapezoidal rule, which has the same exact stability function), the implicit mid-point rule has better stability properties for nonlinear systems.

Considering the test system $\dot{y} = \lambda y$, and a general eigenvalue

$$\lambda = \sigma + j\omega \tag{74}$$

where σ is the real part and $j\omega$ is the imaginary part. It is assumed that $\omega < \pi/h$, that is, ω is assumed to be less than the Nyquist frequency π/h. The local solution of the test system is

$$y_L(t_n; t_{n+1}) = e^{\lambda h} y_n \tag{75}$$

Consider a system $\dot{y} = \mu y$, which has the local solution

$$y_L(t_n; t_{n+1}) = e^{\mu h} y_n \tag{76}$$

The two systems will give the same local solutions at t_{n+1} whenever $e^{\lambda h} = e^{\mu h}$ which is implied by

$$\mu = \lambda + j2k\frac{\pi}{h} = \sigma + j\Big(w + 2k\frac{\pi}{h}\Big), \quad k = 0, \pm 1, \pm 2, ... \tag{77}$$

Therefore, if $\mu = \lambda + 2kj\frac{\pi}{h}, k = 0, \pm 1, \pm 2, ...$, then the system $\dot{y} = \mu y$ where $Im(\lambda) > \pi/h$ will have the same solution as the system $\dot{y} = \lambda y$ where $Im(\lambda) < \pi/h$. This phenomenon is called aliasing.

The test system $\dot{y} = \lambda y$ is stable when $\mathrm{Re}(\lambda) \leq 0$. Consider an integration method which gives $y_{n+1} = R(h\lambda)y_n$ when applied to the test system. If an integration method is stable for all stable test systems, it is called "A-stable" [81]. The definition of this category of stability is therefore that a method is A-stable if $|R(\lambda h)| \leq 1$ for all $Re\lambda \leq 0$. Integration methods that are A-stable will be stable also for systems with dynamics significantly faster than step h of the method. Aliasing can be problematic for A-stable methods, as high frequency oscillations will appear in the computed solution as an oscillation with frequency below the Nyquist frequency π/h.

2.4 Optimization

In order to produce a solution to an optimal control problem, an optimal problem, or optimal program, must be formulated. This way, known theory and principles will lead the way to gain feasible solutions and practically implementable control trajectories. The road towards formulating such a program starts by defining the properties of the problems in order to classify the problem, and hereby identifying what kinds of demands must be put on constraints, objective functions and the implementation of a solver.

An optimization problem can be classified in different ways. Certain properties of a problem will significantly alter the way a solution is found. The different properties defining a problem are:

1. **(Un-)constrained problems:** Whether or not the optimization variables are subject to bounds, or constraints set by functions of some set of the optimization variables.
2. **Continuity:** Whether the problem's object function, constraints and variables displays behaviour which can be characterized as continuous, or discrete (from definition of continuity in [83]).
3. **Linearity:** Whether the objective function or constraints are linear, nonlinear

4. **Convexity:** Whether the objective function or constraints have a positive definite Hessian matrix of their second order partial derivatives.

5. **Size of the problem:** Number of optimization variables and constraints defining the problem

The presence or absence of constraints in an optimization problem, leads to very different outcomes in terms of the pursuit of a solution to the problem. The optimization variables spans a space whose dimension is defined by the number of variables, and the bounds on these variables. The constraints of a constrained problem put on the variables of optimization (which includes the bounds previously mentioned), creates a region of feasible solutions for the variables within the variable space. Continuity is another property which greatly affects the method of solving a problem. An example of a discrete optimization problem, is integer programming. Such problems contain not only integers and binary values for optimization variables, but also more abstract variable objects, such as permutations of an ordered set. The defining feature of a discrete optimization problem is that the unknown x is drawn from a finite (but often very large) set [84].

Linearity simply states that a problem is a nonlinear optimisation problem if either the objective function, or any of the constraints set on the optimization variables, are nonlinear functions. If none of them are, the problem is a linear one. Convexity is yet another property affecting the optimisation approach, and provides a good description of the behaviour of a class of continuous functions. The convexity of a function is identified by a positive semi-definite Hessian matrix of its second partial derivatives [85]. The definition of positive semi definiteness of a matrix, is that it's eigenvalues are non-negative ([86]). In addition, the local minimum of a strictly convex function is the global minimum, making convexity in relation to optimisation a particularly important issue (minimization of the objective function, for instance). Discrete convexity is defined in [85]; Let S be a subspace of a discrete n-dimensional space. A function $f : \quad S \Rightarrow R$ is discretely convex if for all $x, y \in S$ and for $\alpha \in (0, 1)$

$$\alpha f(x) + (1 - \alpha) f(y) \geq \min_{y \in N(z)} f(u) \tag{78}$$

where $N(z) = u \in S : ||u - z|| < 1, z = \alpha x + (1 - \alpha)y$ and $||u|| = \max_{1 \leq i \leq n} |u_i|$. In Figure 8a and Figure 8b, a visual representation of convexity is shown. For a convex function, a straight line going through two of it's points will never cross the part of the line in between these points. For the non-convex function, this is not the case. The visualisation of the local minimum and global minimum in Figure 8b

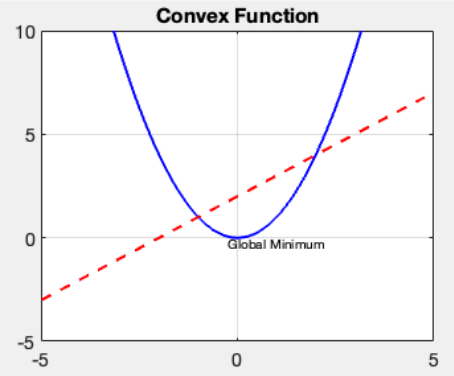

(a) Example of convex function, a straight line demonstrating this property, and its extreme point

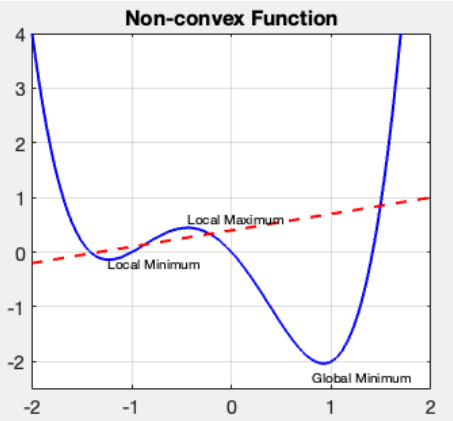

(b) Example of a non-convex function, a straight line demonstrating this property, and its extreme points

Finally, the size of the problem also determines what type of iterative procedure one needs to implement to effectively arrive at a solution. Different algorithms are suited for a certain size

of a problem, making it an essential property to keep in mind when designing a solver for a given problem.

2.4.1 Necessary conditions for a global minimum

[87] defines a nonlinear optimal control program as follows:

$$\begin{aligned} &\min f(x), \\ &\text{s.t. } h(x) = 0, \\ &\quad g(x) \leq 0, \\ &\text{where} \\ &\quad x = (x_1, ..., x_n^T) \in \Re^n, \\ &\quad f(\cdot) : \Re^n \Rightarrow \Re^1, \\ &\quad g(x) = (g_1(x), ..., g_m(x))^T : \Re^n \Rightarrow \Re^m, \\ &\quad h(x) = (h_1(x), ..., h_q(x))^T : \Re^n \Rightarrow \Re^q \end{aligned} \tag{79}$$

x_i for $i \in 1, 2, ..., n$ are the decision variables, $f(x)$ is the objective function, $h(x) = 0$ are the equality constraints and $g(x) \leq 0$ are the inequality constraints. Furthermore, the feasible region is defined as $X \equiv x : g(x) \leq 0, h(x) = 0 \subset \Re^n$. A global minimizer for this scheme is defined as $x^* \in X$ and $f(x^*) \leq f(x)$ for all $x \in X$.

In the case of a constrained optimal control problem, the necessary conditions for a minimum means the fulfillment of the Karush-Kuhn-Tucker (KKT) conditions. Defining the Lagrangian:

$$L(x, \lambda, \mu_0, \mu) \equiv \mu_0 f(x) + \lambda^T h(x) + \mu^T g(x) \tag{80}$$

where μ_i and λ_j for i $\in 1, 2, ..., m, j \in 1, 2, ..., l$ are the Lagrangian multipliers, and μ_0 is the weight parameter for the cost function f. m and l are the number of inequality constraints and equality constraints, respectively. From this we get the gradient of the Lagrangian, and in the end, the KKT-conditions

$$\begin{aligned} \Delta f(x^*) + \sum_{i=1}^{m} \mu_i \Delta g_i(x^*) + \sum_{i=1}^{l} \lambda_i \Delta h_i(x^*) = 0, \\ h_j(x^*) = 0, \quad \text{for } j \in [1, l], \\ g_i(x^*) \leq 0, \quad \text{for } i \in [1, m], \\ \mu_i g_i(x^*) = 0 \quad \text{for } i \in [1, m], \\ \mu_i \geq 0 \quad \text{for } i \in [1, m] \end{aligned} \tag{81}$$

where x^* is a local minimum of the feasible region. For global optimality, these conditions are sufficient in the case of convexity in the objective function, and in the feasible region.

From [87], the definition of convexity lies in the positive semidefiniteness of the Hessian of the objective function. For the objective function $f(x)$, with continuous second partial derivatives, convexity is proven over a certain region if and only if its hessian matrix

$$\begin{bmatrix} \frac{\partial^2 f}{\partial x_1^2} & \frac{\partial^2 f}{\partial x_1 \partial x_2} & \cdots & \frac{\partial^2 f}{\partial x_1 \partial x_n} \\ \frac{\partial^2 f}{\partial x_2 \partial x_1} & \frac{\partial^2 f}{\partial x_2^2} & \cdots & \frac{\partial^2 f}{\partial x_2 \partial x_n} \\ \vdots & \vdots & \ddots & \vdots \\ \frac{\partial^2 f}{\partial x_n \partial x_1} & \frac{\partial^2 f}{\partial x_n \partial x_2} & \cdots & \frac{\partial^2 f}{\partial x_n^2} \end{bmatrix} \tag{82}$$

is positive semi definite.

In the case of Discrete-Time optimal control, [87] shows that applying the KKT conditions (81) leads to the discrete version of Pontryagin's minimum principle. The general problem takes the form of

$$\min Z(X,U) = \Psi(x_q) + \sum_{t=0}^{q-1} F_t(x_t, u_t), \tag{83}$$

subject to

$$\begin{aligned} h(x_t, x_{t+1}) = -x_{t+1} + x_t + f_t(x_t, u_t) = 0 \quad (\tau_{t+1}) \quad t = 0, 1, ..., q-1, \\ g_t(u_t) \leq 0 \quad (\lambda_t) \quad t = 0, 1, ..., q-1, \\ \Phi_0(x_0) = 0 \quad (\rho_0), \\ \Phi_q(x_q) = 0 \quad (\rho_q) \end{aligned} \tag{84}$$

where X and U constitute the entire trajectories of x_t and u_t from $t = 0$ to $t = q$. The first constraint represents the discretized state equations. The corresponding parameters representing each constraint is in parentheses. This gives the Lagrangian

$$\begin{aligned} L(X, U, \rho, \tau) =& \Psi(x_q) + \sum_{t=0}^{q-1} F_t(x_t, u_t) + \rho_0 \Phi(x_0) + \rho_q \Phi_q(x_q), \\ &+ \sum_{t=0}^{q-1} \tau_{t+1}^T (-x_{t+1} + x_t + f_t(x_t, u_t)) + \sum_{t=0}^{q-1} \lambda_t^T g_t(u_t) \end{aligned} \tag{85}$$

and setting $\nabla_x L(X, U, \rho, \tau) = 0$ gives

$$\begin{aligned} \frac{\partial L}{\partial x_0} = \frac{\partial F_0}{\partial x_0} + \rho_0 \frac{\partial \Phi_0}{\partial x_0} + \tau_1^T + \tau_1^T \frac{\partial f_0}{\partial x_0} = 0, \\ \frac{\partial L}{\partial x_t} = \frac{\partial F_t}{\partial x_t} - \tau_t^T + \tau_{t+1}^T + \tau_{t+1}^T \frac{\partial f_t}{\partial x_t} = 0, \end{aligned} \tag{86}$$

Furthermore, defining

$$\tau_0 = -\left[\frac{\partial \Phi_0}{\partial x_0}\right]^T \rho_0 \tag{87}$$

gives the necessary conditions:

$$
\begin{aligned}
\text{Equations of motion}: &\ x_{t+1} = x_t + f_t(x_t, u_t), \quad t = 0, 1, ..., q-1, \\
\text{Initial conditions}: &\ \Phi(x_0) = 0, \\
\text{Terminal conditions}: &\ \Phi(x_q) = 0, \\
\text{Control constraints}: &\ u_t \in u : g_t(u_t) \leq 0 \subseteq R^r \ t = 0, 1, ..., q-1, \\
\text{Adjoint equations (1)}: &\ \tau_0 = \tau_1 + \left[\frac{\partial f_0}{\partial x_0}\right]^T \tau_1 + \nabla_{x_0} F_0, \\
\text{Adjoint equations (2)}: &\ \tau_t = \tau_{t+1} + \left[\frac{\partial f_t}{\partial x_t}\right]^T \tau_{t+1} + \nabla_{x_t} F_t \quad t = 1, ..., q-1, \\
\text{Transvertality condition}: &\ \tau_q = \nabla_{x_q} \Psi + \left[\frac{\partial \Phi_q}{\partial x_q}\right]^T \rho_q, \\
\text{Stationarity condition for the controls}: &\ \nabla_{u_t} \Bigg[\sum_{t=0}^{q-1} F_t(x_t, u_t) + \sum_{t=0}^{q-1} \tau_{t+1}^T (-x_{t+1} + x_t + f_t(x_t, u_t)) \\
&\quad + \sum_{t=0}^{q-1} \lambda_t^T g_t(u_t) \Bigg] = 0
\end{aligned}
\tag{88}
$$

where $x_t \in R^n$, $u_t \in R^r$, x_0 is the initial condition, x_q is the terminal condition and q is the number of time steps. $\Phi_0 : R^n \to R^{m_0}$ and $\Phi_q : R^n \to R^{m_q}$, make up the initial and terminal conditions. τ_t is called the adjoint vector. ∇ represents the gradient of an expression with respect to the given subscript. Pontryagin's minimum principle comes by defining the Hamiltonian:

$$
H_t(x_t, \tau_{t+1}, u_t) \equiv F_t(x_t, u_t) + \tau_{t+1}^T f_t(x_t, u_t) \quad t = 0, ..., q-1 \tag{89}
$$

This allows for the reformulation of the state and adjoint equations as

$$
\begin{aligned}
x_{t+1} - x_t &= \nabla_{\tau_{t+1}} H_t(x_t, \tau_{t+1}, u_t), \\
\tau_{t+1} - \tau_t &= -\nabla_{x_t} H_t(x_t, \tau_{t+1}, u_t) \quad t = 0, ..., q-1
\end{aligned}
\tag{90}
$$

In light of this, the stationarity conditions for the optimal control from (88) can be restated as

$$
\begin{aligned}
\nabla_{u_t} [H_t(x_t, \tau_{t+1}, u_t) + \sum_{t=0}^{q-1} \lambda_t^T g_t(u_t)] = 0, \\
\lambda_t^T g_t(u_t) = 0 \quad \lambda_t \geq 0 \quad t = 0, ..., q-1
\end{aligned}
\tag{91}
$$

The system (91) are the necessary conditions for statically minimizing the Hamiltonian with respect to the controls under the assumption that all other variables are held fixed. Restating this as

$$
H_t(x_t, \tau_{t+1}, u_t^*) \leq H_t(x_t, \tau_{t+1}, u_t) \quad t = 0, ..., q-1 \tag{92}
$$

for all feasible control inputs u_t. This is Pontryagin's minimum principle. The optimal solution u_t^* globally minimizes the hamiltonian.

2.4.2 Optimisation algorithms

The properties of the problem has to be inserted into the framework of an algorithm in order to be solved. [84] presents the building blocks for such algorithms. The authors derive optimality conditions that characterize solutions for general constrained optimization problems like (79). The theory put forth in [84] culminates in algorithms which are all iterative in nature, and seeks to tend toward local solutions of the problem (79). The authors states that one of the main challenges in solving nonlinear programming problems is dealing with inequality constraints, and deciding which of these constraints are active at the solution and which are not.

Active set methods are designed to solve this. The approach consists of starting off with a guess of the optimal active set A^*, where A^* is the set of constraints that are satisfied as equalities at a solution. This guess, called the working set (W). The next step is to solve an optimisation problem in which the constraints in the working set are imposed as equalities and the constraints not in W are ignored. Checking to see if there is a choice of Lagrange multipliers such that the solution x^* obtained for the current W, satisfies the KKT conditions ((81)). Otherwise, a different guess for W is made, and the process is repeated.

The number of working sets W may rise to 2^I, where I is the number of inequality constraints. This can be explained by combinatorics, because each constraint represents two possibilities; either including it, or excluding it from W. This may potentially lead to an exponential increase in possible sets W, which in turn puts demands on the computational ability at hand. This phenomenon is referred to as the 'combinatorial difficulty' of nonlinear programming. The authors advises against designing algorithms that considers all choices for W. Active set methods might utilise the functions defining the problem, and exclude choices for W. Having enough knowledge about the functions and their derivatives, might aid in excluding guesses which leads to points in the space spanned by the optimization variables, which are infeasible, or for some other reason, obviously does not represent a solution. Another approach, which is called interior-point methods, generate iterates that stay away from the boundary of the feasible region defined by the inequality constraints. As the solution of the nonlinear program is approached, the barrier effects are weakened to permit an increasingly accurate estimate of the solution. Active-set methods are effective for small- and medium sized problems ([84]).

Sequential quadratic programming (SQP) is suitable for constrained nonlinear programs, solving general nonlinear problems and honors bounds at all iterations [88]. Such methods model the (79) by a quadratic programming sub problem at each iterate and define the search direction to be the solution of this sub problem ([84]). In the basic SQP method, we define the search direction p_k at the iterate (x_k, λ_k) to be the solution of

$$\begin{aligned} \min_p \frac{1}{2} p^T \Delta^2_{xx} \mathcal{L}(x_k, \lambda_k) p + \Delta f(x_k)^T p \\ \text{subject to } \nabla c_i(x_k)^T p + c_i(x_k) = 0, \quad i \in \varepsilon, \\ \nabla c_i(x_k)^T p + c_i(x_k) \geq 0, \quad i \in I, \end{aligned} \tag{93}$$

where $\mathcal{L}$ is the Lagrangian function defined in (80). According to [84], SQP algorithms show their strength when solving problems with significant nonlinearities in the constraints.

3 Modeling the remaining anaerobic capacity

3.1 Linear model across entire domain

The simplest model of the remaining anaerobic capacity, is one linear in the difference between input power u and CP, based on (22), and the work of [45] (and utilised in [53] to find optimal pacing strategy):

$$\begin{aligned} \frac{dw}{dt} &= CP - u, \\ \Rightarrow w(t) &= w(0) + (CP - u) * t \end{aligned} \tag{94}$$

An obvious limitation at first glance, is the sum of $w(0) + (CP - u) * t$. For $u < CP$, the w is in recovery, and would add even more capacity to its "storage". The absolute maximum anaerobic capacity is AWC. This upper bound must therefore be implemented in other ways in order to represent the physiologically correct scenario. In an optimisation framework, this is no problem, as upper and lower bounds are needed anyways. However, a proposed model containing the upper limit of $w_{max} = AWC$ implicitly, might be preferable, in order to safeguard against any potential numerical errors (or errors as a result of erroneous implementation of the w-dynamics).

Using this model, both recovery and expenditure of the remaining w develops in time in the same, linear rate (linear in power). At the onset of severe intensity coming from an intensity below (as marked by the known parameter CP) the cyclist will start to expend anaerobic capacity, and this shift occurs instantaneously at this level if input power. This means that at exactly CP, one would be able to achieve an infinite endurance. This is, as previously mentioned, a major simplification. CP denotes a border separating the heavy and severe intensity power domains. A more realistic representation would perhaps not allow for recovery of the anaerobic capacity right up to just below this border. This border is more likely to be an interval, or a smooth transition from recovery to expenditure.

However, the simplification can be justified for a number of reasons. Firstly, when used to simulate simpler (less variations in the inclination of the track over a longer segment) the fine details of the dynamics of w are not as important to capture entirely. It would suffice only to capture raw features of the rate of change of w. In the case of the w recovering or expending non-realistic levels of capacity around the borders of CP, a possible solution could be to simply adjust the constraints setting the bounds of what values the input (u) is able to have during those specific segments on the track.

The conditional model (23) presented in [4] and, represent an attempt at differentiating the recovery domain ($u < CP$) from the expenditure domain ($u \geq CP$). Therefore, it is possible to also alter the model in a way that probably fits physiological reality better. However, this calls for additional parameter estimation, which means additional experimental work, in order to determine the values of the parameters. Another slightly problematic aspect to this approach, is the fact that a conditional statement would have to be implemented. This, in turn, could lead to non-convexity of the optimisation problem, due to the binary property of the conditional statement.

3.2 Nonlinear recovery

Research points to a more complex situation, especially in terms of the recovery of the capacity ([57], [89]), as several studies argue for a nonlinear nature of the recovery dynamics. At first glance, this might suggest that the two processes (expenditure and recovery) should be viewed as two separate systems. This might be justified, however, one should not remiss the fact that they operate on the same variable, and are both affected by the input power, somehow. The different variants of nonlinear recovery models present different properties both in terms of how to implement them, and in terms of the physiological interpretation.

The model for nonlinear recovery of w ((28)) proposed by [66], assumes an already expended amount of energy being recovered back to the state variable $w(t)$. This hints at the possibility of a first-order ordinary differential equation describing the state dynamics of the anaerobic capacity. In order to uncover this equation, one has to trace it back from the integral presented in (28). But before this trace-back, certain assumptions have to be made. The most obvious shortcomings of the mono-exponential model, are listed as follows:

1. The already expended energy is assumed known, and is not meant to be continuously updated, rather extracted from a data set having already recorded the power output of a cyclist

throughout a physical exercise, thereby calculating the estimated recovery and expenditure of the remaining anaerobic energy post-exercise

2. The time-constant which governs the rate of recovery, which depends on the power level, will also be calculated post-exercise, and the power level used in the parameter is set as the average power level below CP through the recovery period

Analyzing the integral from (28) helps shed light on its properties. w_{exp} is the expended energy when the cyclist had $u > CP$, and $\tau_w = \tau_w = 546e^{-0.01D_{CP}} + 316$ is the time constant of the recovery. $(t - l)$ is the time spent below CP, resulting in the reconstitution of $w(t)$.

$$w(t) = AWC - \int_w^t W_{exp} e^{-\frac{t-l}{\tau_w}} dl \tag{95}$$

In terms of tracing this solution of the state $w(t)$ back to its original dynamic equation, some questions arises regarding the possibility of this; firstly, is it possible to find an expression for w_{exp} by using known variables and parameters? And how does one interpret the variable D_{CP}? The variable w_{exp} is problematic, due to the fact that it is used as an estimated value after-the-fact in the model (28). This means that the model does not help in describing the expenditure, and leaves this as a case of itself. Therefore, some mathematical unity between expenditure and recovery will have to be developed in order to represent both in one dynamic equation.

However, the behaviour of $\frac{dw}{dt}$ during expenditure ($u > CP$) and recovery ($u < CP$) have shown through experiments and research to be different. The model of recovery always seeks to want to reach the value AWC, and therefore acts with a fixed-point reference. The expenditure model, on the other hand, acts with a free trajectory, dependent on the level of $u > CP$. The latter does have a constraint in that $w(t) \geq 0$, but is not affected directly by the current level of $w(t)$. It is, however, affected by the state $w(t)$ in the constraint setting the maximum level of attainable power P_{max}. This means that there is an lower bound for the time it takes to empty all remaining w. But the rate of negative change of the remaining capacity can potentially be much greater than the rate of positive change.

[90] presents mathematical theory useful for formulating differential equations which gives rise to time responses. The author defines the first-order linear differential equation as

$$\frac{dy}{dt} + a(t)y = 0 \tag{96}$$

This differential equation is homogeneous (equal to zero). The solution of the equation is obtained by integrating both sides of (96) between t_0 and t:

$$\begin{aligned}
\int_{t_0}^t \frac{d}{ds} ln|y(s)| ds &= -\int_{t_0}^t a(s) ds, \\
ln|y(t)| - ln|y(t_0)| = ln\left|\frac{y(t)}{y(t_0)}\right| &= -\int_{t_0}^t a(s) ds, \\
\Rightarrow \left|\frac{y(t)}{y(t_0)} exp\left(\int_{t_0}^t a(s) ds\right)\right| &= 1, \\
\Rightarrow y(t) = y_0 exp\left(-\int_{t_0}^t a(s) ds\right)&
\end{aligned} \tag{97}$$

Non-homogeneous differential equations (in the format of an IVP) takes the general form

$$\frac{dy}{dt} + a(t)y = b(t), \quad y(t_0) = y_0 \tag{98}$$

which can be interpreted as $\frac{d}{dt}$("an expression") $= b(t)$. The authors of [90] argues this to be a logical interpretation in light of the method of solving the homogeneous equation (97). The authors choose to introduce a term $\mu(t)$, representing a continuous function which, by multiplying both sides of (98).

$$\mu(y)\frac{dy}{dt} + a(t)\mu(t)y(t) = \mu(t)b(t) \tag{99}$$

In doing so, the goal is to choose a $\mu(t)$ so that $\mu(t)(dy/dt) + a(t)\mu(t)$ is the derivative of some simple expression. Observing that

$$\frac{d}{dt}\mu(t)y = \mu(t)\frac{dy}{dt} + \frac{d\mu}{dt}y \tag{100}$$

Hence, $\mu(t)(dy/dt) + a(t)\mu(t)y$ will be equal to the derivative of $\mu(t)y$ if and only if $d\mu(t)/dt = a(t)\mu(t)$. But this is a first order linear homogeneous equation for $\mu(t) \Rightarrow (d\mu/dt) - a(t)\mu = 0$, which has a known solution (setting $\mu_0 = 1$):

$$exp\bigg(\int a(t)dt\bigg) \tag{101}$$

Which yields

$$\begin{aligned}
\frac{d}{dt}\mu(t)y &= \mu(t)b(t), \\
\mu(t)y &= \int \mu(t)b(t)dt + c, \\
\Rightarrow y &= \frac{1}{\mu(t)}\bigg(\int \mu(t)b(t)dt + c\bigg), \\
&= exp\bigg(-\int a(t)dt\bigg)\bigg(\int \mu(t)b(t)dt + c\bigg)
\end{aligned} \tag{102}$$

This means, that for an IVP such as (98), the solution becomes

$$y = \frac{1}{\mu(t)}\bigg(\mu(t_0)y_0 + \int_{t_0}^{t} \mu(s)b(s)ds\bigg) \tag{103}$$

In the words of the authors [57], the amount of w remaining at any time t (expressed here as $w(t)$) is equal to the difference between the known w (equal to AWC) and the total sum of the joules of the w expended before time t in the exercise session, each joule of which is being recharged exponentially during recovery ($u < CP$). A proposed dynamic equation for a mono-exponential recovery of $w(t)$ back to its steady state AWC (where u is the power output of the cyclist), could be

$$\begin{aligned}
\dot{w}(t) &= \frac{1}{\tau_w}(AWC - w(t)), \\
\tau_w(u) &= 546 * e^{0.01D_{CP}} + 316, \\
w(t_0) &= w_0,
\end{aligned} \tag{104}$$

In this framework, u will not be considered as a time-varying variable. This leads to $D_{CP} = u - CP$ simply being passed on as the same expression into the equation, and interpreted as a fixed value for some time interval $[t_0 \quad t]$. Expanding on this proposed model, and finding the solution as in (103), means expressing (104) as

$$\begin{aligned} \dot{w} &= \frac{1}{\tau_w}(AWC - w), \\ &= \frac{AWC}{\tau_w} - \frac{w}{\tau_w}, \\ &= b(t) - a(t)w, \\ \Rightarrow &= \mu(t) = exp\left(\int a(t)dt \right) = e^{\frac{t}{\tau_w}} \end{aligned} \tag{105}$$

which, in turn, results in the proposed time-varying solution

$$\begin{aligned} w_p(t) &= \frac{1}{\mu(t)} \left(\mu(t_0)y_0 + \int_{t_0}^{t} \mu(s)b(s)ds \right), \\ &= e^{-\frac{t}{\tau_w}} \left(w_{p,0} + \int_{t_0}^{t} \frac{AWC}{\tau_w} e^{\frac{s}{\tau_w}} ds \right), \\ (\text{For } t_0 = 0) &= e^{-\frac{t}{\tau_w}} \left(w_{p,0} + \frac{AWC}{\tau_w}(\tau_w(e^{\frac{t}{\tau_w}} - 1)) \right), \\ &= w_{p,0}e^{-\frac{t}{\tau_w}} + e^{-\frac{t}{\tau_w}} AWC(e^{\frac{t}{\tau_w}} - 1), \\ &= AWC - (AWC - w_{p,0})e^{-\frac{t}{\tau_w}}, \\ w_{p,0} &= AWC * q, \quad 0 \leq q \leq 1, \\ \Rightarrow w_p(t) &= AWC(1 - (1 - q)e^{-\frac{t}{\tau_w}}) \end{aligned} \tag{106}$$

where q represents the amount of w left at time t, relative to the individualized value AWC. Referring back to the solved integral (95), the solution of the proposed dynamics (106) shows similar properties. Both models approach the value of AWC. Both operate with the time constant τ_w as the defining property of the exponential dynamics. However, as the former model treats this as a fixed value for a given recovery power u_rec, the latter model will treat this as a function $\tau_w(u)$, where $0 \leq u \leq P_{max}$. This means that the larger the value of $u < CP$, the slower the rate of recovery of the anaerobic capacity will happen. The solution shown at the last line in (106), strongly resemble the solution derived from chemical kinetics by the authors of [58], in (27).

In order to get a broader overview of the proposed model (104), a contour plot and a 3D-plot shows the rate of change of $w(t)$, i.e. $\frac{d}{dt}w(t)$, across the domains of $0 \leq w(t) \leq AWC$ and $0 \leq u \leq CP$. Values for physiological parameters are set to $CP = 250w, AWC = 10kJ$:

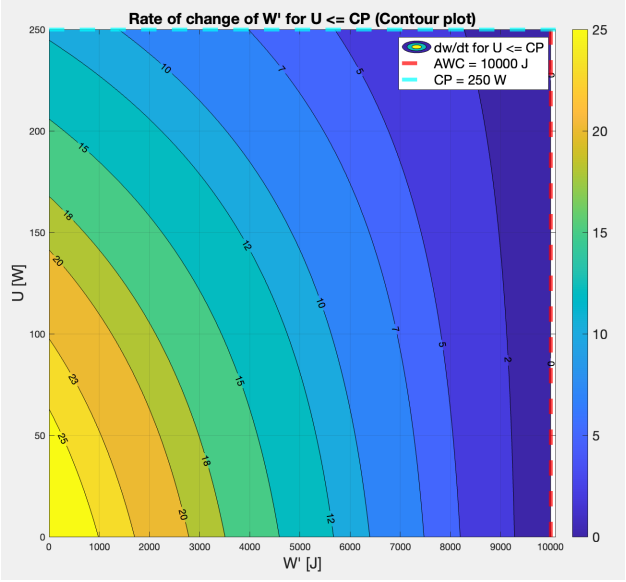

Figure 9: A contour plot showing the rate of change of $w(t)$ with respect to the variables u and w.

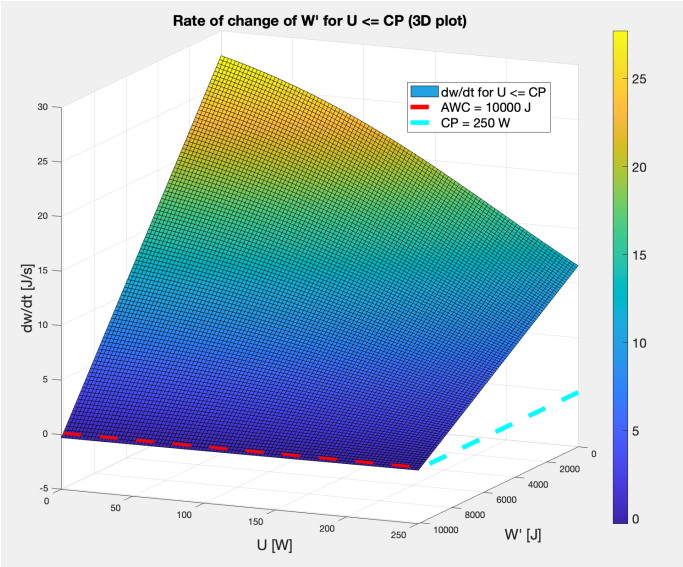

Figure 10: A 3D plot showing the rate of change of $w(t)$ with respect to the variables u and w.

Figure 9 shows the rate of change increasing as $u, w \Rightarrow 0$. This means that the recovery of W' will be fastest when the cyclist's anaerobic capacity is completely empty. An increasing positive rate of change for a decreasing input power u is in line with the findings of [57] and [89]. However, a discussion could be had about whether $\frac{d}{dt}w(t)$ increases at the rate it does in Figure 9, when $w \Rightarrow 0$.

The question arises, as to how one unifies the expenditure and the recovery of w. A possible solution, is through the use of hyperbolic tangent-functions, activating the expressions for expenditure, and recovery when input power is over, and under CP, respectively. This happens gradually, as the hyperbolic tangent-functions are continuous expressions. A proposed setup would be for each metabolic category (anaerobic and aerobic) having its own expression, activating its respective dynamic equation as input power passes the point of CP. This means anaerobic being activated when $u > CP$, and aerobic being activated for $u < CP$. The expressions take the form:

$$\begin{aligned} \text{Anaerobic term: } & \frac{1}{2}\Big(1 + tanh((D_{CP} + \beta_{an})/T_{an})\Big) \\ \text{Aerobic term: } & \frac{1}{2}\Big(1 - tanh((D_{CP} + \beta_{a})/T_{a})\Big) \end{aligned} \tag{107}$$

where $D_{CP} = u - CP$, T_a and T_{an} are "wideness" parameters defining the rate of change of the respective expressions, and β_{an}, β_a are constant, contributing to the metabolic terms shifting to their respective power domains. There is a question of whether the two terms should increase in magnitude equally fast, or if they should reach their steady states at an equal distance away from the vertical line of $u = CP$. For the aerobic term, for instance, the reconstitution (recharging) of w must not take place for any $u > CP$. Discussions in Section 2.2.5, where methods of determining CP showed a tendency to overestimate the actual threshold [50], also supports this idea. Any over-contributing factor of recovery might render the model to predict the cyclists power generation capabilities to be too high.

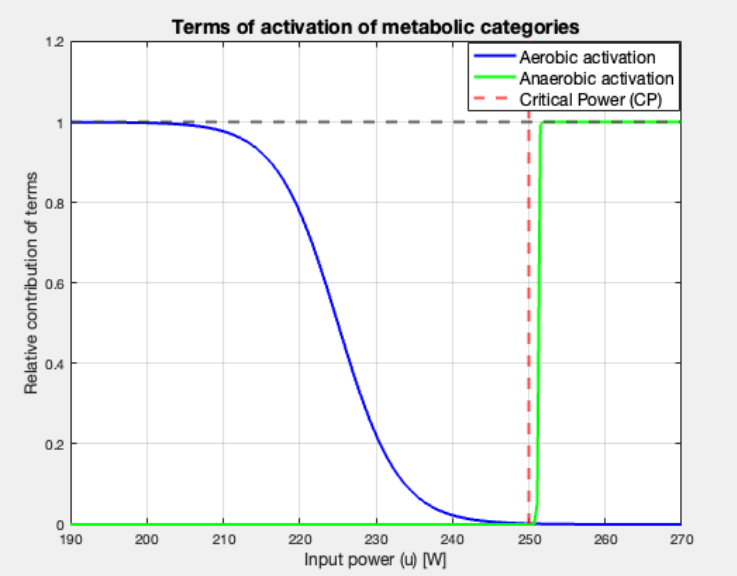

Figure 11: Term multiplied with equation of recovery of w(t) in blue, and term multiplied with equation for expenditure in green.

In Figure 11, an example is shown for the activation terms, for $T_a = 8, T_{an} = 0.1, \beta_a = CP*0.1W, \beta_{an} = CP*0.005$. The proposed parametric values shown in Figure 11 also mimicks the dominating metabolic categories across the power domain, shown in (Figure 5). In this framework, the so-called "aerobic" and "anaerobic" terms would not accurately represent the contribution to metabolism, rather the part of the power domain during which the aerobic contribution is the dominating one, compared to anaerobic contribution. A proposed resulting model in terms on mono-exponential recovery (in time t) and linear expenditure (in input power u) of the remaining anaerobic capacity $w(t)$.

Variables and Parameters:
w : Remaining anaerobic capacity at time t, in joules,
AWC : Anaerobic working capacity, in joules,
u : Input power, in watt,
CP : Critical power, in watt,

Dynamic equation:
$\dot{w} = \frac{A}{\tau_w} * w_{exp} - A_n * D_{CP}$,
where $w_{exp} = AWC - w(t)$, and $D_{CP} = u - CP$,

Hyperbolic functions:
$A_n = \frac{1}{2} * (1 + tanh(\frac{D_{CP} - \beta_{an}}{T_{an}}))$,
$A = \frac{1}{2} * (1 - tanh(\frac{D_{CP} + \beta_a}{T_a}))$,
where T_a and T_{an} are the "wideness" parameters of the aerobic
and anaerobic contribution in the dynamic equation,
respectively, across the power domain,
$\beta_{an} and \beta_a$ are offset,
parameters, shifting the terms to,
their respective power domains, (108)

Time constant of recovery:
$\tau_w(u) = 546 * e^{0.01 D_{CP}} + 316$,

Time response of the system:
$u > CP \Rightarrow w(t) = AWC - D_{CP} * t$,
$u \approx CP \Rightarrow w(t) = AWC + \frac{A_n * D_{CP} * \tau_w(u)}{A} - \frac{w_{exp}}{A} * e^{-\frac{A*t}{\tau_w(u)}}$,
$u < CP \Rightarrow w(t) = AWC - w_{exp} * e^{-\frac{t}{\tau_w(u)}}$

In order to model the transitional dynamics of a final model involving both terms, the dynamics of the proposed model in (108) are simulated and visualised for $u \in [230, 270]$, where $CP = 250W$ and $AWC = 10kJ$. For the proposed values giving the activation terms in Figure 11, the plot of the response of $\dot{w} = \frac{dw}{dt}$ is shown in Figure 12 (3D-plot) and Figure 13 (contour-plot).

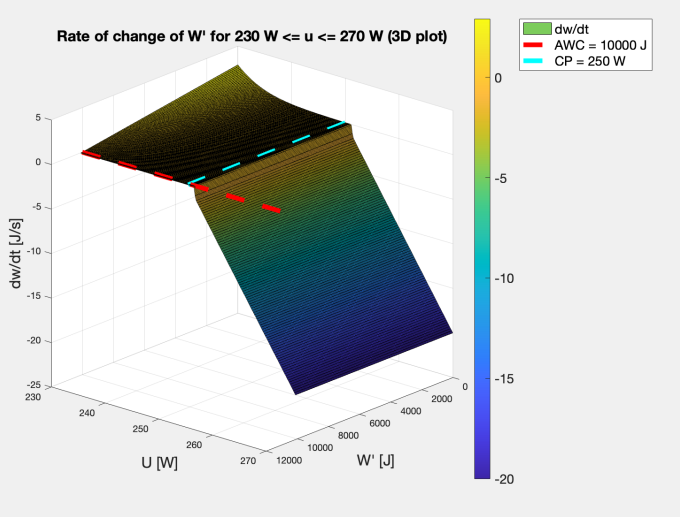

Figure 12: 3D plot of the response of $\frac{dw}{dt}$ for $u \in [230, 270]W$

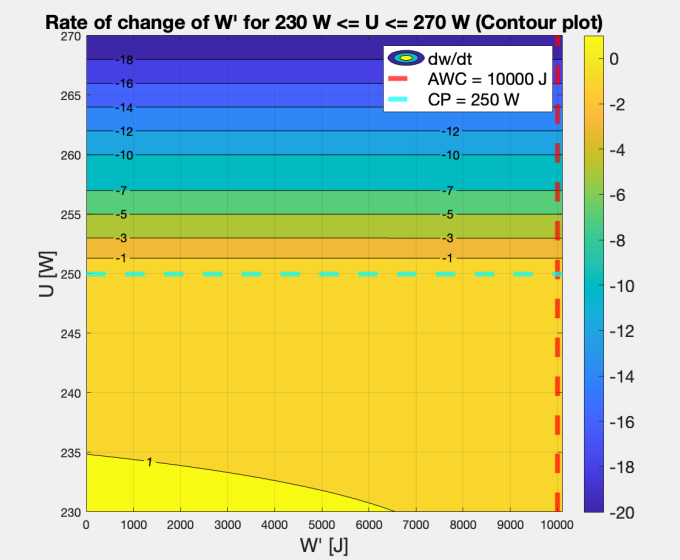

Figure 13: Contour plot of the response of $\frac{dw}{dt}$ for $u \in [230, 270]W$

An observation to note, is the relatively large area of the domain of power output below CP during which the recovery is slow or non-existent. Such a design of a combined recovery and expenditure model, might be motivated by suggestions which points towards the possibility of the critical power acting more as an interval, than as a line in the power domain ([20]). Combined models of expenditure and recovery are scarce (as discussed in [91]), but under the assumption that the two models should not instantly shift the moment critical power is reached, the model presented in (108) and Figure 12 may be used to represent the time evolution of anaerobic capacity.

4 Design of the optimal program

4.1 Problem hierarchy

The longer an activity is, the less likely it is, that a model consisting of CP and AWC is going to be valid ([47]). Therefore, it is natural to focus on shorter duration (30-60 minutes) when looking at relevant cases for this project. During a run-through of a typical TT course, there would be

periods of no change in elevation, to periods of the opposite (or turns, for instance, in the case of adding an extra dimension). This fluctuation of external disturbance on the system (in the form of inclination in the track) means that the use of optimisation theory and techniques would only be necessary during parts of the track. In other words, the actual optimisation problems appears only a few times during the activity. Typically, a cyclist will only have to design a pacing trajectory during certain specific situations in a TT. Examples of these are areas of steep uphill segments, followed by a downhill segment, or flat segments followed by an uphill run. During situations like these, the exact timing of the increase in power output (in the case of the flat-uphill), or the timing of the decrease in power output (in the case of the uphill-downhill).

In this framework of energy distribution, a hierarchy of problems might render itself useful in order to limit the amount of simulation or function evaluations during a typical case of nonlinear optimisation. To build on the framework, one could semantically name the upper level of the hierarchy, the "strategy" of distributing the available energy resources across the track. The lower level of the hierarchy could be named the "tactics" of pacing the power output in a smaller situation. The simulation of the dynamics describing both the mechanical and physiological states in the system contributes in setting up boundaries and possibilities in regards to how one should model the system when dealing with each of these levels in the hierarchy. The step size of the system will determine the accuracy, and the accuracy, in turn depends on the type of situation the cyclist is currently in. If they are cycling on a flat segment for 500 m, and have yet to expend any energy, the system dynamics may be strongly simplified (or possible even neglected) for this segment. The complex dynamics underlying recovery of w during the exercise may become more important during the lower level situations previously mentioned.

The strategic level of optimisation would simply act as a set of constraints on the evolution of w through the track. The design of these constraints would be based upon the shape of the track, and the frequency of situations where tactical pacing would be necessary. An example would be a track starting with a long flat segment, followed by a small uphill segment, a small downhill segment and ending with a longer flat segment. With the objective demand of minimizing the time spent along the course, the upper level of the hierarchy of optimisation would put constraints upon the w at the start, then somewhere before the uphill segment, atop the hill, at the bottom of the hill, and at the very end. Another design of these constraints could see the upper level only constraining the w at the start, and finish of this entire episode. If several small episodes like this occurs throughout the track, the tactical pacing would be more like the aforementioned constraint-setting, whereas the strategic pacing would be the combination of several situations like these, with constraints set on stats at the start- and finish-points for all of them.

The accuracy of the time evolution of the states, and the total duration of the activity, do not really matter for the upper level problem. The goal of the upper level is to produce a feasible solution, respecting the constraints set by the program design, and result in a decrease in total time spent during the track. In so doing, the energy is distributed across the most important points on the track, and the lower level problems has a reference for the energy available at these points. Therefore, the error associated with leaving out exact dynamics in the shift from one segment to another, would not be important. The difficulty for a cyclist of following power level instructions accurately, motivates the design of the optimal program to mostly consider larger distance steps in general.

4.2 Dynamic models

In order to simplify the optimization program to a satisfying level, where most doubts over whether the program will be solved are removed, one could insist on the dynamic models describing the states to be continuous in their nature. This means, no conditional statements leading to non-smooth functions, like the dynamic equation describing the rate of change of w in [4]. The model consisting of the state equation for w (108), provides one single, continuous mathematical expression for the dynamics of this variable. However, this might only be useful in certain situations describing smaller segments with a smaller step size (measured in distance).

The conditional statements (if(true statement) $\Rightarrow$ then(switch dynamics)) can be avoided

using a type of term which was discussed in Section 3. A model which both describes expenditure and recovery dynamics, uses these terms to phase in, and phase out the equations describing the two processes, thereby gathering them into one equation. This was demonstrated in Section 3. In order to simulate the states for the overarching energy distribution problem, it is beneficial to develop expressions for the steady-state responses of the system. Possessing the state equation for velocity (16), the steady state response was found setting $\frac{dv}{dt} = 0$, and solving for the steady-state velocity v_{ss}. u is input power, and θ is the inclination on the segment.

$$-d * v_{ss}^3 - [b * sin(\theta) + c * cos(\theta)] * v_{ss} + a * u = 0 \tag{109}$$

Solving in MATLAB, using the function `roots(Sys)`, for the system parameters $Sys = [-d \quad 0 \quad -B_t \quad a * u]$, solving for v_{ss} in $-d * v_{ss}^3 + 0 * v_{ss}^2 - B_t * v_{ss} + a * u$, gives the roots to the equation, where $B_t = b * sin(\theta) + c * cos(\theta))$. However, these run the risk of having imaginary parts. In an optimal program of little varying elevation, the input power (measured in watt) can be thought to be constrained to a small range $[CP - \beta, CP + \beta]$, where β is a constant. Also, it is reasonable to consider only inclinations ranging from $45°$ to $-45°$ (downhill). Using all other aforementioned parameters $a, b, c, d, u = CP$, θ can vary in order to analyse the behaviour of the expression B_t. For $B_t < 0$, the first root in the output of `roots(Sys)` has an imaginary part equal to zero. For $B_t \geq 0$, the third root in the output is the one with an imaginary part equal to zero. Solving for θ:

$$\begin{aligned} B_t = bsin(\theta) + ccos(\theta) &= 0, \\ bsin(\theta) + bC_R cos(\theta) &= 0, \\ sin(\theta) &= -C_R cos(\theta), \\ tan(\theta) * cos(\theta) &= -C_R cos(\theta), \\ tan(\theta) &= -C_R, \\ \Rightarrow \theta &= atan(-C_R) + \pi n, \quad \text{for} \quad n = 0, 1, 2, ... \end{aligned} \tag{110}$$

We know that $\theta < \frac{\pi}{4} < \pi$ Therefore, $\theta \leq atan(-C_R)$ gives $B_t \leq 0$. One way to solve this is to simply iterate through the roots in the output of the MATLAB function, check for zero imaginary parts in them, and assign this value as the correct steady-state velocity for the segment, based on the current pair (u, θ). Another way of implementing the steady-state velocity, is to simply use the expression for the only root having no imaginary parts already in its expression. Looking at the output of the function `roots(Sys)`, shows the following relation for the real root:

$$\begin{aligned} &B(\theta) > 0, \\ &\Rightarrow v_{ss,R} = \left[\sqrt{\frac{B(\theta)^3}{27d^3} + \frac{(au)^2}{4d^2}} + \frac{au}{2d} \right]^{1/3} - \frac{B(\theta)}{3d \left[\sqrt{\frac{B(\theta)^3}{27d^3} + \frac{(au)^2}{4d^2}} + \frac{au}{2d} \right]^{1/3}}, \\ &B(\theta) < 0, \\ &\Rightarrow v_{ss,R} = \left[\sqrt{-\frac{B(\theta)^3}{27d^3} + \frac{(au)^2}{4d^2}} + \frac{au}{2d} \right]^{1/3} + \frac{B(\theta)}{3d \left[\sqrt{-\frac{B(\theta)^3}{27d^3} + \frac{(au)^2}{4d^2}} + \frac{au}{2d} \right]^{1/3}}, \\ &B(\theta) = 0, \\ &\Rightarrow v_{ss,R} = \sqrt[3]{\frac{au}{d}} \end{aligned} \tag{111}$$

where $v_{ss,R}$ is the potential real root of the system. The potential imaginary part arises within the square root $\sqrt{\frac{B(\theta)^3}{27d^3} + \frac{(au)^2}{4d^2}}$. The cubic roots will not give out an imaginary part if the expressions within them are negative. However, if the same is said for the square root, the opposite is true. The only parameter that has potential negative values is $B(\theta)$. Looking closer at the expression reveals that for $B(\theta) < 0 \Rightarrow \frac{B(\theta)^3}{27d^3} + \frac{(au)^2}{4d^2} > 0$. This means, that for all θ, the expression in (111) provides a real answer for the steady-state velocity.

One must also ensure that the answer is positive for $u > 0$ W at all times. For both $B(\theta) > 0$ and $B(\theta) < 0$ the problematic case is if the absolute value of the last fraction is larger than that of the first term in (111). Setting $Q = \frac{B(\theta)}{3d}$ and $H = \frac{au}{2d}$, the demand for a positive steady state velocity becomes visible.

$$\begin{aligned} \left(\sqrt{Q^3 + H^2} + H\right)^{1/3} - \frac{Q}{\left(\sqrt{Q^3 + H^2} + H\right)^{1/3}} \geq 0, \\ \left(\sqrt{Q^3 + H^2} + H\right)^{2/3} \geq Q \end{aligned} \tag{112}$$

Remembering that $u > 0$ W, and that all parameters except for $B(\theta)$ are positive, the expression $H > 0$. Also, the observation that $\sqrt{Q^3 + H^2} + H \geq Q^{3/2}$ proves that all solutions to the real root of the system results in a positive steady-state velocity. For instance, for the environmental parameters given in (20), and a rider of weight $m_r = 84kg$, height $h_r = 1.87m$, on a bike with mass $m_b = 9.25kg$ and wheel radius $R_w = 35cm$, riding in a time trial position ($C_d = 0.6$, Figure 3b) at a constant input power $u = 200W$ on a flat surface ($\theta = 0 \Rightarrow B(\theta)$), the steady state velocity would be 10.7 m/s $\approx$ 38.5 km/h.

Using steady-state velocity as an equality constraint for the velocity optimization variables across each segment on the track, simplifies the problem in a couple of ways. First, this automatically gives a maximum and minimum bound for the optimization variable of time across a segment (given the knowledge of the longest and shortest segment on the track). It also allows for the algorithm to forgo the cumbersome calculations associated with the complex dynamics that actually describes the state of velocity. It is a significant simplification, but only active over parts of the track where the optimizing of resource management is redundant.

A problematic aspect of using the mathematical expression for the steady-state velocity in an eventual implementation, is the fact that the two expressions for $B(\theta) < 0$ and $B(\theta) > 0$ are different in form. However, simulating different expressions for the steady-state velocity for $-pi/4 \leq \theta \leq pi/4$, shows that the function giving the most intuitive response is

$$v_{ss}(\theta, u) = \left[\sqrt{\frac{|B(\theta)|^3}{27d^3} + \frac{(au)^2}{4d^2}} + \frac{au}{2d}\right]^{1/3} - \frac{B(\theta)}{3d\left[\sqrt{\frac{|B(\theta)|^3}{27d^3} + \frac{(au)^2}{4d^2}} + \frac{au}{2d}\right]^{1/3}} \tag{113}$$

which coincides with the findings of (111). The expression of (113) gives the response

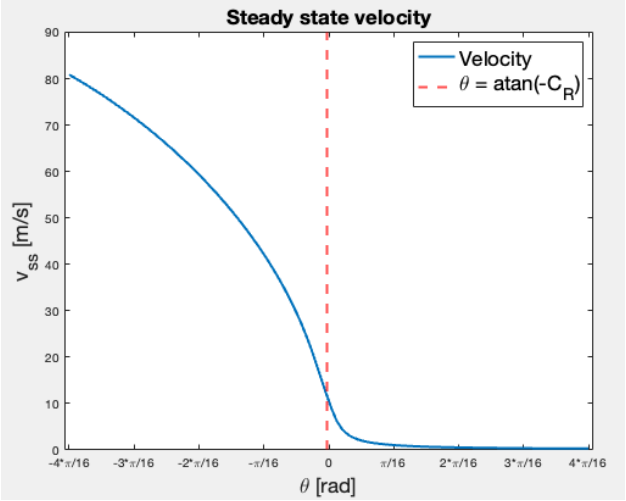

Figure 14: Plot of the expression from (113) for $-pi/4 \leq \theta \leq pi/4$

for a constant input power $u = CP = 192W$, and the parameters given in (20). Including the expression of absolute value results in non-smooth behaviour around the value of $\theta = atan(-C_R)$. A problematic consequence of this is that it might affect the feasibility of the solution. The equations (111) has behaviour could justify an equivalent model using binary variables in the form of absolute values for $B(\theta)$. This alters the nature of the optimal program, and might introduce binary variables. The fact that there is a non-smooth behaviour of the steady-state velocity around $B(\theta)$ also poses a danger for the continuity of the model. However, due to the fact that the optimal program being formulated is fundamentally a discrete one, this might have little effect. Also, it is the derivative of the term $B(\theta)$ with respect to θ, which will have an essential discontinuity on the interval $-\pi/4 \leq \theta \leq pi/4$. This term is not used in the implementation.

Another problematic aspect of the steady-state approach is if $u = 0$ W. This may allow for the value of the steady state velocity to reach 0. However, one is assured against this happening if the input power is constrained in some way, resulting in $u \neq 0$. This seems quite obvious, given that the power given into the bicycle by the cyclist is the only source the system relies on to traverse through the track. In addition, in light of a possible assumption mentioned earlier, one might constrain the input power to an interval $CP - \Delta U \leq u \leq CP + \Delta U$, where $\Delta U << CP$.

For the tactical situations describing a segment of significant alteration of the track, different dynamic models are needed. The reason for this is that these changes in external factors presents potentially huge implications for the pacing strategy of the cyclist. In close vicinity of the situation, the net change of w, namely Δw will be relatively large compared to the relatively short distance along the segments. Also, in relation to the entire time-trial optimization problem, these situations therefore play a huge role in the distribution of capacity throughout the run. The general idea of the splitting of the optimisation task into two different levels, is to solve the overarching problem of energy distribution using one set of constraints (describing the track as a whole), while solving another problem of optimal power input on the ergometer during short sprints using other constraints. This leads to the revelation that the sprint segment must be contained within segments of considerable change in inclination. This means that the entry into such a segment represents the end (or some point before the end) of a homogeneous part of the track (constant inclination), and the exit from such a segment represent the onset (or some point a bit after the onset) of a new, homogeneous segment. Therefore, the initial, and terminal conditions of the sprint optimisation problem is set to the values which were calculated from the energy optimisation. In this way, the sprint problem is constrained by the energy distribution, and the optimal solution from the sprint problem serves as a guide for the power trajectory during the sprint.

4.3 Nature of the problem

The problem at hand needs to be categorised in light of its properties (linearity, convexity, size and continuity, Section 2.4). Clearly, due to the equation of motion ((16)) of the bicycle/rider system, and the proposed model of (108), the problem is nonlinear. The dynamics will in the form of constraints make the problem a nonlinear one, while the objective function (for the simplest case) will be linear, as simply a sum of the time spent on all steps through the track. The size of the problem will vary with the discrete resolution of the track (in distance or time) and how detailed the dynamics are simulated through the setting of constraints. But no matter the resolution, the problem seems to be a medium- to -large sized one. A time trial, for instance, takes normally 20 minutes to 1 hour, making it necessary for quite a number of optimization variables (in the form of discrete steps for the states, time and input) to be implemented.

The problem is obviously discrete due to the dynamics being solved using numerical integration methods. This leads to the question of convexity. The definition of convexity given in [85], tells a story of "curvedness" of a function. For instance, an objective function being simply a sum of time duration of each small segment of distance on a discrete representation of the track, would be a convex objective function, because linear functions are both convex and concave (no curve equals curved both ways). However, the duration of each discrete segment would depend on the velocity (time = distance/velocity), resulting in a potential non-convex objective function. Checking for the non-convexity of the problem, the constraint set by the discrete dynamics are analyzed. For velocity, and an arbitrary solver, here the simplest Euler method (63), the constraint of one step-evolution of the state, is set as:

$$\begin{aligned} v_{k+1} &= v_k + h * dv(v_k, u_k, \theta_k) \\ &= v_k + h * (a * \frac{u_k}{v_k} - b * sin(\theta) - c * cos(\theta) - d * v_k^2) \\ \Rightarrow F_{vCon} &= v_{k+1} * v_k - (v_k)^2 - h * dv(v_k, u_k, \theta_k) = 0 \end{aligned} \tag{114}$$

for the optimization variables v_{k+1}, v_k, u_k (and an arbitrary step in the simulation k, where $k = 1, 2, 3, ...N - 1$, and N is the number of points in the array of points marking accumulated distance, starting at 0). Using MATLAB's function `hessian`, the hessian for the constraint defined by the last line (114) is found for the constraint function F_{vCon}:

$$\begin{bmatrix} 2d - \frac{2au}{v_k^3} & 0 & \frac{a}{v_k^2} \\ 0 & 0 & 0 \\ \frac{a}{v_k^2} & 0 & 0 \end{bmatrix} \tag{115}$$

The eigenvalues of the matrix in (114) is found using the MATLAB function `eig`. This gives the values

$$\begin{aligned} \lambda_1 &= 0, \\ \lambda_2 &= (\sqrt{(au)^2 + (av_k)^2 - 2aduv_k^3 + d^2v_k^6} - au + dv_k^3)/v_k^3 \\ \lambda_3 &= -(\sqrt{(au)^2 + (av_k)^2 - 2aduv_k^3 + d^2v_k^6} + au - dv_k^3)/v_k^3 \end{aligned} \tag{116}$$

Since $a, b, c, d > 0$, and a bound will be set to ensure that in the program, $v_k, v_{k+1}, u_k > 0$, the last eigenvalue λ_3, will be negative. This means a Hessian which is not positive semi-definite, resulting in non-convexity for the system. Given that the upper-level (and possibly the lower-level) would utilise steady-state dynamics for each distance segment, the same procedure done for checking the convexity of the velocity dynamics, was performed for the work dynamics (108). The expressions for these eigenvalues were much larger, and the first of these gave negative values for the same parameters, an initial anaerobic work capacity at 1 J, and an input power at 1 W (along with

the same parametric values for $a, b, c, d > 0$). The problem at hand is therefore a nonlinear, non-convex, discrete optimization problem of medium- to large size. It consists of several constraints, both in the form of bounds on optimization variables and in the form of dynamic constraints (equations of motion and state dynamics). The former results in a number of inequality constraints, whereas the latter results in equality constraints. Considering the optimization problem is to be split into two different types of problems, one has to evaluate bounds in both cases, and how their differences affects the calculation of a solution.

For the overarching problem using larger distance intervals and steady-state velocity, the optimization variables must have bounds. For instance, the anaerobic capacity can never exceed AWC, or be lower than 0. Also, the input power has the constraint $u \leq P_{peak}$. Implementing constraints representing each distance point and it's corresponding states, might be done by simply constraining states to static values which can be represented by their steady states. The way to do this for velocity has already been demonstrated. However, the situation is a bit different for the input power, seeing as this has a coupled dependence on the variable w. The input u will be in danger of exceeding the maximum possible power for parts of a segment, if the remaining anaerobic capacity w is estimated only at the start of the segment.

The inequality constraint for the maximum power generation introduced in (38) and (41), is simplified through the assumption of the cyclist staying at an ideal cadence at all times (an assumption made by the authors in [4], as well). This is in accordance with the scope of the project, but further work could investigate cadence dynamics. From here on out, the maximum power generation given by (37) will be called P_{max}. The value of the remaining anaerobic capacity w at the current point on the track, will set the upper bound for the variable u_k at the same point, through the linear relation $P_{max} = \alpha w + CP$ (from (38)). Therefore, if the intervals of distance between each function evaluation of this upper bound are long enough, the bound might be broken if Δw for this segment is large enough to make the constraint of maximum power active (when w starts to be significantly reduced). The bounds previously mentioned for input power, constraining it to a small interval around CP might aid in avoiding such a situation. However, more consideration needs to be put into the design of the optimal program in order to guarantee feasible solutions. The upper level of optimisation therefore has the following structure in terms of discrete optimization variables:

$$\begin{aligned} t &: 1xN-1 \\ v &: 1xN-1 \\ w &: 1xN \\ u &: 1xN-1 \end{aligned} \tag{117}$$

where N is the number of points on the discrete interval of distance representing the track. For the lower level problem, using the dynamics of velocity directly (16), the number of velocity variables are increased to N, making the total number of variables, at most, equal to $4N-2$. For a significant length of the distance intervals, the constraint setting a dynamic upper bound for u (P_{max}) would be in danger not being respected. In between situations of varying elevation, where the track is flat, or has a constant inclination for a relatively long distance, the power output could be reduced to a smaller interval. These values could be over or under CP, depending on the demands put forth by the overarching strategic pacing plan. Between two consecutive tactical pacing situations, the power output recommendation could be slightly under CP, if the upcoming elevation variations demands a bit of extra w. The recommendation could be slightly over CP, should the situation prove to be less strenuous. The bounds on the variables are given as:

$$
\begin{aligned}
&t_{min} \leq t_k \leq t_{max} \\
&v_{min} \leq v_k \leq v_{max} \\
&1 \leq w_k \leq AWC \\
&1 \leq u_k \leq P_{max} AWC + CP \\
&\text{For k = 1,2,...,N}
\end{aligned} \tag{118}
$$

The dynamic constraints for the upper level problem can be stated as

$$
\begin{aligned}
&\text{Steady-state dynamics (upper level):} \\
&\text{For k = 1,...,N-1} \\
t_k &= \frac{2 * (D(k+1) - D(k))}{v_{k+1} + v_k} \\
v_{k+1} &= v_k + t_k * dv(v_k + (t_k/2) * dv(v_k, u_k, \theta_k), u_k, \theta_k) \\
w_{k+1} &= w_k + t_k * dw(w_k + (t_k/2) * dw(w_k, u_k), u_k)
\end{aligned} \tag{119}
$$

where $D(k)$ is the accumulated distance at point k in the track, and θ_k is the corresponding inclination at that point. dv, dw are velocity and work dynamics, given by (16) and (108), respectively. The dynamic constraints for the lower level problem can be stated as

$$
\begin{aligned}
&\text{Detailed dynamics (lower level):} \\
&\text{For k = 1,...,N-1} \\
t_k &= \frac{2 * (D(k+1) - D(k))}{v_{k+1} + v_k} \\
v_k &= v_{ss}(u_k, \theta_k) \\
w_k &= w_{k-1} + t_k * dw(w_k + (t_k/2) * dw(w_k, u_k), u_k)
\end{aligned} \tag{120}
$$

There are also additional equality constraints in the form of initial and terminal conditions on the states. These could be altered, in order to zoom in or out on different sub-problems, or tailor the optimal program to a very specific situation. Ultimately, the setup for the different levels of optimisation leads to two different regions of feasibility. Constraints on variables, both in the forms of equality and inequality constraints, spans a feasible region. Regions of feasibility, whose principles were explored in Section 2.4, are possible to present visually. For a number of optimization variables larger than 3 (in this case, as many as $4 * N - 2$, for the lower level problem), it is not possible to showcase the region in its entirety.

4.4 Numerical integration

In order to formulate the most suitable implementation for the final optimisation format, one should investigate the nature of the dynamic models describing the bicycle and cyclist, and their respective behaviours during different numeric integration schemes. Also, how the track is discretized and segmented is an important step in choosing and designing a scheme. When a cyclist moves through a track, the position will decide the current inclination on the ground, relative to a horizontally flat surface. Therefore, it is natural to opt for a track discretization consisting of points spaced equally in distance along the track (meaning the actual distance travelled along the track, regardless of inclination). Making distance the independent variable, in this way, might be advantageous for a number of reasons:

1. The objective function will have to include the time spent across the distance between each point on the track. In order for the optimisation routine to be able to minimize the sum of

these time steps, one may make these variable, whereas the distance between each "measured" step is fixed. The alternative would be a minimization of the number of time steps, which would potentially introduce a mixed-integer behaviour of the optimisation problem. This might, in turn, require more complex optimisation schemes to solve

2. The inclination of the track at each discrete distance-step would be reliably predicted, as it would be predetermined, just like the distance. This removes the need of calling a function returning the inclination based on the total distance travelled along the track, which would be necessary in the case of using time as the independent variable

3. The dynamics of distance, however simple, would not be necessary to include, as it falls out of the category of state, and into the category of an independent variable. This might simplify some calculation requirements for the optimisation scheme.

MATLAB's built-in functions for solving ordinary differential equations (ode45, for instance [92]) would seem like good candidates for solving the system dynamics in order to pass numerical values onto the constraints put on the optimisation variables at each point in time. The dynamics derived from Section 2 are based time-varying functions. This means that all numerical solvers eventually implemented, would depend on the step size in terms of time steps. For both the upper level (longer distance segments and simple dynamics) and lower level (short step size in distance, more complex dynamics) optimisation, this step in time varies. In the case for the upper level optimisation, distance might vary as well. However, for this optimal program, no numerical solvers are needed due to the highly simplified nature of it.

Figure 7 visualises the discrete implementation and calculation of states for the lower level of optimisation. Discrete points on the track and their corresponding states, input and inclination, are separated by distance segments of equal length. The differential equation describing change in velocity of the cyclist is given by (16). In order to study its behaviour, it is useful to expose it to different numerical integration schemes and step lengths. During these simulations, the fastest dynamics must also be considered, when the systems might be the most sensitive to step size variation.

Simulating the dynamics for velocity for a duration of 20 seconds with a constant inclination of 5%, one can view the influence a varying step length can have on the response. An initial velocity of 1 m/s was used. Three methods were tried as numerical integration methods (the Explicit Euler's method (63), the implicit midpoint-rule method (73) and the explicit Runge-Kutta 4th order method), whereas MATLAB's ode45 solver (source) acts as the exact solution to the problem. Step lengths $h = 10, h = 1, h = 0.1$ were evaluated. The parameters found in (20) were used.

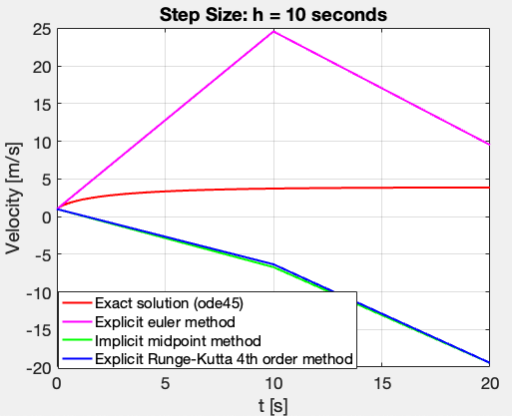

(a) Step size $h = 10$

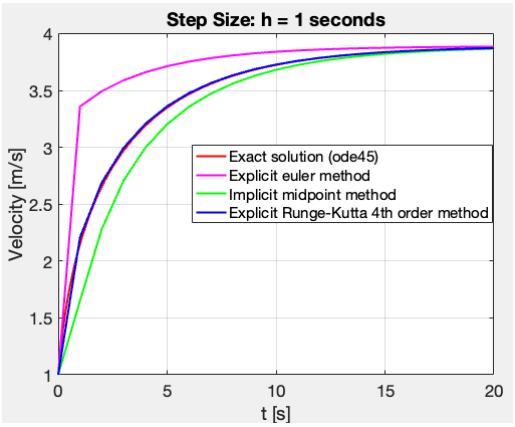

(b) Step size $h = 1$

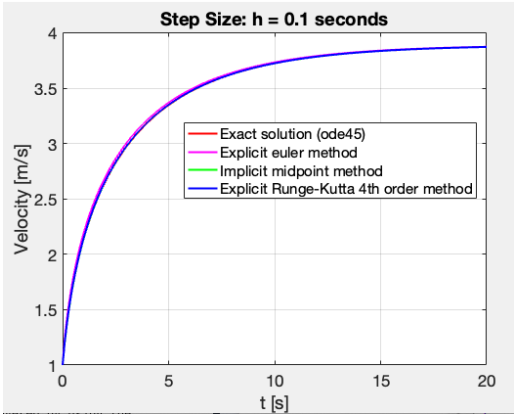

(c) Step size $h = 0.1$

Figure 15a, Figure 15b and Figure 15c shows the effect of a decreasing step size, and how the velocity dynamics becomes increasingly inaccurate for too large step sizes. Using the values in (20), and the same physiological values as has been used in Figure 12 ($CP = 250W, AWC = 10kJ, T_a = 8, T_{an} = 0.1, \beta_a = CP * 0.1W, \beta_{an} = CP * 0.005$), the system in (108) was simulated for a starting anaerobic capacity at 0, and an input power at $u = 0$, in order to uncover the fastest exponential dynamics for the physiological model. The duration was now set to 30 minutes, and step sizes explored were $h = 60$ seconds (1 minute), $h = 300$ seconds (5 minutes), $h = 600$ seconds (10 minutes).

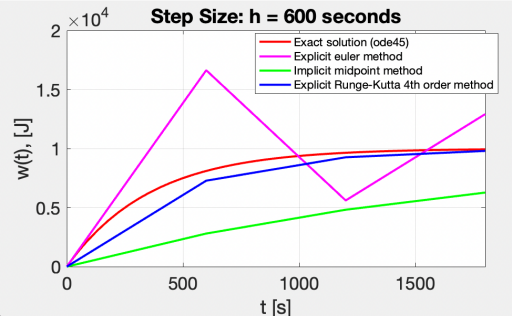

(a) Step size $h = 600$

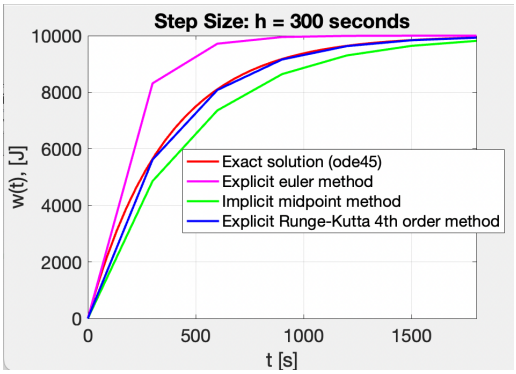

(b) Step size $h = 300$

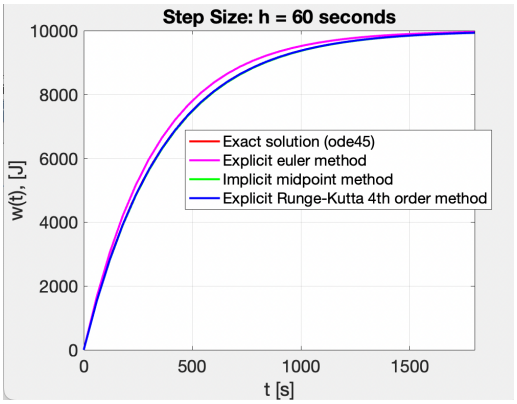

(c) Step size $h = 60$

For the system equations

$$\begin{aligned} \dot{v} =& f_1(v,w) = a\frac{u}{v} - bsin(\theta) - ccos(\theta) - dv^2, \\ \dot{w} =& f_2(v,w) = \frac{A(u)}{\tau(u)}(AWC - w) - A_n(u)(u - CP) \end{aligned} \tag{121}$$

the jacobian ([81]) is given as

$$J = \begin{bmatrix} \frac{\partial f_1}{\partial v} & \frac{\partial f_1}{\partial w} \\ \frac{\partial f_2}{\partial v} & \frac{\partial f_2}{\partial w} \end{bmatrix} = \begin{bmatrix} -\frac{au}{v^2} - 2dv & 0 \\ 0 & -\frac{A(u)}{\tau(u)} \end{bmatrix} \tag{122}$$

The resulting jacobian shows a system whose stability does not depend on the inclination θ for the state of velocity $v(t)$, and does not depend on the anaerobic expenditure model in terms of the state of remaining anaerobic capacity $w(t)$. The latter dynamics does not depend on the AWC, either. In addition, velocity can not be evaluated for $v \leq 0$. Based on Figure 14, the ranges for velocity are set to $v \in [0.1 \quad 80]$. Numeric values are already determined for a, d in (20). However, u, CP might vary, so the stability function must be evaluated for a range of values for these. Ultimately, the CP is estimated to stay in the range $CP \in [190 \quad 300]$. The input power, on the other hand, might vary in the range of $u \in [0 \quad 800]$. The numeric values in the ranges for CP, u are in this case simply guidelines for potential upper and lower bounds based on observed data from [4],[50],[49] and [67].

First, the eigenvalues for the jacobian are found by solving the equation

$$det(J - \lambda I_2) = \begin{bmatrix} -\frac{au}{v^2} - 2dv & 0 \\ 0 & -\frac{A(u)}{\tau(u)} \end{bmatrix} = 0 \tag{123}$$

for the $2x2$ identity matrix I_2, and λ represents the eigenvalues of the system. Using the function `eig` in MATLAB for the matrix J, gives the diagonal elements of the matrix itself, resulting in the eigenvalues

$$\begin{aligned} \lambda_1 &= -\Big(\frac{au}{v^2} + 2dv\Big), \\ \lambda_2 &= -\frac{\Big(\frac{1}{2} - \frac{tanh(\frac{u-(1-0.1)CP}{8})}{2}\Big)}{546e^{-0.01(CP-u)} + 316} \end{aligned} \tag{124}$$

Lastly, considering the extreme values of the intervals of u, CP, the largest, and smallest possible eigenvalues are found using arrays of the intervals and expressions for the eigenvalues in (124). Having established that the implicit midpoint method has acceptable accuracy for the predicted step length of the system (in Figure 15a,Figure 15b,Figure 15c and [81]), this method will be used when numerically integrating going forward. It is partly due to it's relative simplicity as well, compared to, for instance, the Runge-Kutta 4th order method ((64)), which demands four times the number of function evaluations for each step. The stability function for the midpoint method is

$$R(h\lambda) = \frac{1 + \frac{h\lambda}{2}}{1 - \frac{h\lambda}{2}} \tag{125}$$

where h is the step length and λ is the eigenvalue of the system. The demand for A-stability ([81]), states that $|R(h\lambda) \leq 1|$ for all $\mathrm{Re}(\lambda) \leq 0$. Both eigenvalues of (124) are real, and below 0, because $a, d, u, v \geq 0$, and $A(u), \tau(u) \geq 0$ for all u. The region of stability for the two systems are shown below, given the intervals $u \in [0 \quad 800]$, $CP \in [190 \quad 300]$ and $v \in [0.1 \quad 80]$. Firstly, for velocity (and the corresponding eigenvalue λ_1), for the extreme cases of input power:

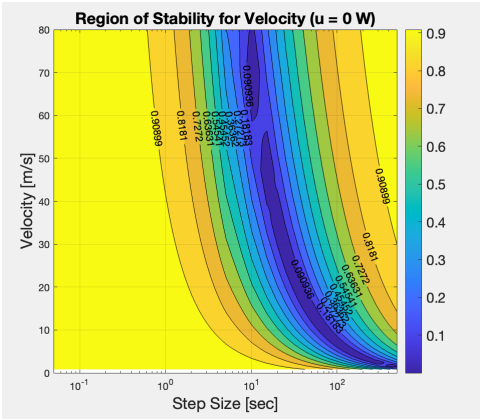

(a) The stability function for velocity when $u = 0W$

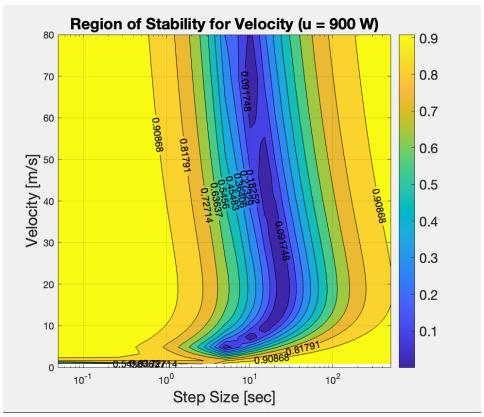

(b) The stability function for velocity when $u = 800W$

Secondly, for remaining anaerobic capacity (and the corresponding eigenvalue λ_2), for the extreme cases of CP:

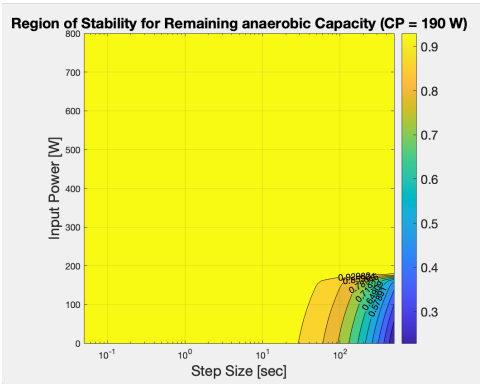

(a) The stability function for velocity when $CP = 190W$

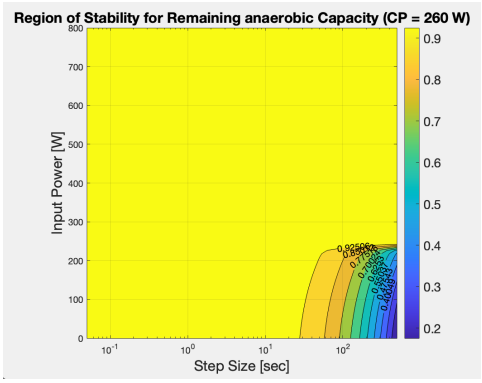

(b) The stability function for velocity when $CP = 260W$

No values of the stability function in Figure 17a, Figure 17b, Figure 18a or Figure 18a are above 1. However inaccurate the solution of Figure 15a, with a step size of $h = 10s$, the solution seems not to be unstable, based on the plots of the regions of stability. It is rather very inaccurate, which leaves the notion that for step sizes well over 1 second, the dynamics of (16) are not reliable when solving using a numerical integration scheme like the implicit midpoint rule (73). The same could be said for the region of stability for remaining anaerobic capacity. This might be a reflection of the good stability properties of the method for nonlinear systems. However, it might also be a reflection of the well placed bounds on the variables involved ($v \in [0.1 \quad 80], u \in [0 \quad 800], CP \in [190 \quad 260]$). Observing the simulated states and their transients, along with the region of stability, it seems the optimal step length for the velocity dynamics is $h \leq 1$, while for the remaining anaerobic capacity (especially its recovery dynamics) it is $h \leq 300s$ (5 minutes). This final observation, ultimately supports the idea of keeping with the detailed dynamics of the remaining anaerobic capacity (108) for the upper level dynamics (where segments of distance cause the system to take discrete step, $k+1$ to k, ranging from 100-500 seconds).

4.5 Final Problem Formulation

The total formulation of the optimal program can be seen below for both the upper level (126), and lower level problem. For the upper level program,

$$
\begin{aligned}
\text{States and input: } & x_k = [t_k \quad v_k \quad w_i]^T, \quad u_k = u(k), \text{ where } k = 1, 2, ..., N-1 \text{ and } i = 1, 2, ..., N \\
\text{Objective Function: } & \sum_{k=1}^{N-1} t_k, \\
& \text{for } t_k = \frac{D(k+1) - D)(k)}{v_k} \\
\text{Initial conditions: } & x_0 = [t_{ss,0} \quad v_{ss,0} \quad AWC]^T, \\
\text{Dynamic constraints: } & v_k = v_s s(u_k, \theta_k) \\
& w_{k+1} = w_k + t_k dw(w_k + (t_k/2)dw(w_k, u_k), u_k), \\
\text{Inequality constraints: } & S_{min}/v_{ss}(u_{max}, \theta_{min}) \leq t_k \leq S_{max}/v_{ss}(u_{min} \\
& v_{ss}(u_{min}, \theta_{max}) \leq v_k \leq v_{ss}(u_{max}, \theta_{min}) \\
& 1 \leq w_k \leq AWC \\
& u_{min} \leq u_k \leq P_{max}(w_{k+1}) = \alpha w_k + CP
\end{aligned}
\tag{126}
$$

where v_{ss} is the expression in (111), $t_{ss,0}, v_{ss,0}$ are initial conditions related to an arbitrary (but feasible) initial guess (mentioned later), S_{max}, S_{min} is the longest and shortest distance intervals

respectively, $\theta_{max}, \theta_{min}$ are the steepest inclination and declination, and N is the number of points on the track for the accumulated distance at each point D (from 0 m to the total distance covered throughout the time-trial). For simplicity (and potential numerical issues, see for example fraction $a * u/v$ in expression for acceleration (16)), no states (nor the input) has a lower bound of 0, but 1, representing the 0. u_{min} might have to be tuned and tested for both problems.

$$
\begin{aligned}
\text{States and input: } & x_k = [t_k \quad v_i \quad w_i]^T, \quad u_k = u(k), \text{ where } k = 1, 2, ..., N-1 \text{ and } i = 1, 2, ..., N \\
\text{Objective Function: } & \sum_{k=1}^{N-1}(t_k) \\
& \text{for } t_k = \frac{D(k+1) - D)(k)}{v_k} \\
\text{Initial conditions: } & x_{init} = [t_{ss,0} \quad v_{ss,0} \quad wInit]^T, \\
\text{Terminal conditions: } & x_{term} = [\qquad wTerm]^T \\
\text{Dynamic constraints: } & v_k = v_s s(u_k, \theta_k) \\
& w_{k+1} = w_k + t_k dw(w_k + (t_k/2)dw(w_k, u_k), u_k), \\
\text{Inequality constraints: } & S_{min}/v_{ss}(u_{max}, \theta_{min}) \leq t_k \leq S_{max}/v_{ss}(u_{min} \\
& v_{ss}(u_{min}, \theta_{max}) \leq v_k \leq v_{ss}(u_{max}, \theta_{min}) \\
& 1 \leq w_k \leq AWC \\
& u_{min} \leq u_k \leq P_{max}(w_{k+1}) = \alpha w_k + CP
\end{aligned}
\tag{127}
$$

where A_n is the anaerobic term activating energy expenditure for $u > CP$ and $wTerm$ is the preferred final remaining anaerobic capacity for the end-point of the corresponding segment. The states t_k, v_k do not have terminal conditions in this case.

4.6 MATLAB framework

The different optimization problems are implemented in the optimization framework developed by MATLAB. It has a simple, effective structure, allowing for quick re-iteration of the optimization design. The interface also allows for quick troubleshooting and debugging of the code. The structure is composed of a built-in class called 'optimproblem'. The optimization variables are tied to the class 'optimvar', being initialised by their respective dimensions (for example a 1x20 row vector of optimization variables) and their bounds (maximum and minimum value). This class treats logic statements containing the variables as constraints (for example $v(0) == 0$, where v is an array consisting of the velocity at the discrete distance point at zero). This way, the constraints set by the dynamic trajectories of the states throughout the track can be set. The optimization variables can included in the constraints set for the other variables (for example $u(k) \leq P_{max}(w(k)) = \alpha w(k) + CP$, where $0 \leq k \leq (N-1)$, and N is the number of points on the track, which constitutes the discrete interval that is the track).

To solve the optimal control problem, the program in Section 4.5 is implemented in MATLAB. Using simplified tracks and examples at first, to demonstrate the behaviour of the program, makes identifying potential shortcomings easier. Firstly, the strategic problem of distributing the anaerobic capacity across the entire track is being explored. Thereafter, the tactical, short-duration optimal control problems are solved in order to provide pre-calculated solutions for the overarching problem. The two levels of optimization are both based on `fmincon` as the optimisation algorithm and framework in MATLAB. However, the dynamic models, constraints and resolution of the track, as laid out in Section 4, are different in the two cases.

The tuning parameters related to the optimisation framework are

- 'Algorithm' - Type of algorithm used to find the solution. Alternatives:

  - SQP
  - Active-set
  - Interior point
  - SQP-legacy
  - Trust-region-reflective
- 'MaxIterations' - Maximum number of iterations of the otpimisation algorithm
- 'MaxFunctionEvaluations' - Maximum number of function evaluations for the oprimisation scheme
- 'ConstraintTolerance' - Tolerance of the sum of constraint violation
- 'StepTolerance' - Tolerance of step size in optimisation variables
- 'FunctionTolerance' - Tolerance of change in objective function
- 'OptimalityTolerance' - Tolerance of the first-order optimality measure (maximum absolute value of the gradient of the objective function)

where each run of the program reports which of the tolerance parameters or maximum bounds that resulted in the termination of the program. In the MATLAB framework, one must choose between problem-based and solver-based. [93] mentions simplicity in the set-up and debugging as advantages of problem-based implementation. The ease with which one may try different solvers on the same problem, as well as efficiency in calculation of solutions are also listed as advantages.

In addition to implementing the optimal program, an initial guess must be produced. This is necessary for the algorithm to have a basis from which to start its iterative search for a solution. This guess must set all the optimization variables t_k, v_k, w_k, u_k for $k = 1, ..., N$ in accordance with the dynamics for the given problem. This guess must also be feasible. In the case of the energy distribution, the initial guess is quite straight forward to produce. Setting the value AWC for all steps in distance for the variable w_k, and the power level CP for all steps for the variable u_k, results in an initial guess which is feasible.

In the case of the sprint-optimization, the initial guess is a bit more complicated. Each step is mathematically bound to its preceding step, in the sense that the transition from one to the other has to have come naturally from the dynamical equations, otherwise the next step in the solution contributes to in-feasibility. An initial guess which is infeasible makes it a lot more complicated for an algorithm to solve for an optimal solution. A possible solution to this problem, is to solve the equation (113) for the unknown variable u_{ss} which renders the expression $\frac{dv}{dt} = 0$, making the initial guess coincide with the dynamics. This means that the initial guess for the optimal power in each point on the track is set to that power which leads to a constant velocity.

4.7 Track selection

The Bologna TT (Figure 19) is a course which invites the idea of implementing a pacing strategy throughout the course profile. This stems from its simple, yet relevant elevation profile. The track consists of a relatively flat segment of approximately 5 km of length. The track then enters a small segment of 1 km of moderate inclination. After this segment, it enters a segment of very steep terrain, varying around 10-17 % inclination. This segment has a length of approximately 2 km. All segment lengths mentioned in this case are measured along the track (i.e. actual distance covered by the cyclist along the slope). The course is available on the software Zwift, and can be run for more than one lap. The optimisation of a pacing strategy becomes more intricate, when given the task of solving this problem for a variant of the Bologna TT going up the hill, down and up again. In other words, going 3 laps on the track is an interesting track selection for the optimisation problem formulated so far.

1 lap of the track in the Zwift software equals 8.1 km of distance. However, succeeding the goal line atop the hill, as well as the starting line (when returning during the 2nd lap), there are

small segments of extra distance, where the simulation runs a few hundred meters, then forces the cyclist to make a u-turn. This adds about 400 m tor the total distance. The total length along the slope (actual distance covered by a cyclist) then becomes 24.7 km. This increased length of the track makes it ideal in terms of duration of typical time trials (which varies around 50 - 70 minutes, obviously depending on the physiological parameters and quality of performance of the subject). Models utilizing the parameters CP and AWC are also most reliable for durations in this range (Figure 6). This variant of the track has an elevation profile shown in Figure 19.

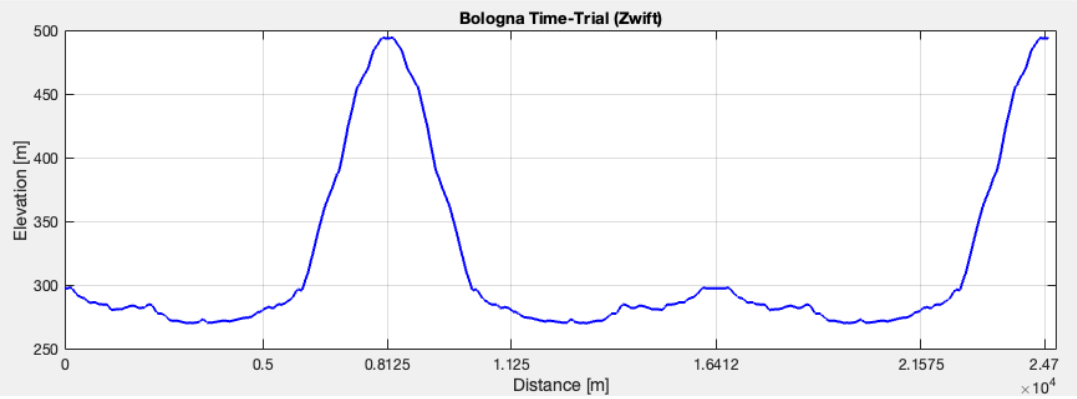

Figure 19: Elevation profile (in 2 dimensions) of the track Bologna TT, run through for 3 laps (up-down-up).

The track will have to be segmented into parts in a manner which allows the optimisation scheme to effectively solve the problem. The upper level optimisation, which features the entire track, and consists of segments of average inclination over a given distance, could utilise a simplification of the track visualised in Figure 20.

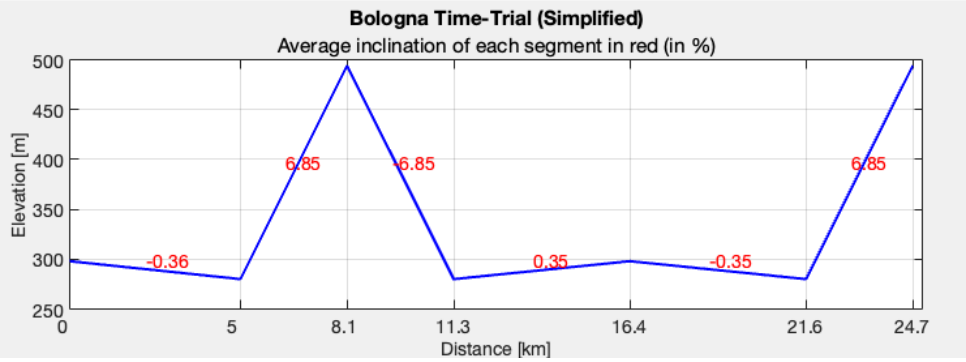

Figure 20: Simplified version of elevation profile (in 2 dimensions) of the track Bologna TT, run through for 3 laps (up-down-up). Mean inclination of each segment shown in red (in %)

The first, relatively flat segment (length of 5000 m) has an average inclination of -0.36%, while the steep segment (length of 3125 m) has an average inclination of 6.85%. The segments and their mean inclinations are simply replicated after the first ascension (Figure 19), as the cyclists will turn around and go through the same elevation profile, only now going downhill. The flat segment after the descent, and before the second ascent, is slightly longer than $5 * 2 = 10$ km, because of the small extra distance designed for turning around after having returned to the starting line at approximately 16 km. This segment is split into two halves, which are identical, only flipped. The length of these are 5612 m, whereas the inclination is 0.35% and -0.35%.

The segments of the simplified track in Figure 20, needs to be split further into even smaller segments, in order to specify the exact optimal power trajectory in finer details. The demarcations for the segments are set at 0, 1.2,

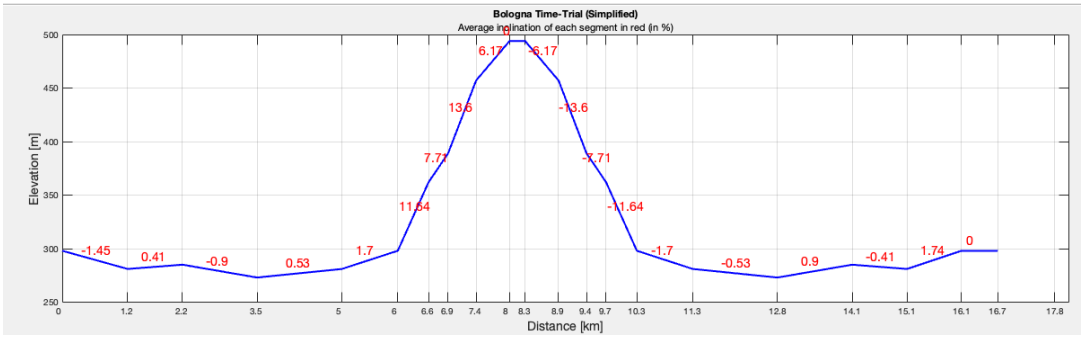

Figure 21: Simplified version of elevation profile (in 2 dimensions) of the track Bologna TT, run through for 3 laps (up-down-up). Mean inclination of each segment shown in red (in %). This time, at a higher resolution.

In Figure 21, the rest of the track from the last segment (at 16.7 km) which is excluded, is simply the mirror image of the track going back up the hill at 494 meters of elevation.

4.8 Upper Level Strategy: Distributing Anaerobic Capacity

For the strategic implementation shown in Section 4, a class defined as 'upperLevel' is constructed (Section A.2,Section A.3, Section A.4). It has the properties of an optimization problems, and the three optimization variables time (t), velocity (v), remaining anaerobic work capacity (w) and input power (u). The constructor method of the class initialises the properties as an optimization problem with optimization variables, corresponding bounds and constraints, and an objective function. Starting off, a simple track, with a varying length of distance segments, was used in the optimal program defined in (126). The state responses, the optimal solution of input power on the ergometer, as well as the elevation profile of the simple track is shown below.

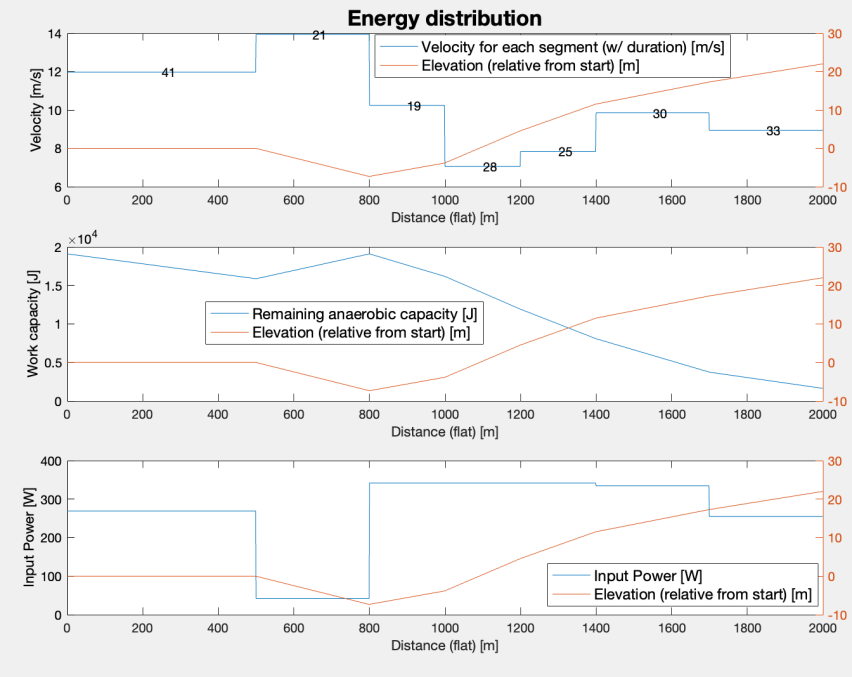

Figure 22: State variables (velocity (v) and remaining anaerobic capacity (w), along with duration of each segment (in black over the velocity curve, measured in seconds)), elevation profile, and input power, all plotted against the distance of the track seen from above (as opposed to actual distance travelled). Elevation corresponds to the red y-axis on the right in the plots

The time spent through the track was 3 minutes and 17 seconds. The plots shows a response that can be explained somewhat by intuition regarding cycling and endurance sports in general. One such example is the fact that the solution chooses a lower input power, or 'rest', for the little downhill segment (starting approximately at 500 m 'flat' distance).

In this example, implementing the upper bound of input power ($u_k \leq P_{max}$) with the current power constrained by the remaining anaerobic capacity at the next step in accumulative distance, the solution will perform slightly better regarding this constraint. As previously mentioned, the upper bound of input power is in danger of not being respected, due to the simplified implementation of the overarching capacity-problem. However, forcing this constraint to adhere to the next step of remaining anaerobic power (meaning $u_k \leq P_{max} = \alpha * w_{k+1} + CP$), as well as lowering the constraint tolerance in the MATLAB framework (from $10^{-10} to 10^{-13}$) even further, makes the solution respect the constraint at more points in the track. However, this might challenge the connection that the optimal program has, to the theoretic principles motivating the dynamics of the w. Considering one whole step forward in distance does not coincide with the state dynamics represented in (94).

It is important to measure the effect of this tuning of parameters (in this case, tuning the 'ConstraintTolerance') in terms of the influence it has on performance. Tuning this value from 10^{-10} to 10^{-13} results in a response respecting the P_{max} constraints for all but the last distance segment. For the former value, this constraint was not respected for the last two segments. The time performance is the same, 200 seconds. Changing even further, to 10^{-15} gives a time performance which is 24 seconds slower, namely 224 seconds. However, now all constraints in the form of upper bound for input power, are respected.

The same strategic optimisation structure is utilised as the one used in Figure 22, now with the simplified Bologna track in Figure 20. A different optimisation solver algorithm is also used, namely the 'active-set' method ([84]). Verifying that the optimal solution renders a better time performance, the solution is compared to an input power trajectory set just above CP, resulting in an almost completely empty (and lower, compared to the varying power trajectory) anaerobic capacity when passing the goal line (372 J left for a constant input power, 449 J left when using the optimised power trajectory). The time performance for the constant power trajectory was 1 hour 11 minutes and 24 seconds. The MATLAB framework concludes that a local minimum was found, which satisfies all constraints. The algorithm stopped searching, due to the objective function being non-decreasing in feasible directions, to within the 'optimality tolerance'. This parameter has so far not been tuned. The constraints are also satisfied within the value of the constraint tolerance. The tuning parameters of (Section 4.6), 'MaxIterations', 'ConstraintTolerance', 'MaxFunctionEvaluations' and 'StepTolerance' were set to $10^{10}, 10^{-10}, 10^{10}, 10^{-10}$, respectively.

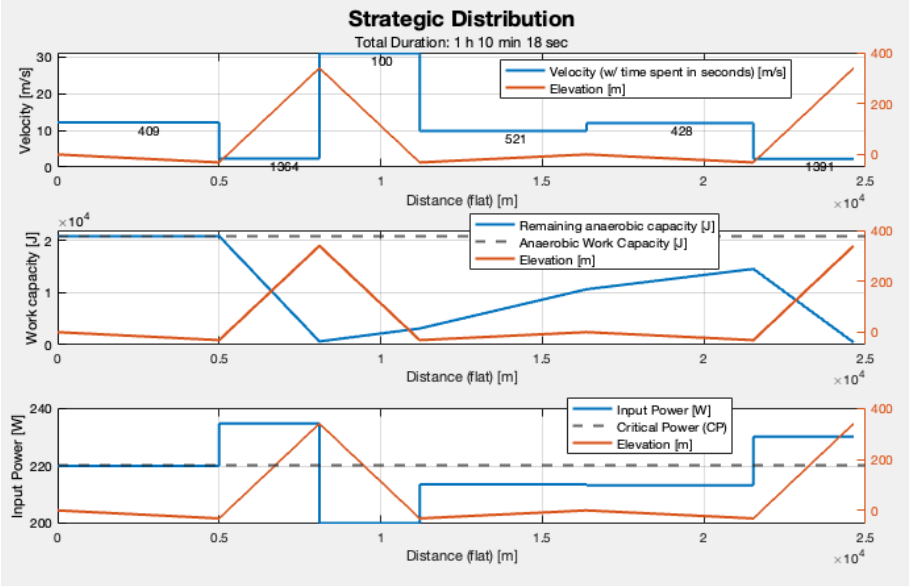

Figure 23: Optimal power trajectory and energy distribution with state responses for the simplified Bologna TT track. The time spent (in seconds) is shown in black above each segment of steady state velocity. The axis with orange numbers on the right, corresponds to the elevation profile (in meters)

Figure 23 shows the response for an optimal input trajectory in the plot on the bottom, using physiological values $CP = 220$ W, $AWC = 20870$ J and $\alpha = 0.0227$ 1/s. These values were based on the model verification shown in Figure 30. The time performance, 1 hour, 10 minutes and 18 seconds, is an improvement of 1 minute and 6 seconds to the constant strategy. The response shown in Figure 23 was a result of the bounds for the input power being set to $u \in [CP - 20 \quad CP + 20]$. By changing these bounds to $u \in [CP - 150 \quad CP + 20]$, the response becomes 3 seconds faster (1 hour, 10 minutes and 15 seconds). In doing this, the cyclist is able to rest more during the downhill segment. The anaerobic work capacity left is now 468 J, indicating that it is possible to achieve an even faster performance. This value is also greater than the remaining anaerobic capacity at the end of Figure 23. The tuning parameters for the optimisation framework were unchanged. The solution and responses are shown in figure Figure 24.

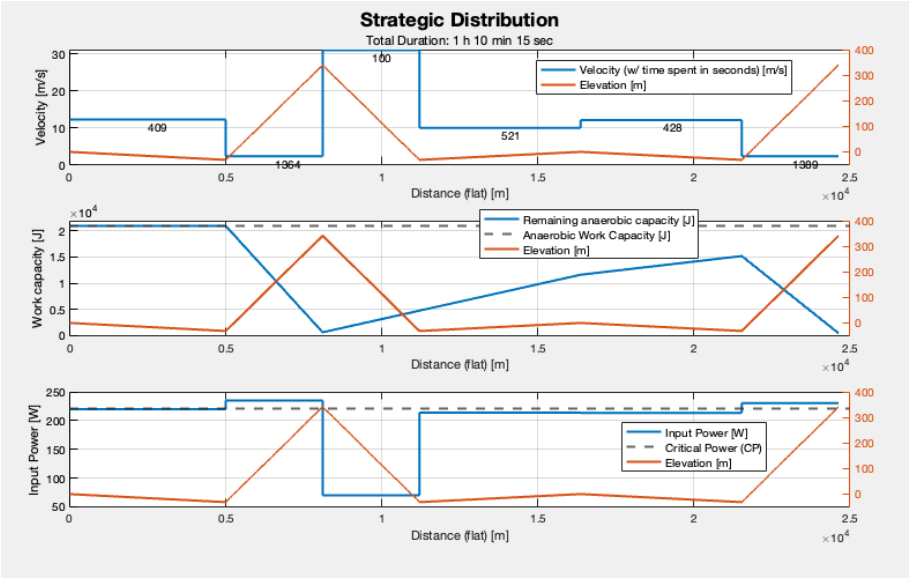

Figure 24: Optimal power trajectory and energy distribution with state responses for the simplified Bologna TT track. The time spent (in seconds) is shown in black above each segment of steady state velocity. The axis with orange numbers on the right, corresponds to the elevation profile (in meters)

The optimization framework comes to the same conclusion as for the response in Figure 23. The solution is a local minimum that satisfies the constraints. An observation in this case, is the 'sqp' algorithm struggled to compute solutions for intervals of input power larger than the one used for the response in Figure 23 (meaning, $u \in [CP-20 \quad CP+20]$). The algorithm either gave infeasible solutions, or took too long to compute. This might have to do with the fact that active-set algorithms takes larger steps ([84]), which adds speed. Regarding the remaining anaerobic work capacity at the end of the activity, this has so far not been forced to empty fully to 1 W (lower bound).

The optimisation attempts shown in Figure 23 and Figure 24 used a physiological model with aerobic and anaerobic terms overlapping somewhat. The models were refined to act more like the response in Figure 12 and Figure 13. Additional tuning parameters for the optimisation framework in MATLAB were added ('OptimalityTolerance' and 'FunctionTolerance'). This was done as a response to the frequent termination of the optimisation routine due to the numeric values of these tolerances not being low enough. The now newly shaped overarching strategy for energy distribution, given the simplified version of the Bologna track shown in Figure 20, is shown in Figure 25. The physiological values used were found in a modified test, which will be explained in Section 5.2, and performed prior the first iteration of verification of a pacing strategy developed using optimisation (Section 6.2).

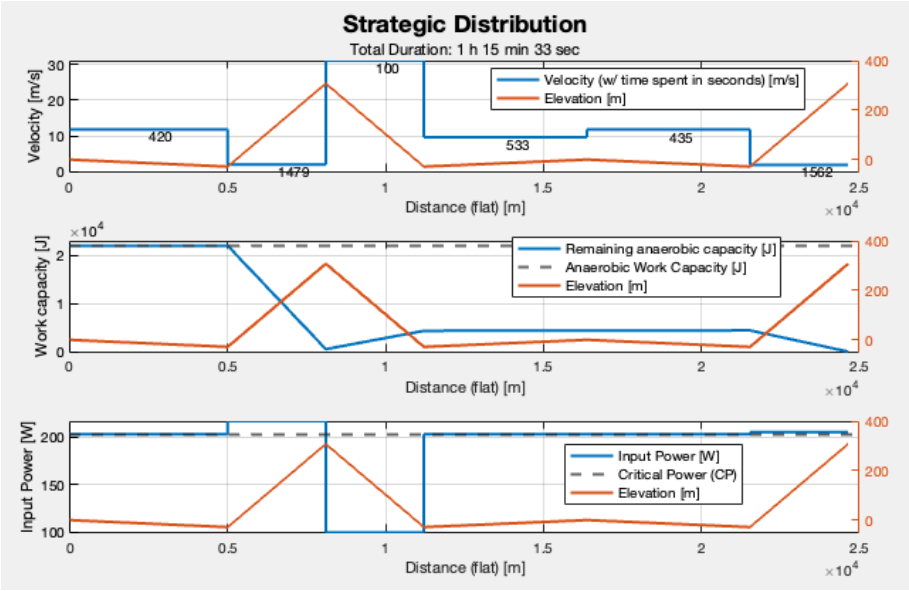

Figure 25: Optimal power trajectory and energy distribution with state responses for the simplified Bologna TT track. The time spent (in seconds) is shown in black above each segment of steady state velocity. The axis with orange numbers on the right, corresponds to the elevation profile (in meters)

The bounds on input power were set to $u \in [CP-100 \quad CP+50]$, whereas the tuning parameters for the optimisation framework, compared to the responses in Figure 24 were a bit higher. The new parameters (for function and optimality tolerance) were set to 10^{-9} and 10^{-6}, respectively. The time performance (1 hour 15 minutes and 33 seconds), is worse than the response in Figure 24, due to the refined model for recovery. This new model does not allow for such a high positive increase in the model for rate of change of remaining anaerobic capacity when u decreases right below CP. This behaviour was refined using the numeric settings for the hyperbolic tangent terms (representing the dominating metabolic category of energy expenditure, shown in Figure 11).

The strategy in Figure 25 is clearly different, in that it expends roughly the same amount up the first ascent, but struggle to recover the same amount as the previous strategies did. This does not allow for the same expenditure of energy up the second ascent, and triggers the need for the cyclist to lie closer to, or at, the estimated critical power. The loss of this increased power output during the final ascent (seen at the end in last optimised power trajectory Figure 24) may cost some minutes. However, the cyclists ability to actually perform the same during the final ascent,

and increase the power output like both optimised trajectories instructs them to do during the first ascent, might be difficult during the second one. Factors of fatigue which lie outside of the model of CP and AWC, may influence the ability to actually push as hard through the entire final ascent. Such discussions were had in [49], regarding the region of validity of the CP-model in terms of duration of the activity. The final ascent might be on the edge of this region, considering the entire effort is predicted to take just above 1 hour. An observation to note, is that the optimised energy distribution in Figure 25 resulted in an even smaller remaining anaerobic capacity at the goal line than previous attempts (127 J).

4.9 Lower Level Tactics: Formulating an Optimal Power Trajectory

In order to properly identify the optimal power trajectory based on physiological parameters, the track in Figure 20 has its six segments (flat-uphill-downhill-flat-flat-uphill) segments split into even smaller segments, shown in Figure 21. The same optimisation routine as the one used in Figure 24 is now being used as well. The only differences, are the smaller segments, as well as the requirement of meeting the remaining anaerobic capacity levels set by the upper level optimisation prior to the program running. The inclusion of these requirements was implemented as a term in the objective function $((w(N) - wEnd)^2$, where N represents the final step in each segment of Figure 20 for the state w(t), and wEnd represents the value for w(t) at this step coming from the upper level optimisation). However, it revealed itself easier for the optimisation framework to interpret the requirement in the form of an equality constraint at the terminal condition (last step) for the last optimization variable of the state w(t) (i.e. the variable w(N)).

In addition to this newly formed strategy, the more detailed power trajectory, in the 'lower level' optimisation was developed. Starting off with an implicit midpoint solver ((73)) to simulate velocity through the track for the dynamic equation (16), the method was altered, to instead using steady state velocity as constraints for the velocity optimisation variables (117) at each step on the track. This coincided with the method of interpretation of dynamics in the 'upper level' optimisation. The reason for this change, was due to the fact that infeasibility was too frequent when computing solutions for variables and input for the lower problem. This might have to do with the step size of the solver, and the corresponding accuracy properties (explored in Figure 15a) due to the relatively long segments of distance.

A question arises regarding the steady state response and the transient of the dynamic model of velocity. One must make sure that the time constant for the steady state responses under no circumstances are in the same range as the duration of the cyclists ride through each segment. This was a concern at the upper level too, however now this must become more relevant as a concern, due to the more detailed discretization of the track during lower level optimisation (Figure 21). One has to be aware of the bounds on input power, seeing as the time constant of velocity to reach steady state becomes lower as the input power decreases. Another factor, is off course the inclination, which also affects the time constant of the system.

In Figure 15a and Figure 17a, the step size and region of stability for numerical integration through the implicit midpoint method was explored. All though the lower level optimisation seems most effective (and so far, accurate enough) with steady-state velocities, the step size exploration also revealed the transient behaviour of the state. Looking at the eigenvalue for the dynamics of velocity (124), and the shortest distance in the segments of the lower level optimisation shown in Figure 21, reveals whether or not the steady state dynamics can be utilized for the lower level problem.

In setting up six lower level optimisation problems (one for each upper level segment in Figure 20), and solving for initial and terminal conditions for $w(t)$ stemming from the solution of energy distribution in Figure 25, the total optimisation of the power trajectory is now the goal. The lower level problems are therefore guided by the upper level attempt at distributing the energy in the best manner across the track. The upper level problem's main focus is the way the first ascent is handled with respect to energy expenditure, how much the cyclist should rest during the downhill segment, and ultimately, how much energy should be left prior to the final ascent. The lower level problems all have the objective of minimizing the time spent in each of the upper

level segments (each of the straight lines in Figure 20, cut into smaller pieces for the lower level in Figure 21).

Possible changes, and modifications to the optimisation design, in the "upper" and "lower" framework established in this section, are (among others);

1. The exact split of the Lower level problem (the smaller segments)
2. Optimisation tuning parameters
3. Possible injection of sprints, or demands on the upper level instruction for energy distribution, to consider a little extra expenditure (for instance at the 200 m at the start or prior to the descent) - if experience indicates that such efforts are necessary
4. Implementation of the inequality constraint for maximum power output ($P_{max} = \alpha w_k + CP$)

In the following section Section 6, different iterations of the optimisation design is therefore explored, based on experience gained through attempting the time trial without a pacing strategy, and the data processed from the corresponding test protocols (3MT, 5MT, 12MT). However, the basis for all lower level problems is shown in Section A.5, Section A.6,Section A.7.

5 Experimental Approach

The approach to the experimental parts of the project was to set up an environment suitable for testing the physiological parameters, which would make up the model for the remaining anaerobic capacity (108). All procedures completed when testing for parameters, or running a time-trial, aimed to minimize measurement errors and external factors introducing uncertainty. Each session of parameter tests involved a 30 minute warm-up with sprints baked into the session. Every time-trial attempt had a warm-up of approximately 15 minutes prior to the attempt. Equipment was regularly calibrated in order to ensure no drift or other uncertainty introduced into the sensors.

The subject performing the experiments is the author of this document. This put an even higher level of emphasis on the importance of reducing sources of error and uncertainty, due to the possible conflict of interest. The anthropometric parameters for the subject was $m = 84$ kg , $h = 1.87$ m during the project (used in (20)), and had some experience cycling. However, cycling on an ergometer in the form of a smart trainer, as was used in the project, was not something they had tried before. The subject also had limited knowledge and no experience of time-trials, or competition cycling. The training schedule prior to the period of tests and trials therefore included 1-2 activities per week, alternating the sessions between a longer duration effort (1-1.5 hour), and intervals (4x10 minutes, or 6x5 minutes) of higher intensity (in measured power output). This schedule was held for 3 months prior to the first test protocol was performed, and 3.5 months prior to the first time-trial attempt.

5.1 Experimental setup

The exact configuration of equipment used during test protocols and time-trials can be seen in Figure 26. It is set up in order to run a cycling simulation with a smart trainer, using the Zwift software, and ANT+ connection. The bicycle consisted of a saddle, frame, handlebar, and a front wheel, while the rear wheel was removed, where the Tacx Flux Smart Trainer ([5]) was attached instead. This device controls the resistance based on the inclination on the track run in Zwift. The bicycle frame was a Cicli B Rithey Carbon Pro. The shoes seen in Figure 26 were made by Shimano, and the chain set was a Shimano Ultegra. The measurement of power originated from the pedals, namely a Favero Assioma Duo. Many power meters calculate power using the average value of the angular velocity per rotation instead of measuring the instantaneous angular velocity. According to the producer ([94]), this may introduce an additional error of up to 4.5% compared to declared accuracy. Pedalling is never regular or homogeneous (for example during sprints or

climbs), and a direct power measurement could capture these small fluctuations easier. In order to measure core temperature during the activities, a CORE Body Temperature measurement device was used ([95]). A Garmin Heart Rate Monitor Dual was strapped around the upper part of the torso ([96]), and the CORE temperature device was attached to the strap, on the left side of the strap.

Figure 26: Experimental equipment set up as it was during all test protocols, and time-trial attempts

The CORE Body Temperature device was connected to a Garmin Forerunner 945 in order to gather the temperature data during the activity. The smart trainer, heart rate monitor, and the power measurements in the pedal were all connected to a MacBook Pro seen inFigure 26 through an ANT+ connection. In order to both mimick the cooling effect and sensation of air during a cycling time trial, and regulating the core temperature of the body, a fan was placed in front of the ergometer, pointing directly at the face of the cyclist when in a time-trial position. The fan did not have the ability to rotate in the vertical direction (only the horizontal), leading to the cooling effect of the air to only hit the face of the subject while in a time-trial position, and not when in a standing position. In the Zwift software, the Bologna TT track was available through sporadic events held at specific times. These events were entered, and attempted for the time-trials, whereas the test protocols for determining CP, AWC and α were run on tracks that were as flat as possible, in order to prevent cadence dynamics from greatly affecting the power data.

When having performed a test or trial, the power data, gpx.-file (containing the track simulated in Zwift) and data from all other measurements (heart rate, temperature, cadence, velocity) was transferred from Zwift to the Garmin Connect application. From there it could be further extracted, and analyzed in MATLAB. In the Garmin interface, normalized power is presented. This is weighted method of average power estimation, taking into account ride conditions such as inclination. In the training platform Strava, an open source plug-in available on Google Chrome called Sauce for Strava ([97]) was used in order to aid with analysis of power data and other metrics.

The tables of power data come in the form of .csv files, which could be read and formatted as tables in the MATLAB interface. This allows for a walk through of the power, cadence or velocity throughout the activity, and each data point comes with a corresponding timestamp. In order to successfully handle potential errors in the data (such as missing data points), each timestamp is checked. If a timestamp is missing, this has to be accounted for, and evaluated in terms of influence it can have on the results. For the test protocol 3MT for instance, it is important to check whether all timestamps during the 3 minute maximum effort is recorded exactly 1 second after the preceding timestamp. If this is not the case ($\Delta t > 1 second$), data is missing. Other error handling routines which are necessary include the check for non-recordings in the data (such as 'NaN' = Not a number) or unrealistically high values for power or velocity. This can also be checked when plotting the data.

When executing a test protocol, all external factors are kept as unchanged as possible prior and during the test. In order to minimize the effects of carbohydrate intake discussed in [32], a fruit was eaten prior to each test, as well as the time trials. Other external factors during the tests were also kept significantly unchanged, like the fan keeping in place to hit the subjects face at the same angle, and the gear being set to approximately the same level for each test protocol (during time-trials they had to change). Another important factor, is the way the tests and time-trial attempts were set up with respect to rest days in between. A time-trial, and an all-out attempt are two different exercises, the former involving more aerobic dynamics, at a lower average power level and longer duration, while the latter involves more anaerobic metabolism and effort. The time-trial is also a different activity entirely in terms of the mental aspect of maintaining a high level of performance throughout. The properties of these activities, their place in the time schedule of the project, and the external factors affecting their outcome, are all topics of discussion in Section 7.

5.2 Test Protocols

In order to determine the physiological parameters CP, AWC and α, the 3MT test was used initially. Simply conducting the 3 minute long interval of all-out effort without warming having a warm up prior to the bout, results in misleading results. Before a physical activity of severe intensity, the body needs a warm-up phase ([76]). In this case, a warm up of 30 minutes was conducted. Having already conducted a training program, the CP was estimated using the software GoldenCheetah ([98]) by feeding it with data from all prior exercise leading up to this point. This software used the a posteriori method of [57] (shown in (28)) in order to simulate the remaining anaerobic capacity $W' = w(t)$ throughout the exercise based on the power output. This value for the CP, helped predict the power levels for the warm up routine of the first 3MT. In accordance with [67], the 3MT test, the CP is estimated as the mean power output of the last 30 seconds.

$$CP = \frac{1}{N}\sum_{k=0}^{N-1} P_k \tag{128}$$

where $N = 30$ is the number of seconds where the estimation takes place and P_k is the power output from the ergometer at timestamp $k = 0, 1, ..., N-1$. The AWC is calculated by taking the integral of the graph which is above the estimated CP in the curve of power output for the activity. This can be visualised in Figure 27

$$AWC = \frac{1}{M}\sum_{j=0}^{M-1} (P_j - CP) * dt \tag{129}$$

where $M = 3 * 60 = 180 seconds$ (duration of 3 minute test), and the power values P_j in this case are given by

$$\begin{aligned} &\text{if } P_j \geq CP\text{: } P_j = \text{Measured power (in watt) at timestamp j} \\ &\text{if } P_j < CP\text{: } P_j = 0W \end{aligned} \tag{130}$$

The parameter α is found through $P_{max,rec} = \alpha * AWC + CP \Rightarrow \alpha = (P_{max,rec} - CP)/AWC$ where $P_{max,rec}$ is the largest measured power for the activity.

The warm-up phase consists of 25 minutes of pedaling at a constant cadence () and 80% of CP. The first 20 seconds of the 25th minute consists of a bout of heavy intensity at higher cadence and 150% of CP. This is repeated for the 26th minute. For the 27th minute, the first 10 seconds consists of a severe intensity bout of 200% of CP, which is repeated for the 28th minute. The rest of the time up to the 30 minute mark is conducted in the same manner as the first 25 minutes. At exactly 30 minutes and 0 seconds, the bout of maximal effort starts, and lasts for 3 minutes. A constant cadence is advised, in order to minimize the influence cadence can have on the

power dynamics ((39)). Leading up to the first run of the 3MT, the software GoldenCheetah had produced an estimate of CP which was at 192 W. Using the setup explained in (Section 5.1), the following curves was the result from this first run in order to estimate the physiological parameters (CP, AWC and α):

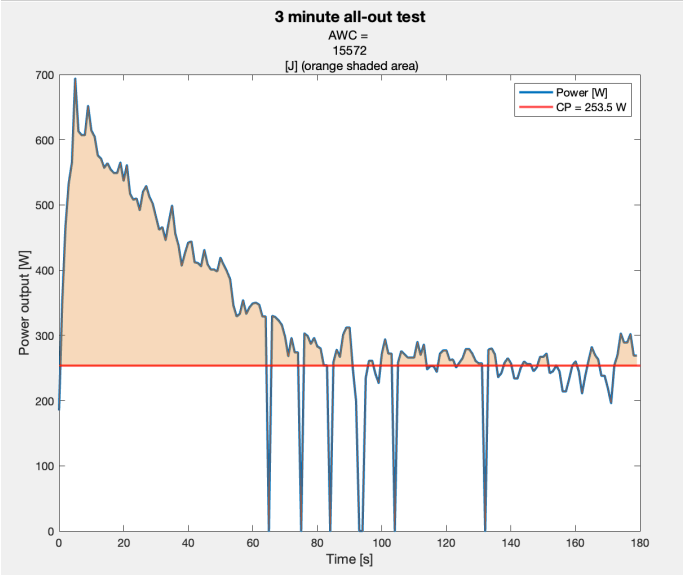

Figure 27: 3 minute all out effort to estimate the parameters CP, AWC and α. The orange shaded area, the integral between the power curve and the estimated $P = CP$, is the total AWC. See results in Section 6.4.1

The values attained from this test was $CP = 253.5W, \quad AWC = 15.57kJ, \quad \alpha = 0.0283[1/s]$ (see also Section 6.4.1). Despite the use of a different method of determination of the parameter α compared to the authors of [4] (where they used a linear fit of peak power data), the value found in this case did not differ too much. For non-professional cyclists included in the experiments, the average value of α was approximately 0.040. The average cadence throughout the entire activity (including the warmp-up) was 70 rpm, whereas the average cadence through the 3 minute maximum effort was 60 rpm. The power curve starts high, reaching its maximal values for the first 10 seconds. Thereafter, the power level steadily decreases as the maximum possible power attained on the ergometer is reduced through the relation (38). The curve levels out during the last minute, and the last 30 seconds can of this interval is what forms the basis for the estimation of the CP. A notable feature of the power curve, are the dips in power level to almost 0 which occurs six times. Luckily, such a dip does not happen during the last 30 seconds. This might be caused by a bit of mechanical slack in the pedals of the ergometer, or some numeric error. The measurement might also just measure correctly, meaning that the cyclist simply did not deliver any power at these specific moments in time.

The estimated value of CP from this test was 60 W higher than the one attained from the software Golden Cheetah. This might be an indication of the activities used in the software not representing the entire interval of possible power outputs on the power-duration curve for the individuals physiological state (i.e. that the activities did not include enough segments of "all-out", or of severe intensity). It might also just be a case of the overestimation of the parameter of the 3MT test, which was discussed in Section 2.2.5. This might be mitigated by tailoring the data processing afterwards more towards the Nonlinear-3 model (35), which also considers the maximum instantaneous power output. Temperature measured as shown in Section 5.1, was steadily rising throughout the activity, from 37.02 °C to 37.93 °C. The experimental equipment involving a fan, in order to mitigate the temperature effects discussed in Section 2, helped with the subjective experience of heat. However, it waits to be seen whether the effects will be mitigated through longer runs, like time trials. The core temperature during the activity was just below the proposed steady state core temperature for running in [30].

In light of the test protocol 3MT, other variants exist, where the duration is increased, and the goal still is to achieve an all-out effort. Examples of these are the Five-minute all-out interval (5MT) and the Twelve-minute all-out interval (12MT). In the section Section 6, different permutations and variants of these are explored and tested. Their results are processed and used in the subsequent optimisation design pertaining to the corresponding iteration. The advantages, pitfalls and controversies with the different variants are then discussed in Section 7, in light of both the experience of conducting these test protocols, as well as the results of the corresponding time-trial attempts using their parameter estimates.

5.3 Verification of a pacing strategy

To test the optimised power profile based on theory and the optimal program formulations ((127),(126)), the variant of the Bologna TT track in Zwift presented in Figure 19, was used. The equipment needed was set up as shown in Figure 26. Each attempt, either with a constant or varying power output strategy, involved a warm-up phase of 10 minutes including 3 sprints of 30 seconds spread out towards the end of the bout. In order to prevent fatigue prior to the time trials, the warm up was shorter than for the test protocols. [76] found that high intensity bouts, like sprints, in particular benefited from longer warm up phases. These two observations led to the decision of keeping the warm up prior to the time trial shorter than for a short test protocol (3 or 5 minutes of maximal effort).

Each iteration would have its own corresponding estimates of CP and AWC. The test protocols necessary to estimate these would be performed prior to the time trial tests. Furthermore, in order to verify that the pacing strategy points the cyclist in a direction of a better time performance (all though it might not be a global minimum for the optimal program), a verification attempt is performed. This attempt will consist of a time trial attempt with the pacing strategy instructions for each segment, and a constant power attempt. There should be at least 1 day of recovery between each attempt, and the constant attempt should be performed after the pacing attempt. All time trials will be run on the track Bologna TT (Figure 19).

6 Results

6.1 Validation of W'-model

Having attempted a Bologna TT (of the up-down-up variant discussed in Section 4), the model of W' dynamics derived in (108) was against the power profile of the activity. In order to measure the validity of the model, the experienced fatigue (as opposed to the muscle fatigue) and general subjective experience of the activity was compared to what the model predicted. The model used the value of CP and AWC from the test protocol iteration plotted in Figure 27. In order to aid in estimating its validity, the subjective experience was also paired with heart rate data, which could help shed light on the intensity of effort in the different segments of the track. This data might also help to determine whether there was sufficient restitution prior to the activity. Data from the activity is shown in Figure 28 and Figure 29, while results can be seen in the first row of the table in Section 6.4.2.

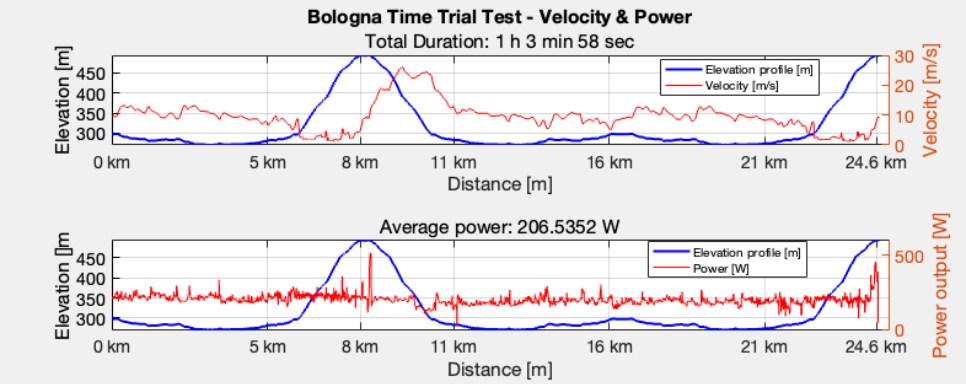

Figure 28: Test of the TT track in Bologna (3 laps). Total duration was 1 hour 3 minutes and 59 seconds, and average power was 205.5 W. The axis on the right with red colored values corresponds to the data, whereas the axis on the left corresponds to the elevation profile (in meters).

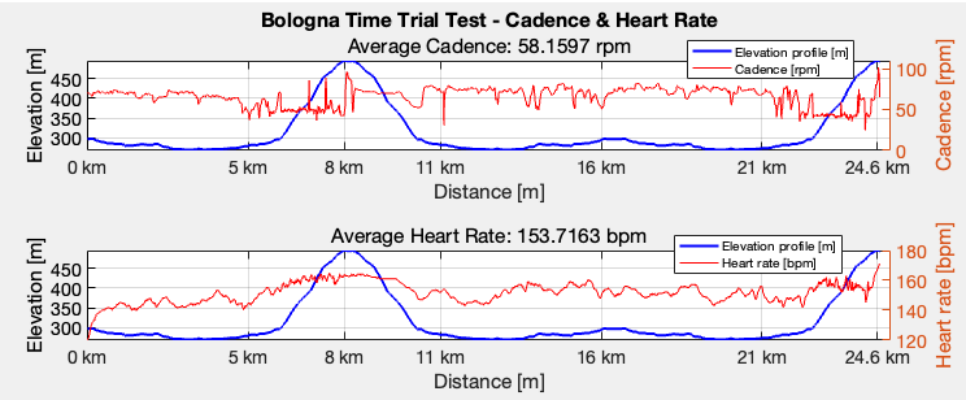

Figure 29: Test of the TT track in Bologna (3 laps). Average cadence was 58 rpm, and average heart rate was 154 bpm. The axis on the right with red colored values corresponds to the data, whereas the axis on the left corresponds to the elevation profile (in meters).

An improvised pacing strategy only based on knowledge of the elevation profile was put in practice. On the relatively flat segments, the subject attempted to stay between the two different estimates for CP, 192 W and 253 W (from Golden Cheetah, and the first 3MT test). Approaching the climb, the subject attempted to decrease the power output somewhat, before increasing it a bit when reaching the top. Going downhill, the subject attempted to gain as much velocity as possible before the steepest segments, then simply rest at very low power outputs. The same strategy is to be repeated for the second ascension, only now emptying even more of the remaining anaerobic capacity, possibly with a sprint of all-out before crossing the goal line.

Figure 28 shows a velocity trajectory which could have been expected. Decreasing when the hill has the steepest slope upwards, and increasing after the cyclist has turned around atop the hill. The power trajectory also shows the sprint which contributed extra to the increased velocity at the start of the first downhill run (spike in power data at around 8.2 km of accumulated distance). A similar type of sprint can be seen at the end of the last ascension. Cadence can be seen to drop during the steepest parts of both ascensions Figure 29. Heart rate increased considerably during the ascent, going from zone 2 (value - value) to zone 4 (value - value) during these segments. The heart rate during the sprint of the final ascent is also barely within zone 5 (value -). The temperature measurements throughout the test showed a relatively stable core temperature around 37.10 °C - 37.20 °C for the first half of the run. From the 20 km - mark up to the goal line on top of the hill, temperature steadily increased from 37.20 °C to 37.40 °C.

The cadence can be seen to drop at different points during the ride (in Figure 29, at approximately the marks of 11 km, 14 km, 15 km and 16 km). This is most likely due to the gear shifting.

Knowing when to shift gears prior to an increase in inclination, comes with the experience of having attempted to traverse a certain track before, or just a high level of experience with cycling. These transitions will inevitably affect the power output at these moments, due to the fact that there is a short period of adjustment to the desired power, at the current cadence. The current gear (and the question of it being the ideal gear for the inclination) greatly affects the cyclist's ability to attain, as well as hold, a certain power level. The proposed relationship between peak power and cadence [4] also points to the fact that there is an ideal cadence for achieving maximum possible power.

From this experience, a conclusion is that the estimated CP from Figure 27 seemed too large, based on subjective experience. At the end of the activity, the storage of remaining anaerobic capacity was experienced to be almost empty. The power profile of the activity was used, in order to create an array of the time response of $W' = w(t)$, based on (108). The choice of CP and AWC greatly affects how this time response appears. Based on the subjective experience of the time trial test, along with the heart rate data, the model was run with a value for CP between the two values coming from GoldenCheetah, and the first 3MT test. The Zwift software provided an FTP estimate after the activity was finished, at 216 W. The software describes this estimate to be the power sustainable for durations ¿40 minutes, based on activities stored on the platform performed by the subject. Using this information, the model in (108) was simulated using a value for CP skewing a bit more to this value, than the value from Figure 27. The final choice landed on 220 W. The curve shown in Figure 27 then provides an estimate of AWC equal to 20.87 kJ. The simulated time response of $w(t)$ using these values were as follows:

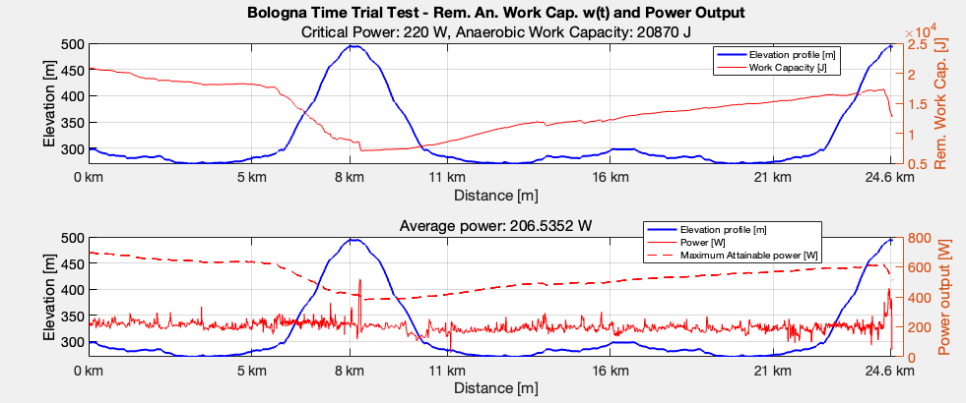

Figure 30: Test of the TT track in Bologna (3 laps). Time trajectory of the remaining anaerobic work capacity (w(t)) for the given power trajectory from the time trial test. In this case, the model from (108) was utilized with values CP = 220 W and AWC = 20.87 kJ. The axis of red colored values on the right corresponds with the remaining anaerobic capacity (in joules).

In Figure 30, the remaining anaerobic capacity seems to not be fully emptied at the end of the last ascent. The subjective experience during the activity indicated that the capacity was not completely empty at the first ascent, in line with the strategy laid out prior to the test. A hypothesis mentioned in the introductory section of this document, Section 1 noted that it might be wise to save energy going downhill, due to the diminishing returns in velocity of burning off anaerobic capacity in the downhill segments. This was remembered a bit later in the descent, as the power curve can be seen to drop to about 120 W around the 10 km mark, which is towards the end of the downhill segment. It is interesting, therefore, to note that during this drop in power, which should lead to a significant increase in reconstitution of the $w(t)$, this does not appear to happen. It might increase its rate of change slightly, but considering that during a time-trial, one rarely finds oneself in very low power outputs (0-100 W), this finding puts an even stronger emphasis on the importance of resting downhill.

The subject's intention while traversing through the segment from 10-15 km, was that the power output was dropped a bit, in order to not expend energy before starting the second ascent. The average power during this segment was 189 W. During the same segment before the first ascent (0-5 km), the average power was 215 W. The average power of the second descent was lower than

the first, which could be explained by the mounting fatigue and mental experience of the hill from the first ascent. The sprint at the very end, was intended to showcase the potential remaining anaerobic capacity. However, as Figure 30 shows, the sprint does not make it up to the estimated maximum attainable power. Another observation regarding the second ascent, is the fact that the expenditure of anaerobic capacity seems to happen later than during the first ascent. As the validation attempt was simply a test of the track with a hypothesized optimal pacing strategy, the power trajectory probably was subject to some reluctance on the subjects part to burn energy early in the second ascent. It might be due to the fact that any considerable effort above CP would simply burn the resources too quickly, and might not allow for a sprint prior to passing the goal line. However, the experience of having gone through the ascent already during the ride, and the subject somewhat struggling to mentally keep a higher power due to mounting experienced fatigue or accumulated pain sensation, could also have influenced this choice of pacing. The heart rate seems to be somewhat lower during the second descent, which might also support the latter argument.

Another observation to note, is the fact that the constraint of maximum attainable power generation is broken during a small sprint segment prior to the first descent down the hill (the spike of power output which can be seen in the lower graph of Figure 30 at around 8.2 km of accumulated distance). In light of these observations, values coming from the Golden Cheetah software were used instead, giving a different response:

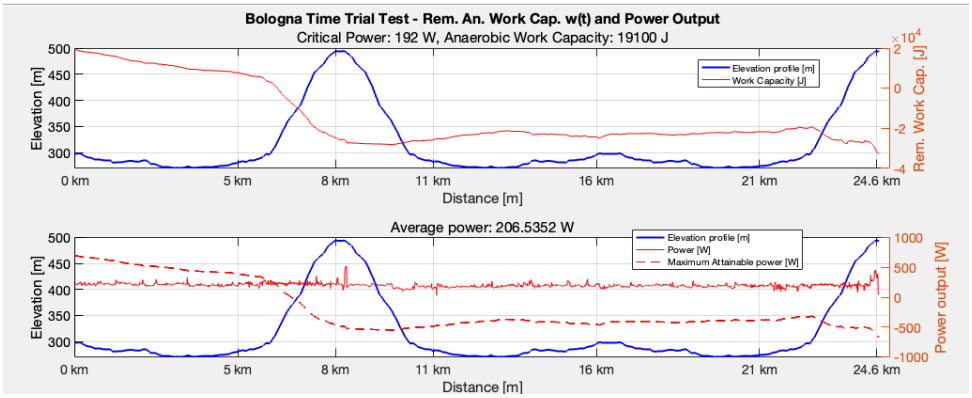

Figure 31: Test of the TT track in Bologna (3 laps). Time trajectory of the remaining anaerobic work capacity (w(t)) for the given power trajectory from the time trial test. In this case, the model from (108) was utilized with values CP = 192 W and AWC = 19.10 kJ. The axis of red colored values on the right corresponds with the remaining anaerobic capacity (in joules).

Figure 31 shows a big undershoot of the remaining anaerobic capacity. This means that the physiological values provided by Golden Cheetah, based on the training period preluding the time trial tests, are not reliable. This might be due to a change in form (for better or worse) of the subject, leading up to the testing period. it might also be due to the fact that the training schedule did not include enough activities of severe intensity, which could help explain an underestimation of the CP. Finally, the model themselves, which were used to calculate the parameters in Golden Cheetah, may also be the source of these errors. Anyhow, the CP (and most likely the AWC) of the subject must have been higher than 192 W at the time the time trial test in Figure 28 was performed. In the training software Strava, the power-duration curve is included in the interface, based on the durations of different power levels during the activity. This curve flattened out at around 206 W, and the estimated power output based on this single activity (Figure 28) for durations of 30 and 60 minutes were estimated to be 215 and 206 W, respectively.

During the first ascent, a possible danger in terms of inefficiency, is the over-use of energy during the first ascent. This segment not only demands expenditure of anaerobic capacity, but also contributes heavily to a mounting, accumulative experienced fatigue, which heavily influences the cyclist's ability to perform when starting the second ascent as well. If measuring perceived exertion in the RPE scale ([35]), the effort up the first hill during the activity in Figure 30 was something like 15 (Hard) for the subject. In comparison, the second ascent was more in the area

of 18 (Very Hard). The subject also took notice of the accumulated experienced fatigue during the second flat segment prior to the last ascent. Going forward, special emphasis has to be put on the pacing during these segments, due to their perceived "flatness" actually often including short, quite but steep segments (up to 8%).

Conclusions from the validation attempt, and the first test of the Bologna TT track, points towards the fact that there is a considerable risk in expending too much of the anaerobic capacity during the first ascent. The segment in between the descent and the second ascent might also present more difficulty with pacing than meets the eye. Developing a thorough pacing strategy through this terrain, where inclination does vary in a non-negligible manner, may reduce the risk of burning too much energy prior to the second ascent, and might optimise the velocity when entering the start of this last climb. A technical, and somewhat tactical conclusion, is the notion that a conscious relationship with gear shifts might reduce some error, when attempting to follow a pacing strategy (in the form of a power trajectory). During small increases in inclination (for instance during the segment between the descent and the second ascent), an optimal timing of a gear shift might reduce the risk of an otherwise unnecessary loss of velocity. As an addition to the hypothesis of having a sprint-like effort in the beginning, and at the top of the hill prior to the descent, the conservation of energy during the flat segment might be a preferred property of a pacing strategy.

6.2 Bologna TT Attempt 1

6.2.1 Physiological Parameters

Based on the experiences of Figure 27 and the known overestimating property of the 3MT test, actions were taken in order to more accurately estimate the physiological parameters. Due to the majority of the time trial being spent in a time-trial position Figure 3b, the test was in this case done in this position throughout. This reduced the estimated parameters somewhat, due to the standing position enabling a higher potential power output during sprints. However, the maximum recorded instantaneous power (which determines the parameter α) was set to the value found from the last test, Figure 27. In addition, the test performed in Figure 27 was modified. An extra 12 minute segment of maximum effort was added. In light of discussion regarding the overestimation of CP using a 3MT-test ([50]), new testing routines were attempted. [99] argues for an alternative processing of the power output data. The method is called a "two-test" method, and estimates the physiological parameters in the following way (CP in watt, AWC in joules):

$$\begin{aligned} CP &= \frac{(12 * P_{12} - 3 * P_3)}{9} \\ AWC &= 240 * (P_3 - P_{12}) \end{aligned} \tag{131}$$

where P_3 and P_{12} are the average power outputs during the 3MT and 12MT, respectively. The entire test consisted of 10 minutes of warm-up at approximately 150 W (the same power output level used for warm-up in the first test showcased in Figure 27), and a cadence of 60 rpm. In the 8th and 9th minute of the warm-up, the first 20 seconds were sprints at 300 W and 100 rpm. Then, at the 10 minute mark, a 3MT test was conducted. Following this, a 30 minute rest period at 100-120 W and 30-50 rpm was conducted. At the 43 minute mark, a 12 minute all-out effort was performed. Cadence topped out at the start at the same cadence held during the 3MT, but stabilised around 80 rpm for the rest of the test.

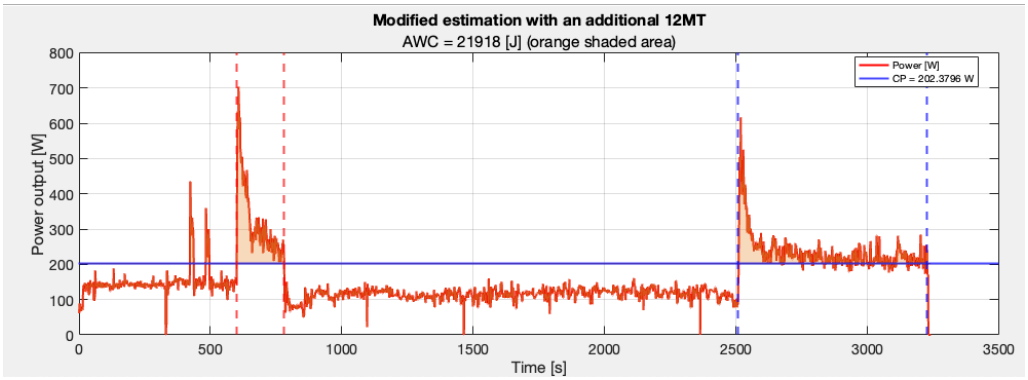

Figure 32: 3 minute all-out effort, along with an additional 12 minute all-out effort to estimate the parameters CP and AWC. The red striped vertical lines marks the 3MT, while the blue sriped vertical lines mark the 12MT. The orange shaded area within these segments, the integral between the power curve and the estimated $P = CP$, is the total AWC. See results in Section 6.4.1

The results were, as can be seen in Figure 32, $CP = 202W$ and $AWC = 21970J$ (see also Section 6.4.1). The average power of the 3MT during the previous CP/AWC test (shown in Figure 27) was 328 W. During the second test (Figure 32), the average power during the 3MT was 324 W. This difference in 4 W might be due to several causes. The variance in the data is a possibility, or the sprints in the warm-up phase prior to the 3MT being somewhat different for the original, and the modified test protocol. The warm-up phase was in both cases performed at an average of 150 W. However, the difference may also be explained by the fact that the first test was performed standing (Figure 3a), while the second was performed sitting. These positions naturally generate a different power level. Insofar as the difference stems from this, it could be argued that it should be even larger, due to the expectation that a standing position generates a significantly higher average power output than sitting in a time-trial position. Therefore, a small improvement in technique, or physical condition during the testing period, might be an explanation of this seemingly small difference in power output. The value for CP from this test coincided with the estimated power level for a duration of 60 minutes of exercise (206 W), based on the power-duration curve in Strava for the activity in Figure 28.

The parameter α was in this case also set to be $\alpha = (P_{max} - CP)/AWC$, where P_{max} is the maximum instantaneous power recorded during both the standing test at first, and the test where the subject performed the test protocols while sitting in a time-trial position. CP and AWC were set to the values found in the modified test protocol. The maximum recorded power output $P_{max} = 694W$, was found in the original test. This resulted in $\alpha = 0.02251/s$. This is the most logical value to use, seeing as the maximum instantaneous power generated on an ergometer, will likely come from a standing position for any individual. The average heart rate during the 3MT for the modified test was 158 bpm. Unfortunately, heart rate monitoring was unavailable during the original test involving only the 3MT. Average cadence during the 3MT for the original and modified tests, were 70 rpm and 90 rpm, respectively. This does indicate the possibility of the gears being set differently for the two tests. The average power, heart rate and cadence during the 12MT were 232 W, 154 bpm and 77 rpm, respectively. The slightly lower heart rate average may indicate the difficulty of staying in the "all-out" mode for the entire test, seeing as the 12MT is four times longer in duration than the shorter 3MT. The core temperature during the test protocol was estimated to stay quite consistently in the area of 37.25°C - 37.32 °C, with no significant increase during the all-out intervals. This might be a reflection on efficient cooling by the fan during the tests, and may be connected to the fact that the fan hit the subject more directly with cool air in the face in a sitting time-trial position, compared to when pedaling in a standing one.

6.2.2 Optimisation

A total optimisation of a power trajectory through the track, was performed as explained in Section 4.9. The program itself is shown in Section A.9,Section A.10. The response is shown in

Figure 33. The values for the tuning parameters of the optimisation framework was found using the same approach described in Section 4.6.

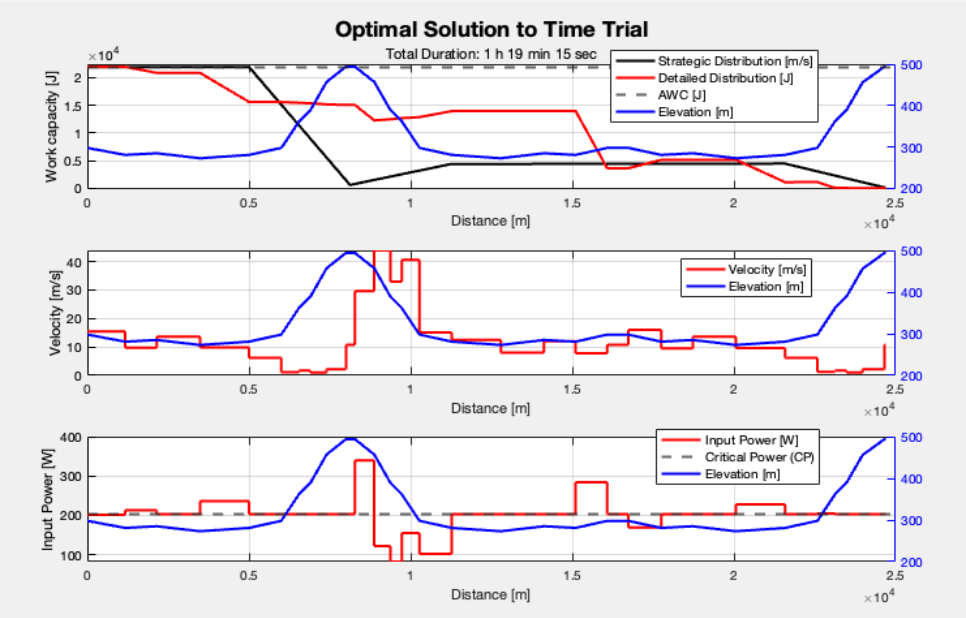

Figure 33: Optimal power trajectory and energy distribution with state responses for the simplified Bologna TT track. The upper level optimised energy distribution is shown in black in the graph at the top.The axis of blue colored numbers on the right corresponds to the elevation profile.

The second overarching segment in Figure 20, representing the first ascent, had its end point attached to the total accumulated distance of 8125 meters, which marks the middle of the flat segment on top of the hill, seen in Figure 21. However, changing this mark to the end of the flat segment on the top, right before the descent starts, in the lower level optimisation, was done in order to see the results. This was tested in light of the hypothesis that a sprint, or some sort of power increase, is necessary, in order to gain a significant velocity increase early in the descent, followed by a resting period when the steady state velocity is reached. The response shows this idea for the power graph (lower graph), only now for the segment which is the start of the descent, rather than the flat segment on the top. However. This allows for the cyclist to recover some energy during the descent. Some additional sprints seems to be preferred by the solution prior to both the first and second ascent. This is interesting, and might be a result of the model evaluating the velocity gained in the segments just before the ascent more important, than the little velocity gains possible during the ascent. It seems the solution aims to maintain a relatively high speed into the start of the hill.

The graph of remaining anaerobic capacity seems to not quite meet the requirement of the overarching strategy, but follows the plan somewhat for the start, and the segments between 15-20 km. The expenditure at the top does not exactly coincide with the recommended expenditure, and after considerable tuning of the optimisation settings, the solution would not budge. It seems as though the solution opts out of expending considerable anaerobic capacity during the ascent, and stays approximately at CP. There are four segments during the ascent, each with its own inclination percentage. One would imagine that the solution could find it advantageous for the objective (minimize time duration) to vary the power output somewhere during the ascent, but this is not seen in Figure 33.

This might have to do with the fact that each segment's optimization variable of input power has an upper limit of maximum attainable power (by the equation (38)), which depends on the optimization variable of the remaining anaerobic capacity of the next step, rather than the current. This implementation was discussed earlier, when it was found that for large steps in distance in the upper level optimisation, the inequality constraint for maximum instantaneous power was respected at most of the points on the track. This might be a shortcoming of the program design, and could

contribute to the solutions consistently failing to render the anaerobic capacity completely empty, leaving some joules left in the "battery".

In order to evaluate the power trajectory further, and in addition scrutinize the potential shortcoming of the maximum power inequality design, the states of $v(t), w(t)$ and were simulated to see the time-evolution. The time-evolution of the maximum power generation attainable was also simulated. The real track (Figure 19) was now considered. The states were simulated using an implicit midpoint method, with step size of 1 second.

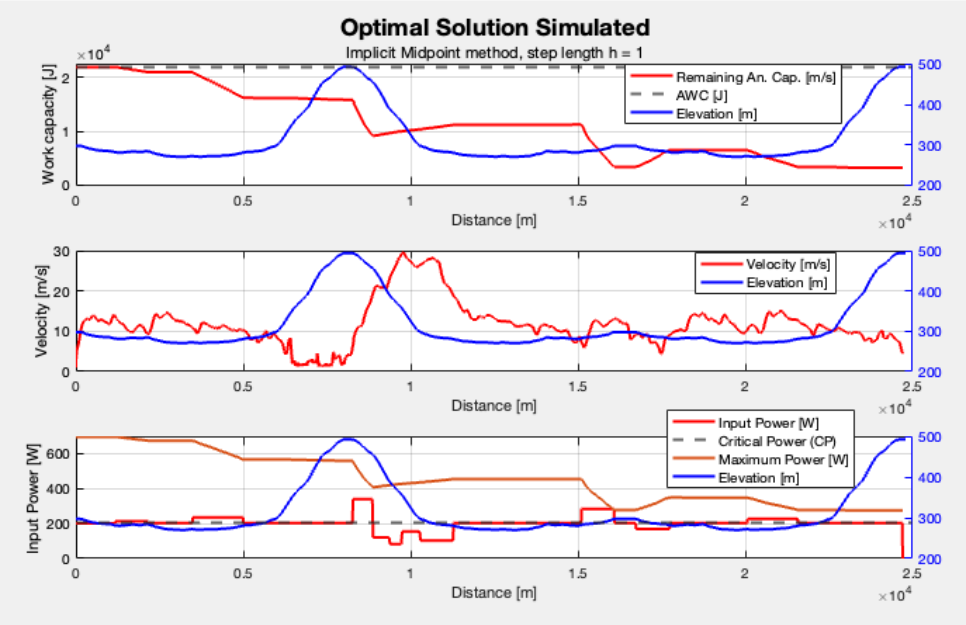

Figure 34: Optimal power trajectory and simulated state responses for the Bologna TT track. The axis of blue colored numbers on the right corresponds to the elevation profile.

Figure 34 shows state responses respecting the actual upper and lower bounds. The maximum power generation inequality is also respected by the power trajectory (for the simulated sate $w(t)$) throughout the entire track. An observation to note, is the fact that the anaerobic capacity is not empty for the last ascent. As much as 4 kJ is left when having reached the top. The state seem to be expended harder as well for the more detailed simulation than for the optimisation program. One example of this, can be seen for the segment from 10 - 15 km in Figure 33 and Figure 34. Between these two plots, for this specific segment, there is a difference in remaining capacity of almost 500 kJ. These disparities were important to note prior to the next iteration of finding an optimal solution to the power trajectory.

6.2.3 Verification of a Pacing Strategy

In an attempt to verify that the proposed optimal power trajectory, generated by the optimal program in MATLAB, actually minimizes time spent during the track, the pacing strategy was performed during a ride in the track Bologna TT. It was performed the same way as the model validation attempt in Figure 28, in the Zwift software. The results of the time trial can be seen in the second row of the table in Section 6.4.2.

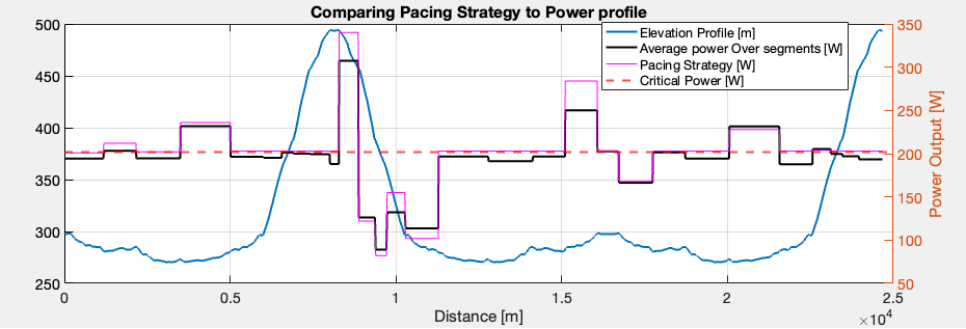

Figure 35: Optimal power trajectory and average recorded power data for the Bologna TT track. The axis on the left corresponds to the elevation profile (in blue). The largest errors between pacing instruction and average power output for a segment (in Watt), was -14% and +11% of the pacing instruction.

The power output instructions (in the color magenta, in Figure 35), were followed quite well during most of the segments. However, it seems that extreme changes (like the one right after the first top had been reached in Figure 35), lead to the most extreme errors between pacing instruction and actual power output. This is natural, due to the increased difficulty of finding the right power on the ergometer, the larger the difference in power between the two segments is. The errors themselves, seem to also have been largest during segments where the pacing instruction increases the power output significantly. During these segments (especially the segment with the largest power output during the start of the first descent in Figure 35, approximately 8 km, and the segment starting at 15 km), the average power output recorded on the ergometer was lower than the pacing instruction. The failure to follow these might then have contributed to some extra seconds of time spent on the track. The largest errors between pacing instructions and measured power output (during the aforementioned segments) are 20 W, while the smallest are down to below 1 W. During the segments with instructions at, or close to CP, the power seems to lie a bit lower than CP. This, along with the peak power values also not meeting their requirements, raises the question of whether the CP recorded in Figure 32 was too high.

The duration of the activity was 1 hour, 5 minutes and 55 seconds, which is 1 minute and 38 seconds slower than the first, non-guided attempt in Figure 28. This indicates that either the pacing strategy solution does not represent a global minimum for the problem, the optimal program design is faulty or lacks accuracy, the power output during the activity had too much error respective of the pacing strategy, or the CP and AWC values found in Figure 32 did not represent the physiological concepts they intend to represent for the subject in question (CP, in that case, being too low). The average power, cadence and heart rate during the activity was 200 W, 57 rpm and 151 bpm, respectively. These are all lower for the corresponding values in the non-guided attempt in Figure 28. The heart rate dropped significantly during the descent (averaging around 130 bpm at the bottom of the hill), indicating the significance of saving energy and recovering during this segment.

All though it is possible to achieve a worse time performance with a larger average power (for instance, through pedaling at a too high power output downhill without gaining much velocity advantage), the power difference between these two attempts clearly indicates that the proposed optimal solution for the power trajectory, is not a global solution. The heart rate also indicates that the non-guided activity was generally performed at a higher intensity level. The cadence is only 1 rpm lower for the guided attempt. This indicates either a better technical gear shift approach, or that the low frequency of new power instructions allowed for a less "random" search for optimal cadence, all though it is difficult to determine what is the optimal cadence (this is not necessarily lower than the average cadence for Figure 28). There were no instances of significant drops in cadence (down to 10-20 rpm, like in Figure 28), indicating a more stable cadence throughout. The temperature varied between 37.25 °C - 37.4 °C.

Simulating the state $w(t)$ for the entire activity in Figure 35 with the power output measured during the ride, using the dynamics of (108), and the physiological values found in Figure 32 ($CP = 202W, AWC = 21970J$)

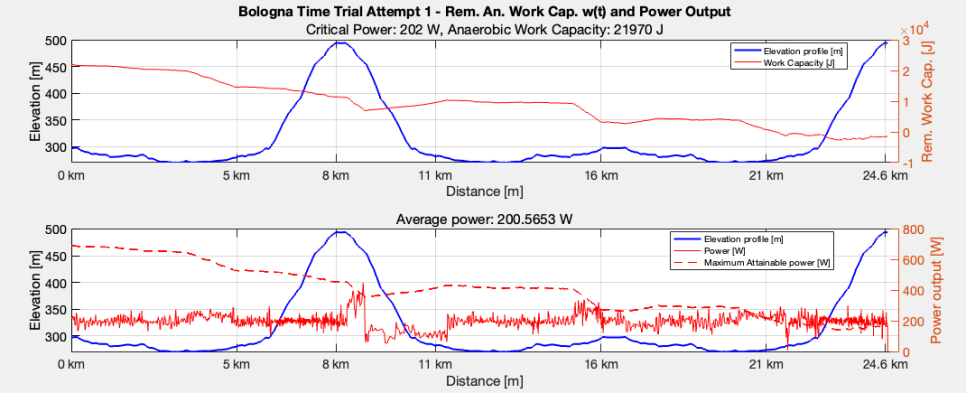

Figure 36: Remaining anaerobic capacity simulated for the measured power output on the ergometer in the upper plot. Power output measured, and maximum power constraint simulated, in lower plot. Axis on the right corresponds to the anaerobic capacity (in joules), and power output (in watt).

Figure 36 shows a simulated anaerobic capacity actually falling somewhat below 0. This indicates an underestimation of AWC. This might in turn relate to an overestimation of CP (given the positive correlation between overestimation of CP and underestimation of AWC reported in [69]).

In order to conclude that the strategy is superior to a constant power throughout (leading to a nearly empty anaerobic capacity, making it comparable to the pacing-attempt), an attempt where the power output at all times were set to the average power output from the activity in Figure 35. If the duration of the activity when passing the goal line was lower, and the pacing-strategy being compared actually was followed successfully by the cyclist, the conclusion would be that the optimisation attempt was successful. As previously uncovered, the subject cycling the Bologna TT, managed to follow the power trajectory to a satisfactory level (with the largest errors being -14% and +11% of pacing instructions). The results of a ride through the Bologna TT track, using the constant power level 200 W, is visualised in Figure 37 and Figure 38, and can also be seen in the third row of the table in Section 6.4.2.

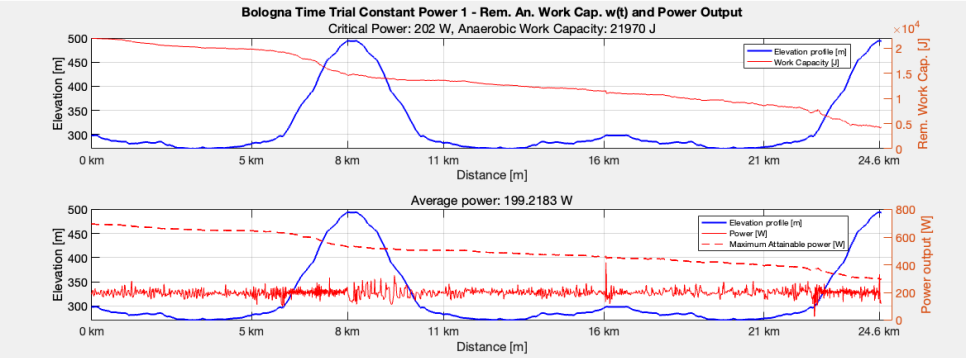

Figure 37: Remaining anaerobic capacity simulated for the measured power output on the ergometer in the upper plot. Power output measured, and maximum power constraint simulated, in lower plot. Axis on the right corresponds to the anaerobic capacity (in joules), and power output (in watt).

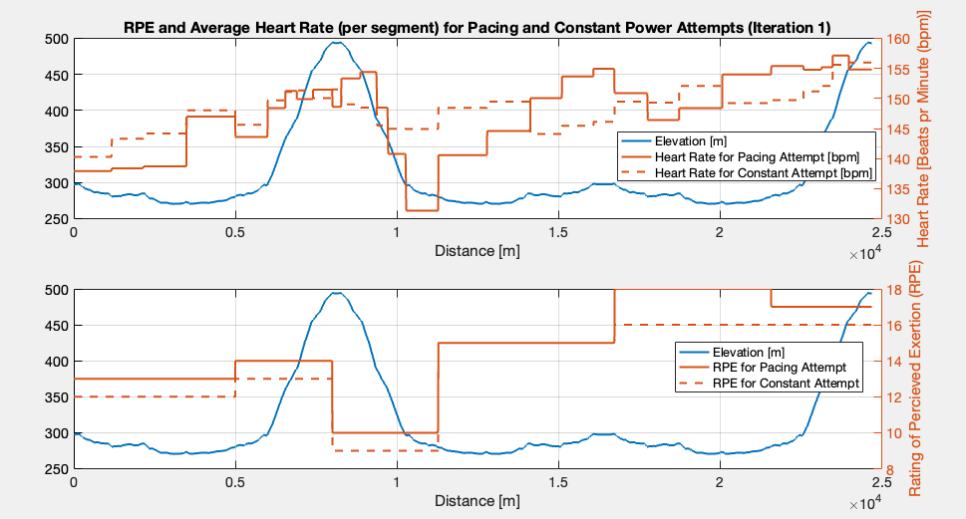

Figure 38: Average heart rate (upper plot) and RPE (lower plot) per segment. Axes for both metrics on the right. Elevation axis on the left.

Ultimately, the constant attempt had a total duration of 1 hour, 6 minutes and 16 seconds. Even though this is a slightly worse time performance than the strategy-based attempt Figure 35, it is only worse by 21 seconds. Having already seen indications of the notion that the solution in Figure 35 might not be the optimal solution for the subjects physiology, this further proves that theory. One would expect a pacing strategy to perform somewhat better. Also, an interesting observation from the results, is that the average power output measured (199 W) indicates that the cyclist could potentially have achieved a slightly better time performance, had the subject's attempt at maintaining this power been just a little more accurate. The power output measured on the ergometer is shown in red in the lower graph in Figure 37. An observation to note is the level to which the subject was able to maintain the constant power throughout. The average power is seen to be approximately the desired value, however, dips and spikes can be observed as well, which might affect physiological transients in the body which are outside of the scope of the models used. The graph also reveals the difficulty of maintaining a very specific power output on the ergometer.

In Figure 38, both the average heart rate per segment, and the perceived exertion for both activities can be seen. The heart rate in the upper graph seems to be more stable for the constant power attempt, which coincides with the strategy. An interesting note is the difference in heart rate for the pacing strategy and constant strategy during the start of the second ascent. The pacing strategy given in Figure 35 had a sudden increase in power at approximately 20 km, and it seems this effort made the entry into the second ascent quite strenuous. The high heart rate set by the sprint is maintained throughout the climb, when the cyclist stands up to pedal.

The RPE-measurements show a generally more strenuous effort for the pacing-based attempt than the constant power attempt. It is especially the segment of approximately 16-21 km which stands out. During this segment, prior to the last ascent, the strategy recommended a sprint to increase velocity. The subject's experience was that this segment was difficult to perform, due to it happening after a long distance already has been covered, as well as the fact that one more ascent is left. This last fact also kept the RPE high during the last ascent, seeing as the mounting experienced fatigue was severe at this point. If the subject is meant to achieve an effective ride up the hill during the last ascent, more energy might be needed in the anaerobic capacity, due to reasons outside of what the mathematical models can explain (mental fortitude, sensation in joints, numbness in knees, toes and buttocks, etc.). Therefore, the optimal solution, in all its mathematical rigour, might have to be aided a bit in order to be even more effective.

6.3 Bologna TT Attempt 2

6.3.1 Physiological Parameters

The experiment conducted in Figure 32 gave by all accounts a more accurate CP. This might be explained by the nature of the CP model, and its need for approximating the power-duration curve (Figure 6) by filling out as many power levels as possible for as many different durations. Ultimately, all testing protocols are simplified regression methods to this curve. Additional durations, with their corresponding power levels (and also just the addition of data), will aid in the accuracy of estimating the CP and AWC. With this as a motivation, the third attempt of estimating the physiological parameters included an additional 5MT interval. It was baked into a test protocol involving a warm-up period of 20 minutes, with 3 sprints in the range of $300 - 400W$ for 30 seconds prior to the bout.

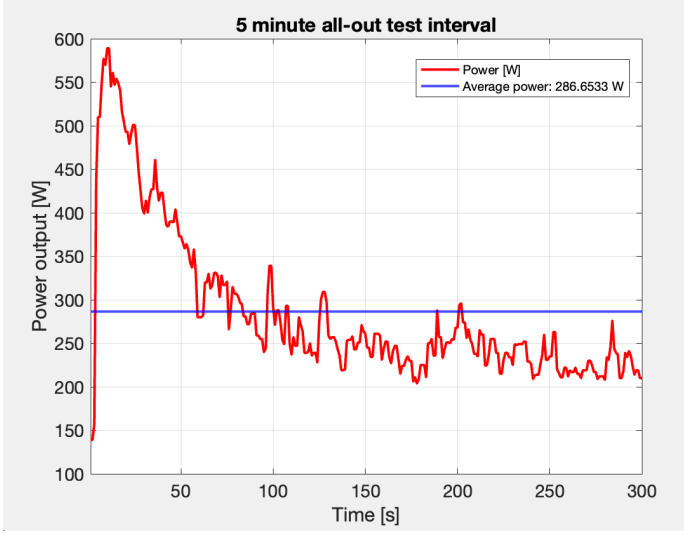

Figure 39: 5 minute all-out effort. Average power for the bout being 287 W. See results in Section 6.4.1

The 5-minute all out interval shown in Figure 39 was conducted the same way as the other all-out efforts (Figure 32), 6 days later. Due to it also happening the day prior to the time-trial attempt with the second pacing strategy, it was convenient for it to be a relatively short test protocol. Since the test protocol were not many days apart, the results were combined to form a single estimate of CP and AWC (hence, also α), based on the critical power-calculator in [100]. The calculator bases its estimate on several bouts of constant, severe intensity, but sustainable power outputs for different durations. Akin to the second test in Figure 32 and its estimation of the parameters, the principle used in [100] is to do a basic regression of the power-duration curve shaped by the power intervals. One may choose one's own intervals duration. In this case, a 3, 5 and 12 - minute interval was used. However, these were all-out intervals. The intervals recorded by the subject, used in the method, were all-out efforts. It is important to interpret the results with this in mind.

Using the calculator with the average power levels of each interval, and inserting their durations, results in the values $CP = 206W, AWC = 22kJ$. The average heart rate for the effort was 161 bpm, which was higher than both attempted 3MTs and the 12MT. A "goodness of fit" is calculated based on how well the data fits the predicted power curve. This means that if a 5-minute bout was paced badly, or the subject had a worse physical form than usual that day, the lower power estimate than expected for this interval would contribute to a somewhat worse goodness of fit. The creators of the calculators states that a goodness of fit above 97% is considered good enough. The inserted power data from the subject resulted in a 98% goodness of fit. As an attempt to add to the physiological insight, the core temperature and heart rate was measured for a short period after the effort. 2 minutes and 30 seconds after the end of the test, the heart rate had steadily fallen to 100 bpm. The heart rate had started decreasing right after the bout was

finished, and seemed to do so quite linearly with time. The core temperature started at 37.10 °C prior to the warm-up. Just prior to the 5MT, it had risen to 37.6 °C. At the end of the effort, it was at 37.5 °C, and it stayed there four minutes after the effort, before it started falling slowly.

6.3.2 Optimisation

As was seen in the last attempts of optimisation, the design segments of the lower level of optimisation Figure 21 has a big impact on the optimal solution. A conclusion gained from last iteration was, that the seemingly "flat" segments before the first, and in between the first and the second climbs, involved small peaks of inclination hidden by the simplified representation of the track (Figure 21). However, the duration, and ultimately the influence these had on the overall performance, were quite low. Also, one must remember the fact that for a cyclist, it is both difficult to maintain a very specific power output (which was demonstrated for the constant power attempt in Figure 37). One can, for the sake of simplicity for the cyclist, as well as the optimisation scheme, conclude that the flat segments (0-5 km, and 11 - 21.5 km) can be kept quite close (possibly somewhat above) CP. It is, in other words, the two ascents, and the descent, which render an interesting optimisation problem. For the second iteration of optimisation, these experiences was kept in mind when attempting to produce the final optimal solution for a pacing strategy.

For the lower level problem, a contentious issue regarding the implementation was the inequality constraint for the maximum power P_{max} ((38)). The implementation used in the first iteration Section 6.2 had simply constrained the optimization variable representing the input power for each segment ($u_k, \quad k = 1, 2, ...N - 1$, where N is the number of distance points). For this iteration, another, slightly different implementation was used. On the surface, the implementation seems quite similar, and it represents the same mathematical model for maximum power generation, only that it also considers the model of expenditure for $u > CP$ in (108). The new power constraint is set to

$$u_k \leq \alpha * (w_k - t_k * (A_n(u_k) * (u_k - CP))) + CP \tag{132}$$

This resulted in the new formulation for upper level optimisation to be

$$\begin{aligned}
\text{States and input: } & x_k = [t_k \quad v_k \quad w_i]^T, \quad u_k = u(k), \text{ where } k = 1, 2, ..., N-1 \text{ and } i = 1, 2, ..., N \\
\text{Objective Function: } & \sum_{k=1}^{N-1} t_k, \\
& \text{for } t_k = \frac{D(k+1) - D)(k)}{v_k} \\
\text{Initial conditions: } & x_0 = [t_{ss,0} \quad v_{ss,0} \quad AWC]^T, \\
\text{Dynamic constraints: } & v_k = v_s s(u_k, \theta_k) \\
& w_{k+1} = w_k + t_k dw(w_k + (t_k/2)dw(w_k, u_k), u_k), \\
\text{Inequality constraints: } & S_{min}/v_{ss}(u_{max}, \theta_{min}) \leq t_k \leq S_{max}/v_{ss}(u_{min} \\
& v_{ss}(u_{min}, \theta_{max}) \leq v_k \leq v_{ss}(u_{max}, \theta_{min}) \\
& 1 \leq w_k \leq AWC \\
& u_{min} \leq u_k \leq\leq \alpha * (w_k - t_k * (A_n(u_k) * (u_k - CP))) + CP
\end{aligned} \tag{133}$$

The optimisation scheme for Section 6.2 also respected this expenditure model, however not so directly. It had to search for optimal input power, while also respecting the constraint of the dynamics of w_k separately. For this iteration, the experience was that the optimal program spent less time finding possible pacing strategies, which may be due to the fact that infeasibility became far less prevalent with the new power constraint (132). Keeping the old constraint implementation for the upper level optimisation, it gave the following optimal solution of energy distribution:

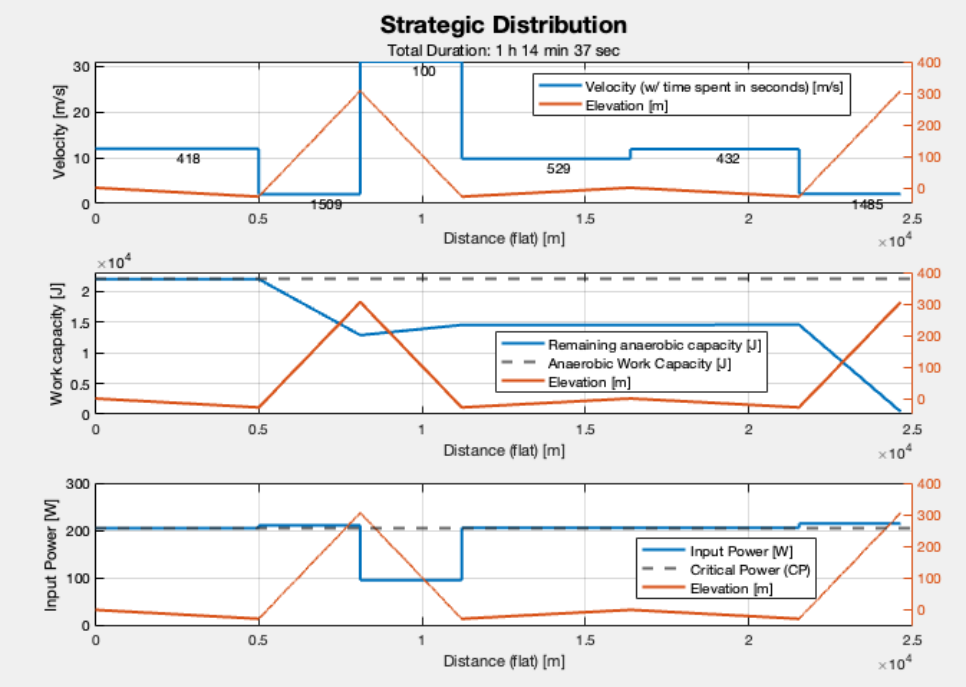

Figure 40: Optimal power trajectory and energy distribution with state responses for the simplified Bologna TT track. The time spent (in seconds) is shown in black above each segment of steady state velocity.

Compared to the previous solution, Figure 40 shows an overarching energy distribution more intent to savour some energy at the first ascent, all though expending half the capacity. The downhill slope is also now used as a recovery period, and the last ascent, possibly thanks to the new inequality constraint (132), allows for the scheme to completely drain the capacity in the end. This, in turn, allows for a more accurate estimate of the remaining anaerobic capacity at the key points in the track; the start, the beginning of the first ascent, the top, the bottom of the descent, the middle of the flat segments, the bottom of the final descent, and finally, the finish.

The experience of previous time-trial attempts, as well as the observation that the predicted P_{max} could sometimes be superseded by the power output measured, simulated sprints were injected into the solution of energy distribution at certain points, in order to completely drain the W'. It seems through exploration of the optimal program design, as well as the difficulty of estimating physiological parameters, that the exact power levels required to fully empty the anaerobic capacity comes with a lot of uncertainty. There are also some very detailed segments where velocity gains could be had, which are difficult to capture entirely with the coded optimal program used in this project. Examples of points where sprints could be injected was the start, in order to gain a high initial velocity relatively quick. The start of the descent was also interesting as a sprint scenario, due to the fact that a high velocity early could potentially result in a longer duration of recovery for the cyclist. Exactly how this would affect the overall performance remained to be seen, but the energy these sprint required would be subtracted from the initial remaining anaerobic capacity in the solution generated in Figure 40 at the corresponding points in the track.

The last place in the track which was deemed a candidate for such a sprint was literally the last place in the track. Prior to crossing the finish line, experience pointed towards there always being some extra capacity left (for the attempts in Figure 28 and Figure 35) which could gain a velocity advantage. The uncertainty of the anaerobic factors involved in sprints like these could explain the possibility of these sprints being highly plausible as executable efforts, despite the seemingly "empty tank" (for instance at the very end of the activity). However, this was not simulated, and only performed during the last part of the final descent of the attempt, in order to see exactly how much power would be possible to squeeze out, if there would be some capacity left.

The start is particularly interesting, due to the fact that the cyclist goes from a stand still,

to some steady state velocity. Below, the results of such a sprint were simulated. The first 175 m are completely flat an ideal for such a sprint. Using the average power from the first 3MT (Figure 27), which was 324 W, a sprint at this average power level took approximately 1.5 kJ to reach a velocity of 8 m/s (30 km/h) which is, based on optimal solutions produced earlier, an acceptable starting velocity. The simulation is only serving as a guide for the energy distribution, which, in turn, serves as a guide for the lower level optimization.

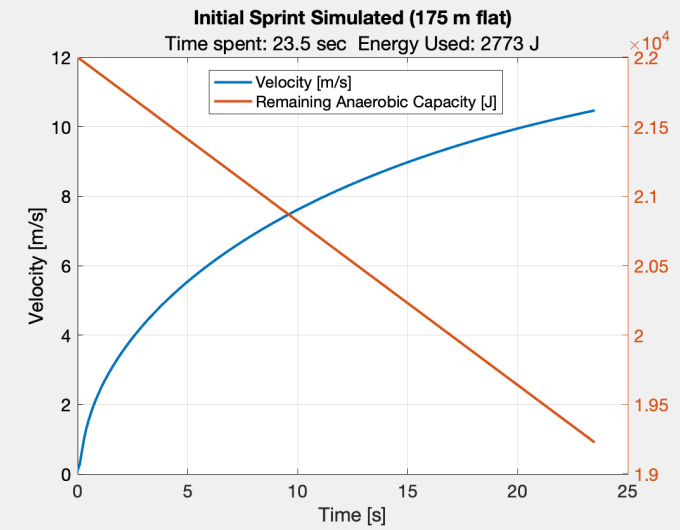

Figure 41: Short sprint simulated in order to predict amount of capacity needed at the moment the activity starts

Figure 41 shows the sprint for a constant power output of 324 W. At the mark of 8 m/s, the remaining anaerobic capacity is seen to have been reduced by approximately 1.5 kJ. This power output is then the guiding value which could be kept by the cyclist for approximately 200 meters at the start. With the sprint in mind, the capacity needed for the sprint was subtracted from the first part of the energy distribution of Figure 40. Meaning, that the shape of the energy distribution was kept, only with the capacity held prior to the last ascent now being 1.5 kJ lower. Additionally, the area of transition from the flat summit to the start of the descent, was made more detailed, involving several, smaller segments. This resulted in an increased amount of infeasibility, and tuning the parameters gave no satisfactory solutions for the power trajectory. A different implementation was pursued.

In order to produce a reasonable, and feasible power trajectory, with a faster time performance, and a more intuitive strategy than the one presented in Figure 33 was achieved. The initial sprint, and its requirement of energy expenditure, in combination with the upper level instructions for energy distribution in Figure 40 was utilised. The flat segments of 0-5 km and 11-21.5 km were kept at a constant power level at the current estimate of CP (= 206 W). Additionally, the first ascent was solved using almost the same lower level implementation as for the first iteration of attempts. A small alteration of this program, saw the objective function include a term representing the remaining anaerobic capacity w_k at the top, and the instructed remaining capacity (minus the energy cost of the initial sprint, which is within the logic the model dynamics in (108), because the flat segment prior to the ascent keeps the $w(t)$ unchanged). The objective function became

$$F(t, v, w, u) = c_1 \sum_{k=1}^{N-1} t_k + c_2((\Delta W) - \sum_{k=1}^{N-1} (A_n(u_k)(u_k - CP)))^2 \tag{134}$$

where N is the number of points of accumulated distance along the track (specific points being 5 km, 6 km, 6.6 km, 6.9 km, 7.4 km, 8 km, with their corresponding elevation levels), ΔW is the total amount of energy (in Joule) to be expended during the ascent based on the upper leven energy distribution (Figure 40), and c_1, c_2 are weight parameters. This resulted in the new

formulation for the lower level optimisation

$$
\begin{aligned}
\text{States and input: } & x_k = [t_k \quad v_i \quad w_i]^T, \quad u_k = u(k), \text{ where } k = 1, 2, ..., N-1 \text{ and } i = 1, 2, ..., N \\
\text{Objective Function: } & \sum_{k=1}^{N-1}(t_k) + \\
& \text{for } t_k = \frac{D(k+1) - D)(k)}{v_k} \\
\text{Initial conditions: } & x_{init} = [t_{ss,0} \quad v_{ss,0} \quad wInit]^T, \\
\text{Dynamic constraints: } & v_{k+1} = v_k + t_k dv(v_k + (t_k/2)dv(v_k, u_k, \theta_k), u_k, \theta_k) \\
& w_{k+1} = w_k + t_k dw(w_k + (t_k/2)dw(w_k, u_k), u_k), \\
\text{Inequality constraints: } & S_{min}/v_{ss}(u_{max}, \theta_{min}) \leq t_k \leq S_{max}/v_{ss}(u_{min} \\
& v_{ss}(u_{min}, \theta_{max}) \leq v_k \leq v_{ss}(u_{max}, \theta_{min}) \\
& 1 \leq w_k \leq AWC \\
& u_{min} \leq u_k \leq P_{max}(w_{k+1}) = \alpha w_k + CP
\end{aligned}
\tag{135}
$$

The optimisation scheme in (135) now excludes a terminal condition for w_N, and simply includes this requirement in the objective function. The same split of segments was used as in Figure 21 for the ascent, and c_1, c_2 were both set to 1. The method of injecting the upper level energy distribution with the initial sprint, led to the initial condition for w_k being $wInit = 20,5kJ$ prior to the ascent. The bounds on power output were set to $u \in [CP \quad P_{max}]$. The remaining capacity at the top of the hill would be $11.4kJ$. This resulted in the following power trajectory:

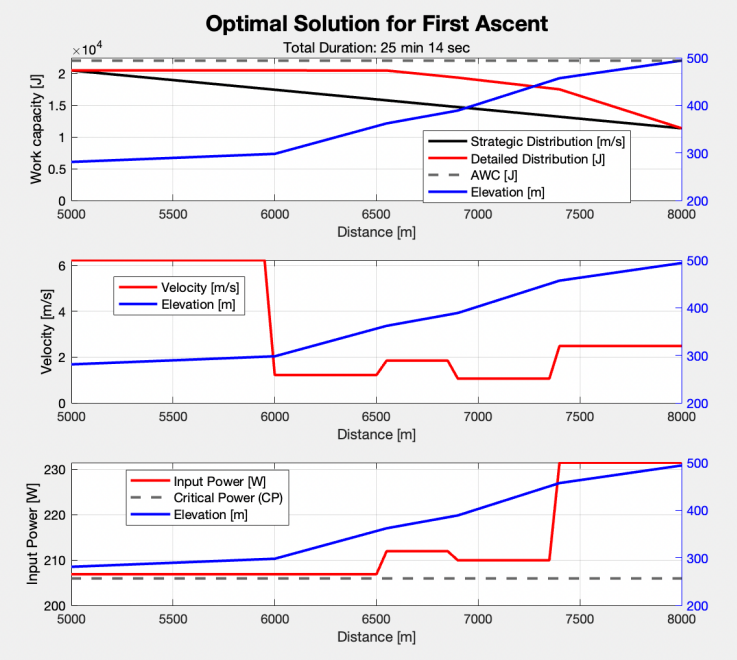

Figure 42: Proposed optimal power trajectory for the first ascent.

Figure 42 shows the remaining capacity (upper plot) being reduced to the amount required by the overall plan, in a much more effective and direct way than for the last iteration (where the relationship between the upper and lower level optimisation was dubious, at best, seen in Figure 24). The relatively low velocity levels seen in Figure 42 coincided with the subject's experienced velocity from previous time-trial attempts up the steepest segments (albeit performed at lower power levels).

Following the proposed optimal solution, a sprint at the top of the hill, prior to the descent, was optimised, in order to gain an acceptable velocity for the downhill segment, before the cyclist would recover capacity by maintaining a power output strictly at 0 for the entire descent. The sprint had the same exact power bounds as the first ascent. Recovery of anaerobic capacity was simulated for a power level $u = 0$ W in order to uncover the minimum required capacity left after the sprint in order to return to the level set at the bottom in Figure 40, minus the requirement of the initial sprint earlier. Descents usually takes 1.5 - 2 minutes, therefore the simulation below (Figure 43) shows that a level of $10kJ$ after the sprint at the top, would result in the desired remaining capacity after the recovery period downhill (figure shows approximately 13 kJ at 1 minute and 40 seconds).

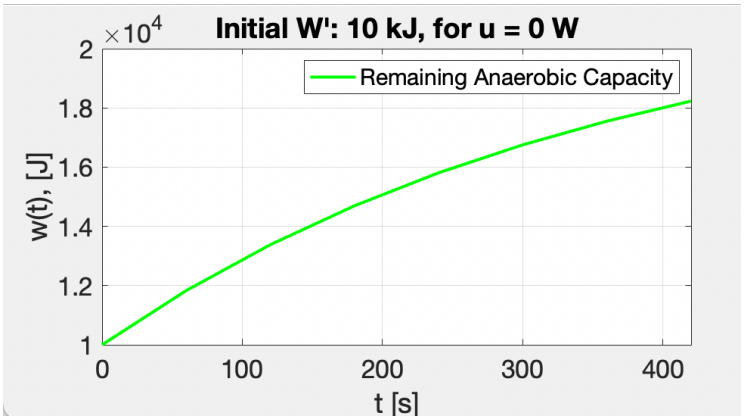

Figure 43: Simulated remaining anaerobic capacity during the downhill segment for a power level $u = 0W$, after the sprint at the top.

The sprint problem on top of the hill prior to the descent was set up in a somewhat different way. The program simulated states for every 100 m, from the 8 km mark, to the 8.4 km mark. Exactly where this interval should start and stop is an open debate, but these limits were decided. The dynamics used to simulate the time evolution of states used the implicit midpoint method ((73)), and the objective function used the same objective function as in (134). The bounds on the input were $u \in [CP \quad P_{max}]$, forcing the program to produce a power trajectory which would expend aerobic capacity. The starting capacity was set to 11.3 kJ, and the end capacity to the level found in the recovery simulation in Figure 43. The result is shown below

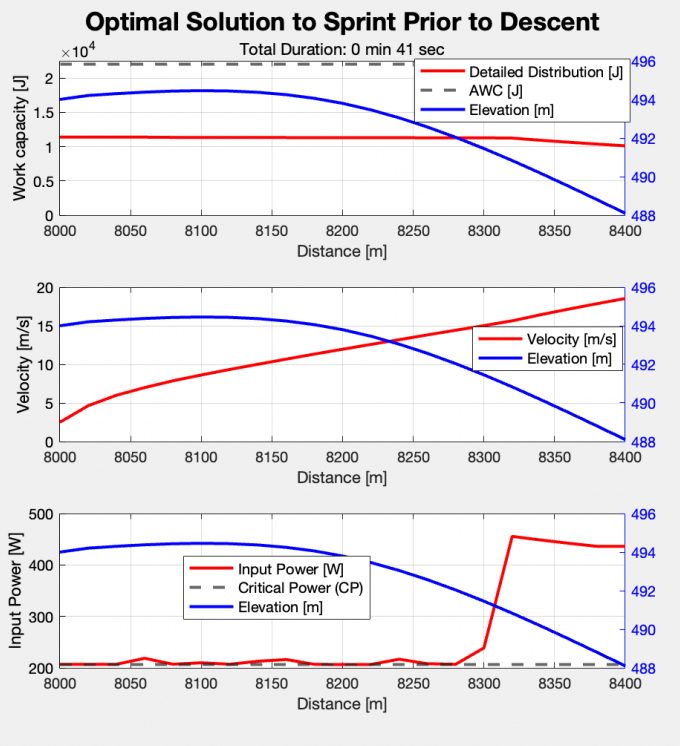

Figure 44: Optimal power trajectory for the short sprint problem prior o the descent, expending 1.3 kJ of anaerobic capacity. Program for this sprint shown in Section A.8

The final ascent was based on the first ascent, taking the same exact shape of the power trajectory. In order to see the effect this had on anaerobic capacity, the overall proposed strategy was simulated using the implicit midpoint method for the every 1 m on the track. The results can be seen in Figure 45

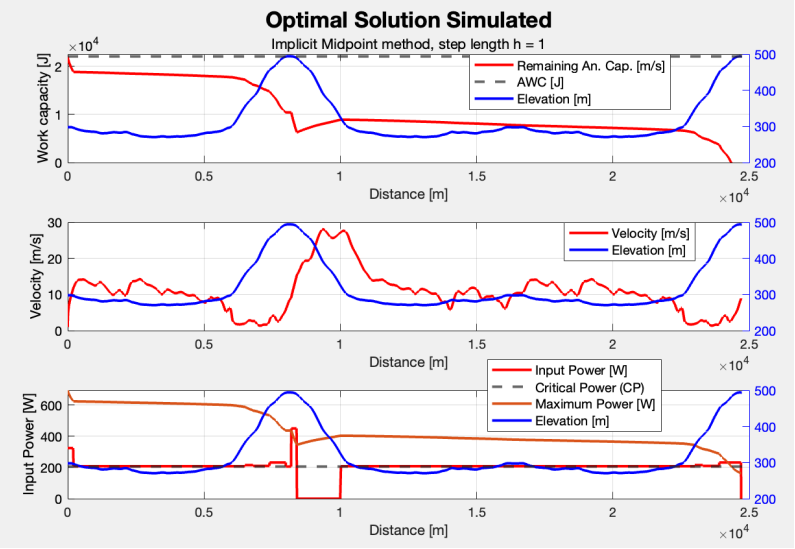

Figure 45: Proposed optimal power trajectory for the entire time trial simulated with states velocity $v(t)$ and remaining anaerobic capacity $w(t)$, as well as the maximum power attainable based on the anaerobic capacity. Time spent projected to be 1 hour and 48 seconds

The upper graph in Figure 45 shows an anaerobic capacity which looks a lot like the proposed upper level energy distribution in Figure 40, even though the total proposed trajectory expends a bit more when it reaches the first top, and goes a bit below zero for the finish line (-1.8 kJ).

Whether or not the cyclist will be able to keep the proposed power instructions, or stay a bit above, remains to be seen, and will be a comment on the estimate of physiological parameters for the subject, as well as the optimal solution produced for the final iteration. Comparing with the first iteration (Figure 34), this iteration of the optimal trajectory focuses more on the peaks, and the energy distribution regarding the entry and exit of those segments. The initial sprint, all though not proposed by the optimal program, also plays a small role in the evolution of the remaining anaerobic capacity throughout the track, and might also aid in achieving important velocity gains at the start.

6.3.3 Verification of a Pacing Strategy

In order to ensure that the optimal solution found in Figure 45 was better than a non-paced, constant power effort needs to be performed throughout the track Bologna TT. The normalized power was planned to be used to set this constant power level, as opposed to the average power output measured throughout the exercise, as has been used in previous attempts. However, due to time constraints in the project, the constant power attempt needed to be completed prior to the pacing attempt. The constant attempt, shown in Figure 46, was completed just the day before the final pacing attempt, which was sub-optimal in terms of recovery and what demands are put on a cyclist for a pacing attempt, compared to a constant power attempt. The former demands more physically due to the bouts of significantly increased power output, and is also experienced as a tougher challenge mentally.

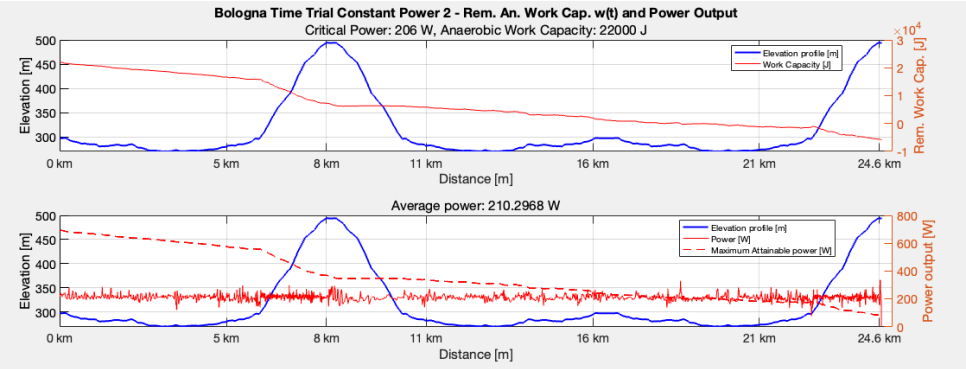

Figure 46: Remaining anaerobic capacity simulated for the measured power output on the ergometer in the upper plot. Power output measured, and maximum power constraint simulated, in lower plot. Axis on the right corresponds to the anaerobic capacity (in joules), and power output (in watt).

The average power held throughout was estimated to 210 W. The normalized power, however, was estimated to 211 W. Average cadence was 58 rpm, average heart rate was 153 bpm (shown in Section 6.4.2). The average temperature, at 37.7 °C, was considerably higher than the other attempts with both constant and varying power trajectories. The temperature measurement was started at the beginning of the warm up for this final time trial attempt. The temperature increased from 37 °C to 37.3 °C after the warm up. This is the same temperature level achieved after longer warm-ups prior to shorter test protocols, indicating that an acceptable body temperature has been reached. An interesting observation is to which level the subject was able to hold the constant power, and avoid all types of pacing.

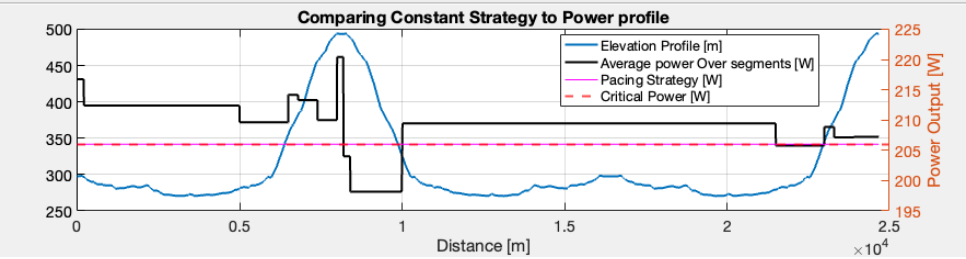

Figure 47: Comparing the constant power attempt to actual constant power, at CP = 206 W.

The attempt shown in Figure 47 show some forms of pacing, but it might also show shifts in power due to gear shifts and the difficulty of finding the right cadence. The pacing strategy attempt based on Figure 45 was attempted the day following the constant power attempt for the second iteration.

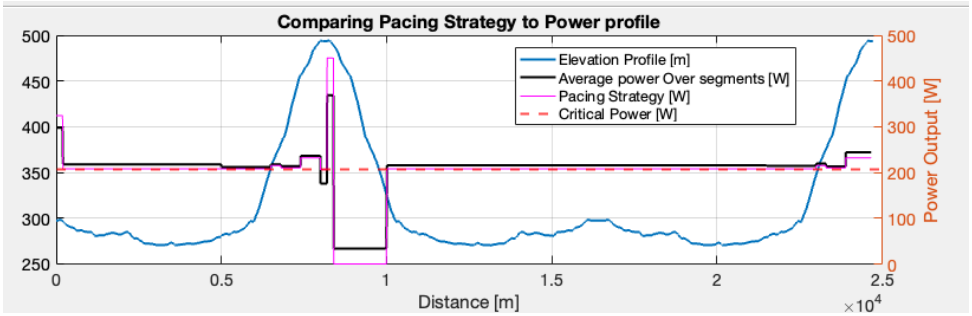

Figure 48: Optimal power trajectory and average recorded power data for the Bologna TT track. The axis on the left corresponds to the elevation profile (in blue). The largest errors between pacing instruction and average power output for a segment (in Watt), was -18% and +5% of the pacing instruction.

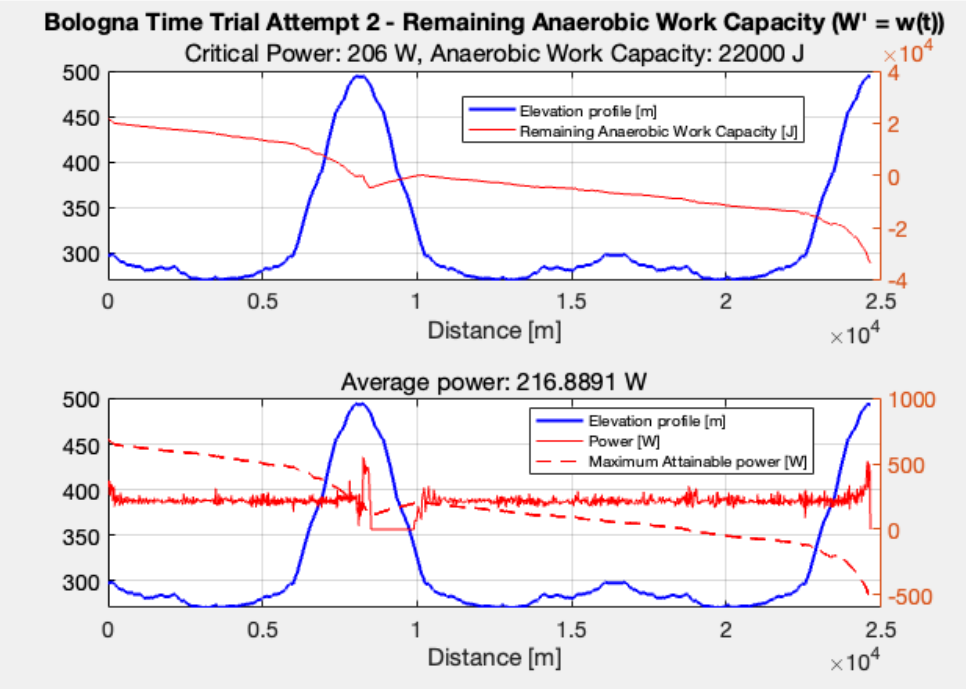

Figure 49: Remaining anaerobic capacity simulated for the measured power output on the ergometer in the upper plot. Power output measured, and maximum power constraint simulated, in lower plot. Axis on the right corresponds to the anaerobic capacity (in joules), and power output (in watt).

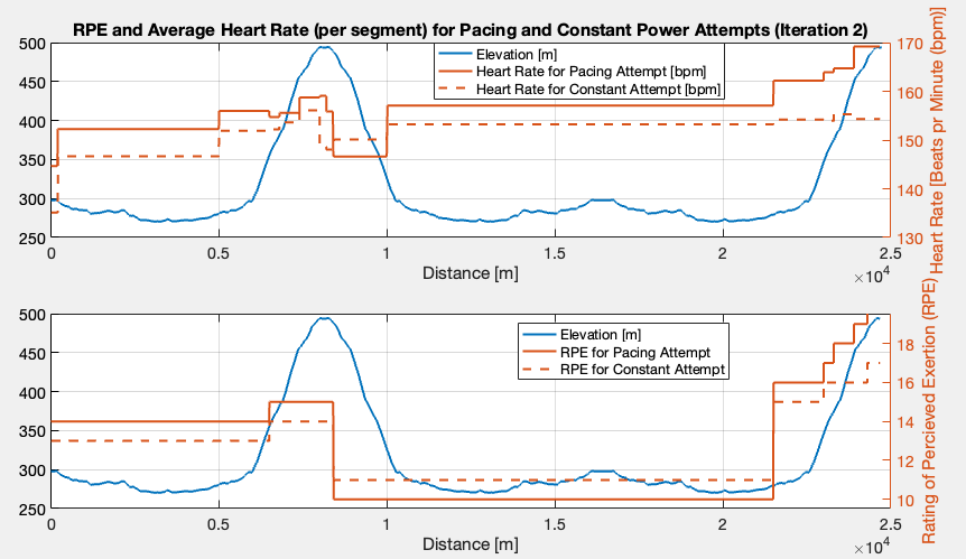

Figure 50: Average heart rate (upper plot) and RPE (lower plot) per segment. Axes for both metrics on the right. Elevation axis on the left.

For the guided attempt in the second iteration, the average power was 217 W. This was 7 W higher than the constant attempt, which will be a source of discussion in later sections. The average metrics are given in Section 6.4.2. Ultimately, the time performance for the last iteration got better with the pacing strategy, albeit with a higher average power. The guided attempt was 1 minute and 42 seconds faster than the constant attempt where the subject intended to maintain the CP level throughout (= 206 W for the last iteration). The subject inserted a sprint in order to test whether the estimated remaining anaerobic capacity was actually empty prior to crossing the finish line. This can be seen in the lower graph in Figure 49

6.4 Overview of Results

6.4.1 Test Protocols for Physiological Parameters

An overview of results from each of the physiological test protocols, determining the model parameters CP, AWC and α. P_{max} was found for the first 3MT test (Figure 27) while standing. The first attempt at estimating the physiological parameters was done through the 3MT method, where the final 30 seconds of the 3MT was estimated to be the CP, area between the graph of the measured power output, and the estimated CP was considered to be the AWC. This test was done in a standing position, and the maximum instantaneous power measured when standing while pedaling (694 W) was used in order to determine α. All the other test intervals were done in a time-trial position (Figure 3b). α was determined in later iterations, also while solving the simple equation $P_{max} = \alpha * AWC + CP$, for the maximum instantaneous power recorded during the first 3MT (standing pedaling, 694 W), and for the corresponding values for CP and AWC.

Row 2 used the two-test method [99] with a 3MT, and a 12MT, using the equations (131) for estimating the parameters. The third estimate used the online calculator [100] in order to estimate parameters in the three-test method. The subscripts of the intervals in the second column defining the protocol, denotes which session of test protocols the interval belongs to (a total of 3 sessions). For the fourth and fifth estimate below, the values from the second (Figure 32) and third (Figure 39) were used in different permutations of the two-test method, now using the online calculator [100] instead of the equations (131).

Est.	Protocol	Position	CP [W]	AWC [kJ]	P_{max} [W]	α [1/s]
1	$3MT_1$	Standing	254	15.6	694	0.028
2	$3MT_2$+$12MT_2$	Time-Trial	202	22.0	694	0.023
3	$3MT_2$+$5MT_3$+$12MT_2$	Time-Trial	206	22.0	694	0.022
4	$3MT_2$+$5MT_3$	Time-Trial	232	16.6	694	0.028
5	$5MT_3$+$12MT_2$	Time-Trial	193	28.3	694	0.018

Table 2: Results from all test protocols involved in determining the parameters CP, AWC, α and P_{max}

6.4.2 Time-Trial attempts

An overview of results from each of the three time-trial attempts on the Bologna TT track (in Zwift). The columns, from left to right, describes the attempt number, along with the corresponding estimated CP prior to the attempt, the average measured power output, the normalized power [101], the average heart rate, the average cadence, the average core body temperature, the strategy (P: non guided, but paced attempt, P+: guided attempt with pacing strategy, or C: constant power attempt), and the duration of the entire exercise. Power, cadence, heart rate and core body temperature are all averages of all measurements done throughout the exercise. Average power, heart rate and cadence in Table 3 are all paired with the standard deviation of their respective data sets (measured in the same units as the mean values). The mean of a data set ([102]) is given by

$$\bar{x} = \frac{\sum_{k=1}^{n} x_k}{n} \tag{136}$$

where n is the number of data points and $x_k, \quad k = 1, 2, ...n$ is the data set. The standard deviation ([102]) of a data set is given by

$$\sigma = \sqrt{\frac{(x_1 - \bar{x})^2 + (x_2 - \bar{x})^2 + ... + (x_n - \bar{x})^2}{n}} \tag{137}$$

TT	CP	AP [W]	NP [W]	HR [bpm]	C [rpm]	T [°C]	S	Dur.
1	254	205 (33)	210	154 (6)	58 (13)	37.2	P	1 h 3 m 59 s
2	202	200 (34)	205	151 (8)	57 (13)	37.3	P+	1 h 5 m 55 s
3	202	199 (23)	200	151 (4)	55 (11)	37.2	C	1 h 6 m 14 s
4	206	210 (20)	211	153 (4)	57 (11)	37.7	C	1 h 3 m 52 s
5	206	217 (47)	221	158 (6)	56 (13)	37.3	P+	1 h 2 m 10 s

Table 3: Table showing the results from time trial attempts of both iterations, their respective attempts of constant power for comparison, and the initial attempt of a strategy based on intuition.

6.4.3 Time Schedule of Tests and Attempts

Time in between tests and time-trial attempts was an important consideration when discussing the results from these tests. First column is the date of the session, and the second is what type of activity it was (TT_p = Time Trial with pacing, TT_c = Time Trial with constant power output, TP_x = Test Protocol, where the subscript, possibly multiple, denotes the duration of the interval(s) performed, in minutes). The third column is the time of day of the session, and the last column is the subjective experience of the level of energy abundance in the body prior to the activity (scale of 0-10). Not getting the proper recovery time in between sessions may have affected the data in some ways, which will be discussed in Section 7.

Date	T.o.D.	Type	S.E.
5 May	18.00	TP_3	8
16 May	19.15	TT_p	9
23 May	21.00	$TP_{3,12}$	8
24 May	10.30	TT_p	8
28 May	09.30	TT_c	7
29 May	20.00	TP_5	8
30 May	20.00	TT_c	7
31 May	18.45	TT_p	7

Table 4: Time schedule listing the total number of activities performed for data collection.

7 Discussion

7.1 Results

7.1.1 Bologna TT Attempt 1

A seemingly clear fault of the first pacing strategy (shown in magenta, in Figure 35), is the lack of a sprint in the end of the activity, which would have emptied the remaining anaerobic capacity completely (optimal program concluding that it lands at 3.8 kJ when passing the goal line). However, the plot in Figure 36 shows a remaining anaerobic work capacity (for the given physiological values CP = 202 W, and AWC = 21970 J) a bit below 0. The latter plot was generated using more accurate dynamics (smaller time steps, and time-varying dynamics for velocity, as opposed to steady state velocities for each segment). This indicates, as previously hinted in Section 6.2, that the parameter AWC was underestimated following the physiological test protocol pertaining to this verification attempt. The disparity between the remaining anaerobic capacity at the end of the activity estimated from the optimal program used in the first verification attempt (Section 6.2), and the simulated remaining capacity, was most likely due to the constraint setting an upper bound for input power u. Comparing this time trial attempt to the first attempt (row 1 in Table 3) further indicates and underestimation of CP, as well.

Table 3 shows standard deviation estimates for the constant and pacing attempts at Bologna TT. For the constant attempts, the standard deviation is less than for the pacing attempts, which coincides with what would be expected, due to the varying nature of a pacing strategy. The relatively high standard deviation values for the constant attempts, further proves the difficulty of maintaining certain power level throughout the activity. The difference between mean power for the constant attempt, and the pacing strategy, for the first iteration (row 2 and 3 in Table 3, respectively), is relatively small compared to the standard deviation. This indicates that the results of this test are reliable in terms of the success of a varying pacing strategy, no matter what flaws lie in the strategy itself.

For this iteration, the steady state dynamics (126) were used for both the upper level and lower level optimisation. The upper level gave, as planned, a strategic distribution of energy throughout the track. The lower level was simply a more detailed version of the same program used in the upper level (a higher number of smaller segments, shown in Figure 21). The pacing strategy however (Figure 35), seemed to also deviate somewhat from the hypothesis that it is beneficial to seek velocity gains during the ascent, more so than during the descent. The segment of relatively high power output (8-9 km approximately), seems to go on for quite some distance down the hill as well. This tendency, which was visible for several other attempted optimal solutions, indicates that the optimal program used for iteration 1 had either not reached the global minimum in its solution, or that the implementation somehow prevented the program from finding the real minimum. The program in (126) uses steady-state dynamics, which means that the velocity reached in one segment, does not affect the next one. For increasingly small segments, this might hide the potential advantage of increasing the velocity prior to the descent from the optimal program. An attempted solution to this was implemented for the next iteration, where the transition from flat

to descent (8-9 km into the track) was split into smaller segments, allowing for the optimal solution now to give more detail into this "sprinting" segment.

The tendency for the program to diverge from the hypothesis of burning more energy when the inclination increases might also be explained by the way the track was segmented for the lower level problem. The details of where each segment starts and stops, and its corresponding inclination, greatly affected the programs ability to produce an optimal solution. An observation which highlights this issue, is the fact that the optimal solution (Figure 35) chooses to significantly increase the power output for certain, relatively flat segments prior to both ascents (0-5 km and 12-22 km), and stays close to CP during them (5-8 km and 22-25 km). The reason for these increases are not completely obvious, but one imagine that the program could have reached optimal solutions for the ascents and descent, but failed to find better time performances overall. This might have led to the solution exploring variations of power output for the flat segments. The program for the lower level optimisation of the first iteration had the same tuning parameters (described in Section 4.6) for the entire track, and was not split into smaller problems, as previously discussed. In order to prevent the program from displaying this behaviour, each larger segment (Figure 20) should be a problem of its own.

Another detail which could reflect an erroneous design choice, or some other fault in the optimal program, is the fact that the proposed energy distribution made by the upper level program is not followed exactly by the lower level optimisation scheme (uppermost plot in Figure 33). This might have been caused by both the inequality constraint for input power (P_{max} in (127)), or the fact that the terminal condition for the remaining anaerobic capacity was simply set as a terminal condition. This might have slowed down the search for an optimal solution, due to increased probability for the dynamics in (108) to produce an infeasible solution. This may, in turn, have led the program to simply struggle to take the right iterative steps towards the global minimum, as the terminal condition was difficult to respect (being under the pressure of both an equality constraint for $wTerm$, as well as an equality constraint for the last step from w_{N-1} to w_N).

7.1.2 Bologna TT Attempt 2

In Figure 48, hints of the same deviation from constant power in Figure 47 can be seen (A spike near the start of the descent, and a small drop in power during the descent). In Figure 48, deviations from CP are as large as 150 W, whereas the deviation in Figure 47 from CP were no larger than 15 W. All though Figure 48 show larger variations in power output, the constant power profile (with its measures of average power output for each segment) skews in the same direction as the proposed optimal power trajectory. This is especially true for the start of the descent, and the rest of the descent, where the power increases momentarily, then drops significantly. This observation might indicate either the track's invitation for a certain behaviour during these parts, or simply point to the difficulty of maintaining a constant power output. The former might help motivate why the total pacing strategy of iteration 2 Figure 48 might point in the right direction of an optimal power trajectory.

The average power output from the two attempts in this iteration (pacing and constant) were not equal (217 W and 210 W). This has to be taken into consideration when deciding whether the final attempt at producing a pacing strategy was success full or not. It was previously argued, that it should be possible to produce a pacing strategy resulting in a lower average power output than a constant power attempt on the same track, and still have a better time performance. Had the average power output of the constant attempt of iteration 2 (row 4 in Table 3) been lower than that of the pacing strategy attempt, one might have observed this. However, due to the large difference in average power (7 W), it is difficult to conclude with the second iteration being successful. The difference in normalized power was 10 W (in favour of the pacing attempt), which is a measure of the increased exertion as a consequence of a higher power output during sprints and climbs. The attempt with a pacing strategy spent 1 minute and 42 seconds less than the constant attempt. For comparison, the difference in average power and time duration between the first and the second constant power attempt were 11 W, and 2 minutes and 22 seconds, respectively. The relation between these two metrics of difference are most likely not linear. But for the sake of trying, the time performance of a hypothetical constant power attempt at 217 W (assuming linearity between

constant power and time performance), would have a time performance of 1 hour 2 minutes and 22 seconds. Here, a simple calculation was performed; (2 minutes + 22 seconds)*(7/11 [W]) = 90 seconds. This would have resulted in a proposed time difference of 12 seconds between the two time trial attempts in iteration 2.

Compared to the very first time trial attempt (row 1 in Table 3), the time performance of the final optimisation attempt was 1 minute and 49 seconds faster. In light of discussions regarding the somewhat failed constant power attempt, one might still argue that this difference in time performance supports the idea of the final pacing strategy attempt being successful. The pacing strategy was followed relatively closely by the subject's power output (Figure 48), with the largest error with respect to the power instructions being +5% (indicating a better followed strategy than the first iteration, which saw +11%). The energy distribution (in Figure 40) intended for a totally empty anaerobic capacity (a bit below zero). The subject was able to perform a sprint prior to crossing the goal line, with an average power output of 480 W over a duration of 20 seconds, resulting in an expenditure of about 5 kJ. This indicates that the model of anaerobic capacity failed to accurately predict the remaining anaerobic capacity, even for an activity where the average power output was above the estimated CP (CP + 11 W). This might also just indicate yet another underestimation of CP.

7.2 Mechanical Model

The mechanical model motivating the equation of motion for velocity (16) is based on a number of limitations to the reality of a cycling situation. Turns, wind conditions, temperature dynamics and more was excluded as external factors in this project. All though some simplifications were necessary to lower the requirement of computational power, one may discuss whether some of them could have been included. Cadence, for instance, could have been implemented as a state. In many situations, cadence greatly affects the power output, and has a relation to the absolute peak instantaneous power through the relation (39) (based on [4]). On a track like Bologna TT, the timing of gear shifts was a challenging task, especially during the slow start of the ascent (Figure 19). It is unclear, however, how the model of remaining anaerobic capacity would adapt to cadence dynamics. The subject did experience somewhat different muscle groups starting to fatigue, based on how high the cadence was.

Other simplifications deserves a mention in part of such a discussion as well. All though it might be safe to assume no drive chain losses ϵ in for the TT bike used in the software Zwift, there will, however, be drive chain losses for the actual bicycle used in the stationary setup shown in Figure 26. This means that one could have included a number below 1 for the ϵ in (16) when implementing the equation of motion for velocity. Another factor, which greatly affects both the interpretation of CP, as well as P_{max}, is the position on the bicycle. In Figure 3a and Figure 3b, the two bicycle positions which were utilised by the subject during test protocols and time trial attempts are shown. The dynamics of energy expenditure should quite possibly have been implemented different for these two. This could simply have been through the modification of the parameters CP and AWC, which seems to be greater in magnitude for the standing position. One could also have modified the inequality constraint for input power, P_{max}, in such a way that the system went into a "standing", and a "sitting" (time-trial position, Figure 3b) mode. This would however, introduce binary variables and behaviour which complicates requirements for the optimisation scheme.

7.3 Physiological Models

7.3.1 The CP-model

The model of CP and AWC describes the maintainable power output for cyclists for the range of duration of exercise from 30 minutes to 1 hour. It is therefore important to mention that all attempts at the Bologna TT were above 1 hour in duration. The specific activity used in this project was, therefore, just outside the range of reliability for the model. As previously discussed,

the model itself (in its most basic form (21)) is based on the power duration curve ([45], Figure 6). However, it is also based on a host of assumptions that are mostly in conflict with the principles of this empirically shaped curve. This creates a double layer of simplification, where a mathematical simplification lies atop an empirical correlation (of power and duration). The distance one creates between the actual physiology and human performance, and the models attempting to predict outcomes of activities, is therefore quite large within this framework. But with careful use of the model with respect to duration of exercise, as well as test protocols to determine the parameters, one may defend its use.

An important note regarding the model is the fact that the CP threshold is simply a line in the intensity domain. This does somewhat challenge the notion of continually overlapping contribution energy systems (Figure 5). One would imagine that there are a host of energy sources available at any time (like the different anaerobic energy sources making up the total AWC [46]). These may be activated fully for a power output significantly above an estimated threshold, yes, but they might as well contribute in a slowly increasing manner below it as well. The lactate dynamics and threshold was kept outside the scope of this project. Compared to the on-line measurement of power, lactate would have been difficult to use as a feedback measure in a pacing strategy for a cyclist (measurements being done only prior to, or after exercise, for instance). However, experimentation with other determinants of energy usage in the body like these, might have helped in painting a broader picture of how to interpret the threshold of CP.

The underdeveloped model of energy recovery, in relation to energy expenditure (which has way more developed models), was also an issue. Almost every model available had equations which described recovery and expenditure, as two separate processes, being activated under and over CP. All though this project used a same interpretation, the threshold became less sudden and "step-like", and the dynamics of the two domains more integrated, when using the hyperbolic tangent functions in (108).

7.3.2 Model of Remaining Anaerobic Capacity

An aspect excluded from the model of energy recovery in (108), is active recovery. [103] showed that when repeated bouts of intensive exercise were followed by active recovery periods, plasma lactate concentration was lower compared with passive recovery levels. In addition higher power outputs were observed with the active recovery protocol. These findings were significant only at high braking forces. This means, that the assumption of the most effective recovery power being 0 W (which is suggested in Figure 10,Figure 9), would have to be altered in order to account for active recovery. Active recovery may also result in a better maintenance of steady temperature in the muscles compared to passive recovery. The model for rate of change of remaining anaerobic capacity $w(t)$ in Figure 10 would in this case have its maximum somewhere in the middle of $0 \leq u \leq CP$.

In Figure 30, the power output dropped during the descent of the hill, from 200 W to 150 W, approximately at the 10 km mark. The resulting rate of recovery (with the power output now being 70 W below the critical power of 220 W), should speed up somewhat. Even though this segment of dropped power output was short, the remaining anaerobic capacity (simulated using the model in (108)) seems to not increase its recovery rate significantly. This is interesting to note, as this shed some light on the sensitivity of the time constant developed by [57], presented in (29). This specific time constant of recovery is modelled after findings from experimental work done in [57], and has fixed numeric values in it's equation. This limits the model's ability to adapt to different physiological properties of individuals. The only physiological parameter affecting this constant, is the individual's CP, and the difference between it, and the current power output. This poses the question of whether the constant might be a source of erroneous modeling of the recovery.

The time constant of recovery developed in [57], was found using experiments recovering at very low power outputs, compared to average power during Figure 28 and Figure 35. The power output rarely becomes low enough, for long enough periods in time, to properly gain the advantage of the increased rate of recovery. This indicates that the time constant might be better suited in models of longer duration, where the average power output might be lower. Furthermore, this

indicates that it might be acceptable to use a simpler model of recovery when performing activities such as time trials, due to the fact that the cyclist rarely produces power outputs far below CP, other than during steep descents. This does, however, support the use of the model for tracks like Bologna TT (Figure 19), due to the relatively long descent (the steepest descent averaging a time duration of 2 minutes for the subject's recorded activities, and constituting 10% of the total distance of the track). During this segment, the mathematical motivation for a lower power output (provided through the time constant dynamics) might aid the optimal program in forcing the power instruction to a relatively low level.

The implementation of the time constant in (108) is an ambitious attempt at integrating the equation formulated in [57], with a complete model of energy recovery and expenditure. One might imagine that the rate of recovery which appears as a consequence of both the current expended energy $AWC - W(t)$, as well as the difference between power output and CP, $CP - u(t)$, results in dynamics which allow for too high rates of recovery. However, findings in [57], [57],[89] and [54] supports this notion. Intuitively, this makes sense as well. The cyclist will not recover the same amount of energy when close to CP, compared to when at 0 W for the power output. Also, when the energy storage is almost completely recovered again, the findings inf [57] indicate a typical first-order transient response, which is what was used in (108) (all though derived and formulated somewhat differently).

The modeling of these equations put together (recovery; (27) and expenditure; (94)) turned out to have a relatively steep increase in recovery rate (dw/dt) for input power slightly below CP. This did not reflect the discussions regarding CP and it's potential role as an interval rather than a discrete line. This motivated the use of hyperbolic tangent expressions, which somewhat damped the increase in rate of recovery just below CP. The inclusion of these expressions produced an interval of CP, starting at about 10% below CP (shown in Figure 12).

7.3.3 Modeling maximum power generation

Whether or not the parameter α can simply be determined from solving (38) based on estimated values for CP and AWC, and measured values of P_{max}, is questionable. In [4], this parameter was found using a linear fit. However, as previously reported, the value of this parameter from the experiments conducted in this project, did at least not diverge from the values of the parameters of the subjects involved in the experiments in [4]. However, it was significantly lower (average 0.024 1/s for this project, whereas the authors of [4] found an average 0.040 1/s).

For the first iteration of optimisation (Figure 35), the maximum power inequality constraint was not even necessary for large parts of the track during the formation of the optimal solution. Only during the descent and the last ascent, where $P_{max} \leq 500$ (because 500 was set as the upper bound), was the inequality necessary. This may reflect the sub optimal nature of this particular solution, or some erroneous part of the implementation of the optimal program. During a sprint in the model validation attempt in Bologna TT (Figure 30, at the first peak - 8 km), the power output is observed larger than the predicted maximum power generation possible by the relation (38). This happening at a moment where the subject had just traversed the hardest part of the track, also raises the question of whether this inequality constraint is a realistic interpretation of reality.

The linear relation in (38) may struggle to capture some anaerobic dynamics which lie outside the model of CP and AWC. After having conducted two iterations of estimating the physiological parameters, 220 W (which was the CP used in the situation in Figure 30) seemed ultimately to be closer to the actual CP than values around 200 W (all though CP also could have increased somewhat throughout the period of 2 weeks). Therefore, based on the assumption that the model has relatively accurate physiological values, the spike in power output, exceeding the maximum power constraint at 8 km, seems to point towards the linear relation itself being somewhat erroneous in relation to reality. On the other hand, power output measurements may also have some uncertainty baked into them. The increased output also only lasts for about 100 m, indicating that such a spike is unlikely to be maintained. This indicates that the maximum power constraint could be reinterpreted as the upper bound for average maximum power over some interval.

7.4 Design of optimal program

7.4.1 Optimisation hierarchy

The relation between the two levels of optimisation is somewhat diffuse. They have quite different dynamics for their respective states. A point of critique in the upper level of optimisation, is its ability to describe the mechanics of the situation. Looking at Figure 23, there are sudden shifts in velocity not achievable in reality. This will, in turn, affect the total estimation of time spent during the course. However, the role of this optimal solution is not to estimate with accuracy, the exact time spent through a course, but the optimal and most effective distribution of energy throughout the course. The minimization of the time spent (even though that estimation of time spent is somewhat inaccurate) is the objective. It is therefore safe to assume, that for an optimal program including the steady-state velocity implementation, a solution which is estimated to result in a shorter duration than some other solution, is going to end up resulting in a shorter duration in the actual ride in the software Zwift.

The optimal solution found for the final iteration of formulating a pacing strategy, was found, not directly by one running program, but somewhat indirectly. Intuition based on physiology, and experience from previous time-trials, resulted an acceptable improvement in time performance. The optimal program therefore proved to be somewhat ineffective at uncovering the exact situations of significant increase and decrease in power output. This had to be forced through by intuition on the author's part. The reason for this failure to produce a total optimal pacing strategy may have come as a consequence of the level of integration between the two optimisation problems - the energy distribution and the power trajectory. The former deals with long segments and low resolution, and is in it's nature quite simple. It uses steady state dynamics for the velocity, and simply distributes the available anaerobic capacity throughout the track. The lower level deals with a higher resolution (possibly with distance intervals of equal length), and attempts to simply shape a power trajectory based on the required anaerobic capacity at the start, and at the end of the segment.

All though the goal of the hierarchy was to separate the problems in this manner, it seems the separation resulted in a gap between the dynamics and optimisation schemes. Am alternative solution could have been to store solutions for sprints and smaller segments, making use of their power trajectories only when the upper level somehow detects the need for them during it's search for optimal energy distributions. This would require a different type of implementation for both levels of the scheme, and bears a strong resemblance to the dynamic programming utilised in [4].

7.4.2 Iterations of the optimisation scheme

When running the optimal program for both iteration 1 (Section 6.2) and iteration 2 (Section 6.3), the tuning of the parameters in the MATLAB framework seemed to give diminishing returns the smaller the step sizes and constraint error tolerances got, and the larger the function evaluation numbers got. In other words, there seemed to be some obvious limits to how numerically "optimal" the generated solutions for the optimization variables could be. In particular, at around 10^{-13} (which is an extremely low number, of course), the optimal programs often struggled to compute anything, as the programs would run for an extremely long time. The difference in run-time going from 10^{-12} to 10^{-13} was colossal compared to going from 10^{-11} to 10^{-12}. The reasoning behind this would have been quite straightforward given the exponential nature of the numbers presented. However, the differences in run-time for larger step size tolerances and constraint errors was not much faster than the move from 10^{-11} to 10^{-12}. It seemed therefore likely, that in addition to how extremely small the numbers were, there were some numerical limit to the program at around 10^{-13} to 10^{-14}.

In practice, the difference between the first (Figure 25), and the second iteration (Figure 40) of the upper level optimisation, was the added opportunity for the latter of being able to expend more energy during the final ascent, as well as have enough capacity for a sprint prior to the descent. The lower level optimisation for the first iteration (Figure 33), however, did not exactly follow the

proposed trajectory, and expended large amounts of energy during the descent, and during parts of the second, flat segment.

The overall strategy formulated by through the tools of MATLAB and the models for physiology and mechanics was, for the last iteration, produced in a manner quite different from what the author had intended, and how it was performed in the first iteration. The first strategy (Figure 35), however flawed in its power trajectory, was produced using an upper level energy distribution, and a lower level power optimisation. The lower level used the entire track as basis for solving the problem, which might have made it more cumbersome than necessary. As previously discussed, this first iteration also failed to some degree to consider each smaller segment as a problem to solve in its own, due to the tuning parameters (Section 4.6) being set the same way (all though each problem had its own optimization variables and constraints). The second iteration, and its additions to the objective function, inequality constraint, and dynamics, was all intended to resolve the problematic issues and inexplicable behaviour of the first strategy. However, both the work flow, and to some degree, the solution itself, did not reach this level of optimality.

During the final iteration, the optimisation scheme for the lower level problem did include elements from the upper level (steady-state dynamics for the velocity for instance). This indicated a somewhat failed attempt at clearly distinguishing between the upper and lower level of the optimisation scheme. The problem hierarchy is therefore debatable as a necessity. As previously mentioned, as long as optimal solutions which produce lower time duration than previous iterations are included in the final solution (no matter if the optimised solution focuses on 1 km, or 10 km), the optimisation is successful. One would, however, miss the opportunity of exploiting velocity gains through simulating acceleration ((16)) for sprints, for instance prior to the descent in Figure 19. The final solution did include a sprint using these "true" lower level dynamics, all though this situation was simply picked by the author for the program to solve. The ideal situation, in the sense of an optimisation hierarchy, would be if the lower level optimisation scheme, as depicted for the first iteration in Figure 35, would itself point out the best points for sprints, and then simulate the exact optimal input power for a given expenditure of energy, set by this lower level optimisation. This effectively takes the total number of levels from 2, up to 3.

7.4.3 The initial guess at a solution

The initial guess is an important factor in the speed of the running program, and the feasibility of the resulting solution. For both the upper level, and lower level, problem, it proved increasingly obvious, that an initial guess was essential in order to prevent the program from converging to an infeasible point. "A good start" for the optimisation routine, with an initial guess setting up the velocity, time and work capacity optimisation variables using the same dynamics as the problem itself, turned out to be a recipe for success for the optimal program. A point of uncertainty regarding this guess, however, is the initial guess of input power. For the upper level, the initial guess was always set to CP for all $N-1$ variables representing the power trajectory of the pacing strategy. For this level of optimisation, where the bounds on input power were not far above or below CP anyway, this initial guess made sense. However, for a lower level scheme, evaluating shorter distances varying in length for the steady state dynamics (200 - 1000 m), and even shorter distances for the detailed dynamics of velocity (50-100 meters, equal length of each segment), this initial guess would not be as obvious. The bounds on input power were wider, allowing for sprints ($\geq$ 350 W) as well as real recovery periods ($\leq$ 100 W).

The final solution, however feasible it was with respect to the constraints set by inequalities, dynamics, and initial and terminal conditions, might with the initial guess be heavily influenced to skew it's power trajectory towards this guess. If the algorithm struggled to take steps in the solution space which were feasible, the initial guess might have been even more influential, seeing as this was all that the scheme had to go on for feasibility. In such a case, the implementation of the optimal program, and a correct interpretation of the constraints based on state dynamics, would be key in order for the program to avoid a case where the initial guess is the best option. Unless, off course, the initial guess turns out to actually be the the global minimum. Based on the elevation profile of the Bologna TT track though, and experience from constant and varying power attempts on it performed by the subject, this should not be the case.

7.5 Experimental Execution

During the experiments (test protocols and time trials), the fan meant to have the cooling effect on the cyclist's face (based on findings in [29]), lacked the ability to rotate vertically, making it stay fixed in the vertical direction. This resulted in the cyclist only getting the cooling effect during segments when the time-trial position was utilised. The accumulated duration of the standing and time-trial positions (shown in Figure 3a, Figure 3b), amounted to approximately 55% and 45% of the time spent through the track for the time-trial attempts, respectively. This might have affected the subject's performance during the segments when the subject was standing, due to the lack of cooling air leading to a potential increase in core temperature.

Ones own subjective experience will undoubtedly have a huge effect on performance, especially in a situation like a time trial. The level of experience the athlete or exerciser has with cycling, gear shifts, and endurance sports, will affect the pain tolerance, power generation and performance in general. The mental part of having performed time-trials previously, is an important issue here. The trials involve strenuous physical activity with an added requirement of focus in order to shift gears effectively (and potentially follow a pacing strategy). The subject gained valuable experience when cycling for the 3 months prior to the time-trial period, but might have tried more individual time-trials in this period as well. All though the subject had built up some competency within cycling, the subjective experience of time trials should have been more prevalent during the training phase.

The subject also noticed the mental side of the physical activity being a huge constraint to the entire model. A cyclist traversing a track will likely save energy when they don't know that is actually what they are doing, especially if the track is a longer one, and they are aware of the lengthy bout they are embarking upon. The ability to push one self to the limit seems to increase with experience level, and in this project, the subject always seemed to have a little bit extra capacity even though the optimal program had predicted it to be empty. In order to limit prior subjective experiences of a track, a more ideal scenario would perhaps be for the subject to try a completely unknown track when attempting a pacing strategy. This would obviously introduce challenges regarding gear shifts and the technical aspects of a track. But for more experience athletes, and possibly involving cadence dynamics as well ((39)), this could be a better approach.

Time constraints in the project, led the subject to perform some tests (as well as omit other, potentially important data collection sessions) in ways which might very well have affected, or diminished the quality of performance of other tests and time-trial attempts. Certain activities may have been performed with too little recovery time in between. An example of this is the recovery time between the two final time-trial attempts (Table 4). All though the final activity actually had a larger average power output, some of the data, like heart rate and temperature, might have been affected. By not having the preferred day in between the activities, heart rate and temperature might be higher in mean value then they would have been with the rest day. The recovery periods between the second test protocol session, as well as the final stages of the testing period involving the last time trials, were all relatively short. The preferred day between was absent, and the subjective experienced energy levels saw a decrease towards the end of the period. This might have affected the performance somewhat, however, the final attempt gave the highest average power outputs. This might be partly due to more accurate estimates of CP and AWC, and puts further emphasis on the notion of the mental "capacity" which is difficult to analyze.

7.5.1 Test protocols

The first iteration of optimisation, clearly had an underestimate of CP. This idea can be supported by the observation that the average heart rate for the pacing and constant time-trial attempts (row 2 and 3 in Section 6.4.2) were 3 bpm lower than for the non-guided attempt in Figure 28. The very first attempt at estimating the physiological parameters (through the 3MT shown in Figure 27) had produced an overestimate of CP. The difference in using the 3MT method alone, compared to using the two-test method (Figure 32), was vast (50 W). This shows the care which has to be put into the planning, design and execution of test protocols when estimating the physiological parameters.

The 3MT test protocol, and it's all-out nature of execution, is based on intuition rather than empirical data, and has been known to overestimate CP [20]. For an all-out scenario, athletes and exercisers with good sprinting abilities, will likely produce a higher estimate for the threshold. This is due to the length of the interval, as well as the "all-out" nature of it. The three test method in Figure 39 relies on a somewhat different principle. This test, prevalent in the cycling community online, instructs the athlete to set the maximum maintainable power output for all intervals, no matter their length in time. This value is then maintained constantly throughout the interval. The two-test method did not distinguish between all-out and the constant power method, resulting in the subject using an all-out strategy for the first iteration (Figure 32).

Even though the constant power throughout the interval was instructed, the subject had to use the data from the second 3MT and the 12MT, due to time constraints. This was performed using the all-out method, during the two-test method Figure 32. For this reason, the final addition to the three-test method, namely the 5MT (Figure 39), had the same all-out routine. In principle, an all-out effort could produce an under estimation of the parameters, compared to the constant power routine. This would especially be true during the longer intervals of 5 and 12 minutes. The initial sprint could potentially lead to a level of fatigue not intended for the constant power attempt, due to processes outside of the scope of the CP model (neuromuscular constraints, or some constraint of the subjective pain tolerance being pushed). The fact that the final time-trial attempt had an average power output of 217 W (and normalized power of 221 W), this seems likely to be the case. Had the subject performed the test protocols in the three-test method at constant power outputs predicted to be maintainable throughout the entire intervals, the estimate of CP could have come closer to 217 W.

An experimental pitfall affecting the estimate of physiological values, is the danger of pacing during the 3MT, 5MT and 12MT tests. An observation regarding this notion, was the 12MT interval performed in Figure 32. The power profile for the 12MT seen in Figure 32, has some spikes in power near the end of the interval. A dip in power leading to a relatively stable power output in between the two spikes (right after 3000 seconds) can also be seen. This might indicate the knowledge of the length of the interval, affecting the subject's willingness to expend power; in other words, pacing. Pacing during the test protocols would lead to erroneous results. For the 3MT, the potential danger would be for the cyclist to save some energy until they know there is little time left, in order to gain a higher estimate of 3MT (due to the estimate being set as the average power output of the last 30 seconds). However, this is as much a fault with the test protocol as it is with the subconscious pacing.

7.5.2 The Bologna Track

The track in Bologna is right at the border of activities which could effectively be utilised in the CP/AWC framework for the subject, due to the time duration of time-trial attempts staying around 1 hour. But the elevation profile offers interesting dilemmas as an optimisation problem. The question of how to distribute energy across the two ascents, as well as the timing of energy expenditure during the ascents, are all problems of optimal control which do not have entirely obvious answers. The sprints are somewhat independent of the track, seeing as they were deliberately placed within the final attempt at the track. Elevation profile and variations in the slop are what makes a time-trial problem into a problem without an obvious optimal power trajectory. However, the power trajectories did end up being set at, or around, CP for large parts of the time trials. The actual power trajectory problem may therefore have been more complicated and less obvious for a different track. This could perhaps be one where the cyclist don't turn around and climb the same hill twice, but enter into the ascent of a new hill, with a different elevation profile. Also, the indication of an optimal solution having relatively few instances of varying power output, may point to the energy distribution problem as a more interesting one for this specific track.

7.6 Further Work

7.6.1 Remodeling

The two component model of recovery of anaerobic capacity introduced in [89],[52], might be suitable alternative to the model used in this project. The interpretation and modification to the model proposed by [57] is criticised by the authors of the former model, which point towards the existence of a slow and a fast component of recovery. The work also indicated the usefulness of designing a time constant which slows w recovery with repeated maximal incremental exercise. In light of the final proposed optimal solution, where sprints of sudden significant power increases define the trajectory (and otherwise CP), such a model would have an impact on the recovery dynamics. This makes it, in principle, a relevant alternative to the model used for the Bologna TT track in this project.

In order to determine the recovery dynamics and the corresponding time constants, the authors of [52] performed several ramp tests, which has previously been described in Section 2.2.4. The model therefore require a much larger number of tests compared to this project. The ramp tests performed in [52] were also investigated for only one resting power output (20 W), and not several. The model formulated by the authors of [57] is more complete in terms of having attempted several recovery powers, but lacks the slowing of the time constants. Since the model in [52] already has many tests related to only one recovery power, the prospect of having to determine the fatigue-induced increase of time constants for an individual, as well as uncovering the behaviour of these dynamics across the entire power domain below CP, leads to a dramatic increase in tests compared to this project. Assuming (worst case, since the dynamics are not known) a nonlinear relation between recovery power and increase of the time constants, three recovery power levels should be tested. Different duration for the recovery intervals, in order to determine the time evolution of the recovery itself (which the time constant in [57] had a proposed universal solution for), would also have to be experimented with. The order of the recovery intervals would have to be alternated between experiments as well, like in [52]. Assuming these dynamics also having a nonlinear behaviour, and combining with the recovery power levels, the total number of experiments results in something like 3*(3!) = 3*3*2*1 = 18.

In order to trace the time evolution of (31) back to the original differential equation, the principles of [90] are used. For the equation

$$a\frac{d^2w}{dt} + b\frac{dw}{dt} + cw = 0, \tag{138}$$

and the constants $a, b, c \in \Re$, the corresponding characteristic equation is

$$(ar^2 + br + c) = 0, \tag{139}$$

resulting in the two roots

$$r_1 = \frac{-b + \sqrt{(b^2 - 4ac)}}{2a}, \quad r_2 = \frac{-b - \sqrt{b^2 - 4ac}}{2a} \tag{140}$$

If $b^2 - 4ac$ is positive, then the roots are real and distinct. This results in the time-varying solution

$$w(t) = c_1 e^{r_1 t} + c_2 e^{r_2 t} \tag{141}$$

for some choice of constants c_1, c_2. In the potential the remodeling of the physiological system, these would correspond to the relative contribution of the slow and fast component of energy recovery (FC_{amp}, SC_{amp}), and the roots r_1, r_2 would correspond to the inverse of time constants $1/\tau_{FC}, 1/\tau_{SC}$.

7.6.2 Alternative methods of optimisation

An alternative method of optimisation, would be to insert the problem formulation into an Model predictive control (MPC) framework. In [104], this procedure is described in detail. Specifically, a Nonlinear Model Predictive Control (NMPC) would have to be implemented, due to the nonlinear system equations involved ((16) and (108)). MPC is a multivariable control algorithm that seeks to control a process to a desirable state, while being subject to a number of constraints on the state and/or the input. Considering the most general case

$$\begin{aligned} x_{j+1} &= f(x_j, u_j) \\ x_0 &= x_s \\ y_j &= G_y(x_j) \\ j &= 1, 2, ... \end{aligned} \tag{142}$$

where y_j is the measured output. When the complete state of the system is not measured, as is almost always the case, the addition of a state estimator is necessary. The principle of MPC is based on optimizing a control strategy on a finite time horizon, based on the minimization of a quadratic cost function. As described in [104], for a system on the form (142), MPC is defined as the feedback law u that minimizes the cost function

$$\Phi = \frac{1}{2}\sum_{j=0}^{\infty}(y_j - \bar{y})^T Q(y_j - \bar{y}) + (u_j - \bar{u})^T R(u_j - \bar{u}) + \Delta u_j^T S \Delta u_j \tag{143}$$

where $\Delta u = u_j - u_{j-1}$. The matrices Q, R and S are assumed to be symmetric positive definite. This approach also assumes that the state of the plant is perfectly measured. The vector $\bar{y}$ is the desired output target and $\bar{u}$ is the desired input target. These targets are normally constant between plant optimizations. For a time invariant setpoint, the steady-state aspect of the control problem is to determine appropriate values for the state and input, as close to the ideal values as possible. However, constraints may limit the possibility of the states or input reaching their desired values, and the states and input has to be feasible with respect to these, as well. The dynamic aspect of the control problem is to control the state and input to the steady state values computed to be as close as possible to the ideal values. The MPC considers constraints generally not active for steady-state values. With no inequality constraints, the feedback law is the linear quadratic regulator. Analyzing the stabilizability, reachability and identifiability would be an important step when attempting to formulate it as an optimal control problem using an NMPC.

7.6.3 Practical Implications

All though the optimal program might be implemented in several ways, the role of the optimisation tool used in this project, is as an a priori optimisation of the power trajectory. For athletes or exercisers to use this method for future time-trials, it would have to be more streamlined in its interface. An application, where the athlete might input their CP and AWC, according to their preferred method of estimation of these parameters, would be ideal. The models would also have to be subject to even more system identification in order to determine the best total model of the remaining anaerobic capacity $w(t)$. In the case of an alternative optimisation method, like solving an optimal control problem using an NMPC, the athlete or exercise would have to be even more in tune with the power instructions. This alternative approach could see the application regulating the instructions on-line, while the cyclist attempts to follow these changes.

Another though on the practicality of an optimisation tool, is the way the instructions are communicated. A beginner within cycling would not have a clue of what level of effort to exert when being told to maintain a power output at CP. A professional athlete within cycling, however, would only have to be told (given regular testing routines of relevant parameters) to stay some relative amount of Watt below or above CP, and the they would be quite accurate in the tracking

of this instruction. The subject involved in this project experienced the difficulty of following power instructions accurately first-hand. The frequency of the commands would also have to be carefully chosen, as the change in power output would not only require a significant shift in power, but gear shifts, and potentially a change of position on the bicycle, as well. An alternative method of instructing the subject, could be through more active use of intervals (in light of the discussion of interpretation of CP as an interval). Telling a subject to stay at CP $\pm$ 10 W, for instance, would be quite practical. This would, in turn, however, affect the a priori simulation of the state $w(t)$, and would complicate the role of power output in the model of remaining anaerobic capacity.

8 Conclusion

Models utilising the CP concept, rely on the fact that the value represent some border between the heavy intensity domain, and the severe intensity domain of power output. This value, however, seems to be a consistent controversy when being used to model human performance. From the moment the model was put into a mathematical framework by [45], it has been shaped and molded by further research. The methods of estimating the parameter will be discussed later. The theoretic principles of the parameter, and its corresponding anaerobic capacity AWC, is based around the power-duration curve (Figure 6). This curve, with its peaks and plateaus, have been refined throughout the years of research. This has led to knowledge of where on the scale of duration of exercise the parameters become relevant, and where they are not. Different methods of estimating the parameters leads to different ranges in duration, all though they mostly focus on the range of 30 minutes - 1 hour.

The lack of a model describing the rate of change of the remaining anaerobic capacity for the entire intensity domain, fuelled the synthesis of a reinterpretation of the already existing ones ((108)). In light of the different simulated scenarios, as well as a relatively successful attempted validation of the model, it proved to describe physiological phenomenons of anaerobic capacity to a satisfying degree. There model did, however, leave out active recovery of it's equations. An individualised time constant for recovery (through rigorous testing) might also have made the model more accurate to the subject in question. The addition of hyperbolic tangent terms proved effective in the discrete optimisation framework. However, in terms of an optimal control problem using an MPC, the dynamics in (108) might pose significant challenges in system analysis. These terms introduced significant complexity to the equations, and the parameter values found in this project (for $T_a, T_{an}, \beta_a, \beta_{an}$) may prove to be difficult to determine.

The experimental results produced during this project were achieved using a number of different estimation methods. By using the (not so theoretically motivated, but empirically more accurate) two- and three test methods ([99], [100]), the subject experienced that the estimates of CP and AWC were more correct. The ideal addition in the experimental approach would have been to perform constant power intervals for these methods, as well (all-out intervals were used in this project). Verification of the pacing strategies proved effective when compared to constant power output. But the constant power attempt is most likely best designed when the power level is set to the average power output from the pacing attempt. All though optimality is difficult to intuitively predict in relation to the track Bologna TT (Figure 19), this seems to be the best approach when trying to verify that the pacing strategy is effective. For potential future work on this problem in relation to professional athletes, the best verification approach might be to use a track unknown to the subject beforehand. For less experienced subjects, cadence dynamics might also be advantageous to introduce, seeing as cadence greatly affects the power generation ability, and often has huge fluctuations when the experience level of the subject is low.

The final iteration of optimisation produced an optimal power trajectory with a better time performance than the constant comparison, all though the average power for the former activity was higher than for the latter. The power trajectory corresponding to this attempt showed behaviour similar with what was hypothesized to be optimal to begin with; namely, to expend energy capacity during climbs, recover during downhill segments, and pursue velocity gains prior to descents and at the start of the activity. With there being relatively few instances of varying power output in the final (and presumed most optimal) power trajectory, the energy distribution problem seemed

most interesting and less obvious than the power trajectory problem. In total 3 hard sprints of approximately 1 minute each, 4 segments of increased power output of 5 minutes each, and a segment of almost zero power for 2 minutes were the significant variations relative to the power output maintained exactly at CP. In order to gain more insight into the pursuit of an optimal power trajectory for time trials, it might be better to evaluate a track with an even more varying elevation profile, and one in which the cyclist does not simply turn around and traverse the same hill. That being said, the track provided a good basis for evaluating the models involved, and validating them to some degree.

The optimisation problem seems to be as much a problem of optimising the specific split of segments of the track in question, as it is a problem of formulating a power trajectory and an energy distribution. The resolution of segments, as well as the mathematical interpretation of the track (using cubic splines, for instance, in [3]), greatly affects the possible solutions for a power trajectory. Algorithms exploring different permutations of straight lines in order to model the track, could be an interesting alternative design of the optimal program.

Bibliography

[1] Zwift Inc. URL: https://us.zwift.com/. (accessed: 02.02.2023).

[2] P. Cangley, L. Passfield, H. Carter and M. Bailey. 'The effects of variable gradients on pacing in cycling time-trials'. In: *International journal of sports medicine* 32.2 (2011), pp. 132–136. DOI: 10.1055/s-0030-1268440.

[3] D. Sundström. 'Numerical Optimization of Pacing Strategies in Locomotive Endurance Sports'. In: (2016). URL: http://www.diva-portal.org/smash/record.jsf?pid=diva2%5C%3A897522&dswid=-7825.

[4] F. Ashtiani, V. S. M. Sreedhara, A. Vahidi, R. Hutchison and G. Mocko. 'Optimal Pacing of a Cyclist in a Time Trial Based on Individualized Models of Fatigue and Recovery'. In: (July 2020). DOI: 10.48550/ARXIV.2007.11393.

[5] URL: https://www.garmin.com/nb-NO/p/690888. (accessed: 01.06.2023).

[6] G. J. van Ingen Schenau and P. R. Cavanagh. 'Power equations in endurance sports'. In: *Journal of Biometrics* 23.9 (1990), pp. 865–881. DOI: https://doi.org/10.1016/0021-9290(90)90352-4.

[7] P. E. di Prampero, G. Cortili, P. Mognoni and F. Saibene. 'Equation of motion of a cyclist'. In: *Journal of Applied Physiology* 47 (1979), pp. 201–206. DOI: 10.1152/jappl.1979.47.1.201.

[8] T.J. LaClair. 'Rolling resistance'. In: *The pneumatic tire* (2006), pp. 475–532.

[9] A. Sommerfeld. 'Ein Beitrag zur hydrodynamischen Erkläerung der turbulenten Flüssigkeitsbewegüngen (A Contribution to Hydrodynamic Explanation of Turbulent Fluid Motions)'. In: *International Congress of Mathematicians* 3 (1908), pp. 116–124.

[10] *Standard Atmosphere*. Standard. International Organization for Standardization, 1975.

[11] URL: https://www.bikelockwiki.com/what-is-a-tt-bike/. (accessed: 21.05.2023).

[12] T. N. Crouch, D. Burton, Z. A. LaBry and K. B. Blair. 'Riding against the wind: a review of competition cycling aerodynamics'. In: *Sports Engineering* 20 (2017), pp. 81–110. URL: https://doi.org/10.1007/s12283-017-0234-1.

[13] C.R. Kyle and E.R. Burke. 'Improving the racing bicycle'. In: *Mechanical Engineering* 106.9 (1984), pp. 34–35.

[14] J.C. Martin, D.L. Milliken, J.E. Cobb, K.L. McFadden and A.R. Coggan. 'Validation of a mathematical model for road cycling'. In: *Journal of Applied Biomechanics* 14 (1998), pp. 276–291. DOI: 10.1123/jab.14.3.276.

[15] D. Du Bois. 'A Formula to Estimate the Approximate Surface Area if Height and Weight Be Known'. In: *Clinical Calorimetry* 10 (1916).

[16] D. R. Bassett Jr, C. R. Kyle, L. Passfield, J. P. Broker and E. R. Burke. 'Comparing cycling world hour records, 1967-1996: modeling with empirical data'. In: *Medicine and science in sports and exercise* 31.11 (1999), pp. 1665–1676. DOI: 10.1097/00005768-199911000-00025.

[17] G. de Groot, A. Sargeant and J. Geysel. 'Air friction and rolling resistance during cycling'. In: *Medicine and science in sports and exercise* 27.7 (July 1995), pp. 1090–1095. DOI: 10.1249/00005768-199507000-00020.

[18] F. Grappe, R. Candau, B. Barbier, M. D. Hoffman, A. Belli and J.-D. Rouillon. 'Influence of tyre pressure and vertical load on coefficient of rolling resistance and simulated cycling performance'. In: *Ergonomics* 42.10 (1999), pp. 1361–1371. DOI: 10.1080/001401399185009.

[19] URL: https://zwiftinsider.com/crr/. (accessed: 21.05.2023).

[20] V. S. M. Sreedhara, G. M. Mocko and R. E. Hutchinson. 'A survey of mathematical models of human performance using power and energy'. In: *Sports Medicine* 5.54 (Dec. 2019). DOI: https://doi.org/10.1186/s40798-019-0230-z.

[21] Ø. Støren, K. Ulevåg, M. H. Larsen, E. M. Støa and J. Helgerud. 'Physiological determinants of the cycling time trial'. In: *Journal of strength and conditioning research* 27.9 (2013), pp. 2366–2373. DOI: 10.1519/JSC.0b013e31827f5427.

[22] P. E. di Prampero. 'Factors limiting maximal performance in humans'. In: *European journal of applied physiology* 90.3-4 (Oct. 2003), pp. 420–429. DOI: 10.1007/s00421-003-0926-z.

[23] K. K. Buttar, N. Saboo and S. Kacker. 'A review: Maximal oxygen uptake (VO_{2max}) and its estimation methods'. In: *International Journal of Physical Education, Sports and Health* 6.6 (Oct. 2019), pp. 24–32. URL: https://www.kheljournal.com/archives/?year=2019&vol=6&issue=6&part=A&ArticleId=1590.

[24] N. Armstrong. 'Aerobic fitness of children and adolescents'. In: *The Journal of Pediatrics* 82.6 (Dec. 2006), pp. 406–408. DOI: 10.2223/JPED.1571.

[25] J. Helgerud. 'Maximal oxygen uptake, anaerobic threshold and running economy in women and men with similar performances level in marathons'. In: *European Journal of Applied Physiology and Occupational Physiology* 68 (Feb. 1994), pp. 155–161. DOI: https://doi.org/10.1007/BF00244029.

[26] S. A. Jobson, J. G. Hopker, T. Korff and L Passfield. 'Gross efficiency and cycling performance: a brief review'. In: *Journal of Science and Cycling* 1.1 (June 2012), pp. 3–8. URL: https://jsc-journal.com/index.php/JSC/article/view/12.

[27] M. J. Joyner and E. F. Coyle. 'Endurance exercise performance: the physiology of champions'. In: *The Journal of Physiology* 586.1 (2008), pp. 35–44. DOI: 10.1113/jphysiol.2007.143834.

[28] C.J. Stevens, A. R. Mauger, P. Hassmèn and L. Taylor. 'Endurance Performance is Influenced by Perceptions of Pain and Temperature: Theory, Applications and Safety Considerations'. In: *Sports Medicine* 48 (2018), pp. 525–537. DOI: https://doi.org/10.1007/s40279-017-0852-6.

[29] Z.J. Schlader, S. E. Simmons, S. R. Stannard and T. Mündel. 'The independent roles of temperature and thermal perception in the control of human thermoregulatory behavior'. In: *Physiology and Behavior* 103.2 (May 2011), pp. 217–224. DOI: 10.1016/j.physbeh.2011.02.002.

[30] J. R. Brotherhood. 'Heat stress and strain in exercise and sport'. In: *Journal of Science in Medicine and Sports* 11.1 (Jan. 2008), pp. 6–19. DOI: https://doi.org/10.1016/j.jsams.2007.08.017.

[31] K. Vitale and A. Getzin. 'Nutrition and Supplement Update for the Endurance Athlete: Review and Recommendations'. In: *Nutrients* 11.6 (June 2019), pp. 1289–1309. DOI: https://doi.org/10.3390/nu11061289.

[32] A. Jeukendrup, F. Brouns, A. J. Wagenmakers and W. H. Saris. 'Carbohydrate-electrolyte feedings improve 1 h time trial cycling performance'. In: *International Journal of Sports Medicine* 18.2 (Feb. 1997), pp. 125–129. DOI: 10.1055/s-2007-972607.

[33] T. D. Noakes. 'Physiological models to understand exercise fatigue and the adaptations that predict or enhance athletic performance'. In: *Scandinavian Journal of Medicine and Science in Sports* 10.3 (June 2000), pp. 123–145. DOI: 10.1034/j.1600-0838.2000.010003123.x.

[34] J. M. Carter, A. E. Jeukendrup, C. H. Mann and D. A. Jones. 'The effect of glucose infusion on glucose kinetics during a 1-h time trial'. In: *Medicine and Science in Sports and Exercise* 36.9 (Sept. 2004), pp. 1543–1550. DOI: 10.1249/01.mss.0000139892.69410.d8.

[35] N. Williams. 'The Borg Rating of Perceived Exertion (RPE) scale'. In: *Occupational Medicine* 67.5 (2017), pp. 404–405. DOI: https://doi.org/10.1093/occmed/kqx063.

[36] V. Bunc and J. Heller. 'Non-invasive determination of the "anaerobic threshold" using heart rate kinetics'. In: *Journal of Czech Physicians* 128.4 (1989), pp. 117–120. URL: https://pubmed.ncbi.nlm.nih.gov/2720744/.

[37] A. Jeukendrup and A. Van Diemen. 'Heart rate monitoring during training and competition in cyclists'. In: *Journal of Sports Sciences* 16 (1998), pp. 91–99. DOI: https://doi.org/10.1080/026404198366722.

[38] J. Johnson. *What is the difference between aerobic and anaerobic exercise?* Ed. by D. Bubnis. June 2020. URL: https://www.medicalnewstoday.com/articles/aerobic-vs-anaerobic-exercises#definitions. (accessed: 03.02.2023).

[39] K. Wasserman and M. B. McIlroy. 'Detecting the threshold of anaerobic metabolism in cardiac patients during exercise'. In: *The American Journal of Cardiology* 14.6 (Dec. 1964), pp. 844–852. DOI: https://doi.org/10.1016/0002-9149(64)90012-8.

[40] A. Ramos-Jimenez et al. 'The Respiratory Exchange Ratio is Associated with Fitness Indicators Both in Trained and Untrained Men: A Possible Application for People with Reduced Exercise Tolerance'. In: *Clinical Medicine Insights; Circulatory, Respiratory and Pulmonary Medicine* 2 (Feb. 2008), pp. 1–9. DOI: 10.4137/ccrpm.s449.

[41] A. M. Jones and A. Vanhatalo. 'The "Critical Power" Concept: Applications to Sports Performance with a Focus on Intermittent High-Intensity Exercise.' In: *Sports Medicine* 47.1 (Mar. 2017), pp. 65–78. DOI: 10.1007/s40279-017-0688-0.

[42] P. B. Gastin. 'Energy System Interaction and Relative Contribution During Maximal Exercise'. In: *Sports Medicine* 31.2001 (Nov. 2012), pp. 725–741. DOI: https://doi.org/10.2165/00007256-200131100-00003.

[43] Sigma. 'Adenosine 5'-triphosphate disodium salt Product Information'. In: *Sigma-Aldrich* (2019).

[44] U. Schlattner, M. Tokerska-Schlattner and T. Wallimann. 'Mithocondrial creatine kinase in human health and disease'. In: *Biochimica er Biophysica Acta (BBA) . Molecular Basis of Disease* 1762.2 (2006), pp. 164–180. DOI: https://doi.org/10.1016/j.bbadis.2005.09.004.

[45] H. Monod and J. Scherrer. 'The work capacity of a synergic muscular group'. In: *Ergonomics* 8.3 (1965), pp. 329–338. DOI: 10.1080/00140136508930810.

[46] H. C. Bergstrom et al. 'Differences Among Estimates of Critical Power and Anaerobic Work Capacity Derived From Five Mathematical Models and the Three-Minute All-Out Test'. In: *Journal of Strength and Conditioning Research* 28.3 (Mar. 2014), pp. 592–600. DOI: 10.1519/JSC.0b013e31829b576d.

[47] P. Leo, J. Spragg, T. Podlogar, J. S. Lawley and I. Mujika. 'Power profiling and the power-duration relationship in cycling: a narrative review'. In: *European Journal of Applied Physiology* 122 (2022), pp. 301–316. DOI: https://doi.org/10.1007/s00421-021-04833-y.

[48] C. B. Scott. 'Energy expenditure of heavy to severe exercise and recovery'. In: *Journal of theoretical biology* 207.2 (Nov. 2000), pp. 293–297. DOI: 10.1006/jtbi.2000.2174.

[49] R. H. Morton. 'The critical power and related whole-body bioenergetic models'. In: *European Journal of Applied Physiology* 96.4 (Mar. 2006), pp. 339–354. DOI: 10.1007/s00421-005-0088-2.

[50] J. Bartram, D. Thewlis, D. Martin and K. Norton. 'Predicting Critical Power in Elite Cyclists: Questioning Validity of the 3-min All-out Test'. In: *International Journal of Sports Physiology and Performance* 12 (Nov. 2016). DOI: 10.1123/ijspp.2016-0376.

[51] J. Denham, J. Scott-Hamilton, A. D. Hagstrom and A. J. Gray. 'Cycling Power Outputs Predict Functional Threshold Power and Maximum Oxygen Uptake'. In: *Journal of Strength and Conditioning Research* 34.12 (Dec. 2020), pp. 3489–3497. DOI: 10.1519/JSC.0000000000002253.

[52] A. Chorley, R. P. Bott, S. Marwood and K. L. Lamb. 'Bi-exponential modelling of W' reconstitution kinetics in trained cyclists'. In: *European Journal of Applied Physiology* 122 (2022), pp. 677–689. DOI: dhttps://doi.org/10.1007/s00421-021-04874-3.

[53] J. de Jong, R. Fokkink, G. J. Olsder and A. Schwab. 'The individual time trial as an optimal control problem'. In: *Proceedings of the Institution of Mechanical Engineers, Part P: Journal of Sports Engineering and Technology* 231.3 (May 2017), pp. 200–206. DOI: 10.1177/1754337117705057.

[54] P. Bickford, V. S. Sreedhara, G. Mocko, A. Vahidi and R. Hutchison. 'Modeling the Expenditure and Recovery of Anaerobic Work Capacity in Cycling'. In: *Proceedings* 2 (Feb. 2018), p. 219. DOI: 10.3390/proceedings2060219.

[55] C. Ferguson, H. B. Rossiter, B. J. Whipp, A. J. Cathcart, S. R. Murgatroyd and S. A. Ward. 'Effect of recovery duration from prior exhaustive exercise on the parameters of the power-duration relationship'. In: *Journal of applied physiology* 18.4 (2010), pp. 866–875. DOI: 10.1152/japplphysiol.91425.2008.

[56] H. B. Rossiter, S. A. Ward, J. M. Kowalchuk, F. A. Howe, J. R. Griffiths and B. J. Whipp. 'Dynamic asymmetry of phosphocreatine concentration and O(2) uptake between the on- and off-transients of moderate- and high-intensity exercise in humans.' In: *The journal of physiology* 542.3 (June 2002), pp. 991–1002. DOI: 10.1113/jphysiol.2001.012910.

[57] P. F. Skiba, W. Chidnok, A. Vanhatalo and A. M. Jones. 'Modeling the expenditure and reconstitution of work capacity above critical power'. In: *Medicine and science in sports and exercise* 44.8 (2012), pp. 1526–1532. DOI: 10.1249/MSS.0b013e3182517a80.

[58] P. F. Skiba, J. Fulford, D. C. Clarke, A. Vanhatalo and A. M. Jones. 'Intramuscular determinants of the ability to recover work capacity above critical power'. In: *European journal of applied physiology* 115.4 (Apr. 2015), pp. 703–713. DOI: 10.1007/s00421-014-3050-3.

[59] T. Moritani, A. Nagata, H. A. deVries and M. Muro. 'Critical power as a measure of physical work capacity and anaerobic threshold'. In: *Ergonomics* 24.5 (May 1981), pp. 339–350. DOI: 10.1080/00140138108924856.

[60] Y. Fukuba, A. Miura, M. Endo, A. Kan, K. Yanagawa and B. J. Whipp. 'The curvature constant parameter of the power-duration curve for varied-power exercise'. In: *Medicine and Science in Sports and Exercise* 35.8 (Aug. 2003), pp. 1413–1418. DOI: 10.1249/01.MSS.0000079047.84364.70.

[61] M. A. Johnson, D. E. Mills, P. I. Brown and G. R. Sharpe. 'Prior upper body exercise reduces cycling work capacity but not critical power'. In: *Medicine and Science in Sports and Exercise* 46.4 (Apr. 2014), pp. 802–808. DOI: 10.1249/MSS.0000000000000159.

[62] A. M. Jones, D. P. Wilkerson, F. DiMenna, J. Fulford and D. C. Poole. 'Muscle metabolic responses to exercise above and below the "critical power" assessed using 31P-MRS'. In: *American Journal of Physiology Regulatory, Integrative and Comparative Physiology* 294.2 (Feb. 2008), pp. 585–593. DOI: 10.1152/ajpregu.00731.2007.

[63] W. Chidnok et al. 'Muscle metabolic responses during high-intensity intermittent exercise measured by ^{31}P-MRS: relationship to the critical power concept'. In: *American Journal of Physiology: Regulatory, Integrative and Comparative Physiology* 305.9 (Nov. 2013), pp. 1085–1092. DOI: 10.1152/ajpregu.00406.2013.

[64] W. Chidnok et al. 'Muscle metabolic determinants of exercise tolerance following exhaustion: relationship to the "critical power"'. In: *Journal of Applied Physiology* 115.2 (July 2013), pp. 243–250. DOI: 10.1152/japplphysiol.00334.2013.

[65] J.C. Bartram, D. Thewlis, D. T. Martin and K. I. Norton. 'Accuracy of W' Recovery Kinetics in High Performance Cyclists—Modeling Intermittent Work Capacity'. In: *International Journal of Sports Physiology and Performance* 13.6 (2017), pp. 724–728. DOI: https://doi.org/10.1123/ijspp.2017-0034.

[66] P. F. Skiba, D. Clarke, A. Vanhatalo and A. M. Jones. 'Validation of a novel intermittent w' model for cycling using field data'. In: *International journal of sports physiology and performance* 9.6 (2014), pp. 900–904. DOI: 10.1123/ijspp.2013-0471.

[67] A. Vanhatalo, J. Doust and M. Burnley. 'Determination of Critical Power Using a 3-min All-out Cycling Test'. In: *Medicine & Science in Sports & Exercise* 39.3 (Mar. 2007), pp. 548–555. DOI: 10.1249/mss.0b013e31802dd3e6.

[68] D. W. Hill. 'The critical power concept. A review.' In: *Sports medicine (Auckland, N.Z.)* 16.4 (1993), pp. 237–254. DOI: 10.2165/00007256-199316040-00003.

[69] T. J. Housh, H. A. Devries, D. J. Housh, M. W. Tichy, K. D. Smyth and A. M. Tichy. 'The relationship between critical power and the onset of blood lactate accumulation'. In: *The Journal of sports medicine and physical fitness* 31.1 (1991), pp. 31–36.

[70] G. A. Gaesser, T. J. Carnevale, A. Garfinkel, D. O. Walter and C. J. Womack. 'Estimation of critical power with nonlinear and linear models'. In: *Medicine & Science in Sports & Exercise* 27.10 (Oct. 1995), pp. 1430–1438. URL: https://pubmed.ncbi.nlm.nih.gov/8531615/.

[71] G. Vinetti et al. 'Experimental validation of the 3-parameter critical power model in cycling'. In: *European journal of applied physiology* 119 (Jan. 2019), pp. 941–949. DOI: https://doi.org/10.1007/s00421-019-04083-z.

[72] B. Clark and P. W. Macdermid. 'A comparative analysis of critical power models in elite road cyclists'. In: *Current Research in Physiology* 4 (2021), pp. 139–144. DOI: https://doi.org/10.1016/j.crphys.2021.05.001.

[73] R. M. Broxterman, C. J. Ade, J. C. Craig, S. L. Wilcox, S. J. Schlup and T. J. Barstow. 'The relationship between critical speed and the respiratory compensation point: Coincidence or equivalence'. In: *European Journal of Sport Science* 15.7 (Oct. 2014), pp. 631–639. DOI: https://doi.org/10.1080/17461391.2014.966764.

[74] A. Vanhatalo, A. M. Jones and M. Burnley. 'Application of Critical Power in Sport'. In: *International Journal of Sports Physiology and performance* 6.1 (Aug. 2003), pp. 128–136. DOI: https://doi.org/10.1123/ijspp.6.1.128.

[75] E.M. Coats, H.B. Rossiter, J. R. Day, A. Miura, Y. Fukuba and B. J. Whipp. 'Intensity-dependent tolerance to exercise after attaining $V\dot{V}O_{2max}$ in humans'. In: *Journal of Applied Physiology* 95.2 (Aug. 2003), pp. 483–490. DOI: https://doi.org/10.1152/japplphysiol.01142.2002.

[76] C. J. McGowan, D. B. Pyne, K. G. Thompson and B. Rattray. 'Warm-Up Strategies for Sport and Exercise: Mechanisms and Applications'. In: *Sports Medicine* 45 (2015), pp. 1523–1546. DOI: https://doi.org/10.1007/s40279-015-0376-x.

[77] B. Saltin and J. Karlsson. 'Muscle Glycogen Utilization During Work of Different Intensities'. In: vol. 11. Springer, 2006, pp. 289–299. DOI: https://doi.org/10.1007/978-1-4613-4609-8_25.

[78] O. Buttelli, D. Seck, H. Vandewalle, J. C. Jouanin and H. Monod. 'Effect of fatigue on maximal velocity and maximal torque during short exhausting cycling'. In: *European Journal of Applied Physiology and Occupational Physiology* 73.1-2 (1996), pp. 175–179. DOI: 10.1007/BF00262828.

[79] B. R. MacIntosh and J. R. FLetcher. 'The parabolic power-velocity relationship does apply to fatigued states'. In: *European Journal of Applied Physiology* 111.2 (2011), pp. 319–320. DOI: 10.1007/s00421-010-1610-8.

[80] R. Hutchinson, K. Edwards, G. Klapthor and L. Shearer. 'Effects of w' depletion on the torque-velocity relationship in cycling'. In: *Medicine and Science in Sports and Exercise* 52.7S (2020), pp. 264–264. DOI: 10.1249/01.mss.0000676420.17268.6d.

[81] O. Egeland and J. T. Gravdahl. *Modeling and Simulation for Automatic Control*. 2002. ISBN: 82-92356-01-0.

[82] C. Lin and L. Segel. *Mathematics applied to deterministic problems in the natural sciences*. 1974. DOI: https://doi.org/10.1137/1.9781611971347.

[83] A. Masahiko. 'Uniform continuity of continuous functions of metric spaces.' In: *Pacific Journal of Mathematics* (1958).

[84] J. Nocedal and S. J. Wright. *Numerical Optimization*. 2nd ed. Springer New York, 2006. DOI: https://doi.org/10.1007/978-0-387-40065-5.

[85] U. Yuceer. 'Discrete convexity: convexity for functions defined on discrete spaces'. In: *Discrete Applied Mathematics* 1197.53 (2002), pp. 297–304. DOI: https://doi.org/10.1016/S0166-218X(01)00191-3.

[86] N. J. Higham. 'Computing a nearest symmetric positive semidefinite matrix'. In: *Linear Algebra and its Applications* 103 (1988), pp. 103–118. DOI: https://doi.org/10.1016/0024-3795(88)90223-.

[87] T. L. Friesz. 'Nonlinear Programming and Discrete-Time Optimal Control'. In: *Dynamic Optimization and Differential Games* 135 (2010). DOI: https://doi.org/10.1007/978-0-387-72778-3_2.

[88] The MathWorks Inc. *Solve nonlinear optimization problems*. URL: https://se.mathworks.com/discovery/nonlinear-programming.html. (accessed: 09.03.2023).

[89] A. Chorley, R. P. Bott, S. Marwood and K. L. Lamb. 'Slowing the Reconstitution of W' in Recovery With Repeated Bouts of Maximal Exercise'. In: *International Journal of Sports Physiology and Performance* 14.2 (Feb. 2019), pp. 149–155. DOI: 10.1123/ijspp.2018-0256.

[90] M. Braun. *Differential Equations and Their Applications*. Vol. Short Version. Springer-Verlag, 1975. DOI: 10.1007/978-1-4684-0053-3.

[91] E. P. Andersson, P. Bachl, A. Schmuttermair, C. A. Staunton and T. L. Stöggl. 'Anaerobic work capacity in cycling: the effect of computational method.' In: *European journal of applied physiology* 122 (2022), pp. 2637–2650. DOI: https://doi.org/10.1007/s00421-022-05038-7.

[92] URL: https://se.mathworks.com/help/matlab/ref/ode45.html. (accessed: 05.06.2023).

[93] The MathWorks Inc. *Decide Between Problem-Based and Solver-Based Approach*. URL: https://se.mathworks.com/help/gads/global-decide-problem-solver.html. (accessed: 09.03.2023).

[94] URL: https://cycling.favero.com/en. (accessed: 01.06.2023).

[95] URL: https://corebodytemp.com/. (accessed: 01.06.2023).

[96] URL: https://www.garmin.com/nb-NO/p/649059. (accessed: 01.06.2023).

[97] URL: https://chrome.google.com/webstore/detail/sauce-for-strava/eigiefcapdcdmncdghkeahgfmnobigha. (accessed: 01.06.2023).

[98] URL: https://www.goldencheetah.org/. (accessed: 04.06.2023).

[99] URL: https://www.bikeradar.com/advice/fitness-and-training/critical-power/. (accessed: 26.05.2023).

[100] URL: https://www.highnorth.co.uk/critical-power-calculator. (accessed: 29.05.2023).

[101] URL: https://apps.garmin.com/nb-NO/apps/fbeafa7b-ee0f-46db-83f0-1cc1b96a8ef7. (accessed: 01.06.2023).

[102] D.K. Lee, J. In and S. Lee. 'Standard deviation and standard error of the mean'. In: *Korean Journal of Anesthesiology* 68.3 (2015), pp. 220–223. DOI: https://doi.org/10.4097/kjae.2015.68.3.220.

[103] S. Ahmadi, P. Granie, Z. Taoutaou, J. Mercier, H. Dubouchaud and C. Prefaut. 'Effects of active recovery on plasma lactate and anaerobic power following repeated intensive exercise'. In: *Medicine and Science in Sports and Exercise* 28.4 (1996), pp. 450–456. DOI: 10.1097/00005768-199604000-00009.

[104] J.B. Rawlings. 'Tutorial overview of model predictive control'. In: *IEEE Control Systems Magazine* 20.3 (2000), pp. 38–52. DOI: 10.1109/37.845037.

Appendix

A MATLAB code

A.1 Parameters

```
%% Environmental and physiological parameters

% ------------------------------------------------------------------------
% ENVIRONMENT:
g     = 9.81;% <-------------------- Gravitational acceleration [m/s^2]
C_R   = 0.004;% <------------------- Rolling resistance (road wheels on pavement,
↪  Zwift) [unitless]
rho   = 1.204;% <------------------- Air density, Standard Ambient Temperature
↪  and Pressure (SATP) (p_0 = 101.325 kPa and T = 20°C) [kg/m^3]

% ------------------------------------------------------------------------
% ANTHROPOMETRICS:
m_r   = 84;% <---------------------- Mass of rider [kg]
h     = 1.87;% <-------------------- Height of rider [m]
A_bsa = (0.2025*h^(0.725))...% <---- Frontal cross-sectional area [m^2] (Du Bois
↪  et al. (1915))
    *(m_r^(0.425));
A     = 0.1447*A_bsa + 0.0604;% <--- Bassett et al. (1999), R^2 = 0.757 (Coef. of
↪  Det.)
C_d   = 0.6;% <---------------------- Time-trial position (upright ~0.8), Crouch
↪  et al. (2017)
CdA   = C_d*A;% <------------------- C_d*A

% ------------------------------------------------------------------------
% ENERGY SYSTEMS:
CP    = 206;% <--------------------- Critical power [W]
AWC   = 22000;% <------------------- Anaerobic working capacity [J]
alpha = 0.0222;% <------------------ Param. for maximum power [1/s]
PMAX  = alpha*AWC + CP; %<---------- Absolute maximum power capability [W]

% ------------------------------------------------------------------------
% BIKE (wheel parameters from Ashtianti et al. (2020)):
m_b   = 9.25;% <-------------------- Mass of bike (Roughly avg. mass of TT road
↪  bike) [kg]
R_w   = 0.35;% <-------------------- Radius of wheel (28 inches) [m]
m_w   = 1.2;% <--------------------- Mass of one wheel [kg]

% ------------------------------------------------------------------------
% SYSTEM (rider + bike):
I_w   = m_w*R_w^2;% <--------------- Rotational inertia of wheel [kg*m^2]
m_s   = m_r + m_b;% <--------------- Mass of Rider + Bike [kg]
m     = m_s + 2*(I_w/(R_w^2));% <--- Effective mass of the system [kg]
% ------------------------------------------------------------------------

% Constructing constants:
a = 1/m;                  % [1/kg]
b = (m_s/m)*g;            % [m/s^2]
c = b*C_R;                % [m/s^2]
d = (1/(2*m))*C_d*A*rho; % [kg/m^2]
```

```
% Vector of parameters:
params = [a;b;c;d;AWC;CP;alpha];
```

A.2 Upper level optimisation

```
% Class definition for the energy distribution problem. W' at certain
% specific points in the track will be constrained, and the state dynamics
% inbetween will be simulated using simplified dynamics with a large step
% size

classdef upperLevel

    properties

        % Optimization problem:
        problem;

        % Optimization variables:
        t
        v
        w
        u


    end

    methods

        % Make optimization problem
        function obj = upperLevel(distance,theta,bounds,params)

            % Track data:
            Theta = pi.*(theta)./200; % Inclination from (%) to [Rad]

            % Number of points on track:
            N = length(distance);

            % Parameters:
            a     = params(1); b  = params(2);
            c     = params(3); d  = params(4);
            AWC   = params(5); CP = params(6);
            alpha = params(7);

            % u/w bounds:
            w_L = bounds(1,1); w_U = bounds(1,2);
            u_L = bounds(2,1); u_U = bounds(2,2);
```

```
            % Inclination term:
            B_t = @(inc) b.*sin(inc) + c.*cos(inc);

            % Steady-state velocity:
            vss = @(u,inc)
↪   (sqrt((abs(B_t(inc))/(3*d))^3+(a*u/(2*d))^2)+a*u/(2*d))^(1/3)...

↪   -B_t(inc)/(3*d*(sqrt((abs(B_t(inc))/(3*d))^3+(a*u/(2*d))^2)+a*u/(2*d))^(1/3));

            % Work dynamics:
            anaerob = @(u) 0.5 + tanh((u-CP-CP*0.005)/0.1)/2;%-----> Anaerobic
↪   activation
            aerob = @(u) 0.5 - tanh((u-CP+CP*0.1)/8)/2;%-----> Aerobic
↪   activation

            tau     = @(u) 546*exp(0.01*(u-CP)) + 316;%-> Time constant of
↪   recovery
            dw      = @(w1,u) (aerob(u)/tau(u))*(AWC-w1) - anaerob(u)*(u-CP);

            % Max/min segment distance [m]:
            Smin = min(diff(distance));
            Smax = max(diff(distance));

            % Max/min velocity [m/s]:
            v_L = vss(u_L,max(Theta));
            v_U = vss(u_U,min(Theta));

            % Max/min duration on a segment [s]:
            t_L = Smin/v_U;
            t_U = Smax/v_L;

            % Optimization variables:
            obj.t = optimvar('t',N-1,'LowerBound',t_L,'UpperBound',t_U);
            obj.v = optimvar('v',N-1,'LowerBound',v_L,'UpperBound',v_U);
            obj.w = optimvar('w',N,  'LowerBound',w_L,'UpperBound',w_U);
            obj.u = optimvar('u',N-1,'LowerBound',u_L,'UpperBound',u_U);
↪

            % Problem:
            obj.problem = optimproblem('ObjectiveSense','Minimize');

            % Objective function:
            obj.problem.Objective = sum(obj.t);

            % Initializing constraints:
            tcons = optimconstr(N-1);
            vcons = optimconstr(N-1);
            wcons = optimconstr(N);
            ucons = optimconstr(N-1);


            % Initial condition for W' and u:
            wcons(1) = obj.w(1) == AWC;

            % States:
            for j = 1:N-1

                % Work capacity (simplified):
```

```
                %wcons(j+1) = obj.w(j+1) == obj.w(j) - (obj.u(j) - CP)*obj.t(j);


                % Time:
                tcons(j) = obj.t(j) == (distance(j+1) - distance(j))/obj.v(j);

                % Velocity:
                vcons(j) = obj.v(j) == vss(obj.u(j),Theta(j));

                % Work capacity (implicit midpoint rule):
                wcons(j+1) = obj.w(j+1) == obj.w(j) +
↪   obj.t(j)*dw(obj.w(j)+(obj.t(j)/2)*dw(obj.w(j),obj.u(j)),obj.u(j));

                % Input:
                ucons(j) = obj.u(j) <= alpha*(obj.w(j+1)) + CP;

            end

            obj.problem.Constraints.timeCons  = tcons;
            obj.problem.Constraints.velCons   = vcons;
            obj.problem.Constraints.workCons  = wcons;
            obj.problem.Constraints.inputCons = ucons;

        end
    end

    methods (Static)
        % Generate feasible initial conditions for opt. var.:
        function [t0,v0,w0,u0] = initialGuess(distance,theta,params)

            % Track data:
            Theta = pi.*(theta)./200;  % Inclination [rad]

            % Number of points on track:
            N = length(distance);

            % Parameters:
            a   = params(1); b  = params(2);
            c   = params(3); d  = params(4);
            AWC = params(5); CP = params(6);

            % Inclination term:
            B_t = @(inc) b.*sin(inc) + c.*cos(inc);

            % Steady-state velocity:
            vss = @(u,inc)
↪   (sqrt((abs(B_t(inc))/(3*d))^3+(a*u/(2*d))^2)+a*u/(2*d))^(1/3)...

↪   -B_t(inc)/(3*d*(sqrt((abs(B_t(inc))/(3*d))^3+(a*u/(2*d))^2)+a*u/(2*d))^(1/3));

            % Initialising (u = CP --> W' = AWC):
            t0 = zeros(N-1,1);   v0 = zeros(N-1,1);
            w0 = AWC.*ones(N,1); u0 = CP.*ones(N-1,1);

            % Work dynamics:
            anaerob = @(u) 0.5 + tanh((u-CP)/4)/2;%-----> Anaerobic activation
            aerob   = @(u) 0.5 - tanh((u-CP+5))/2;%-----> Aerobic activation
```

```
            tau      = @(u) 546*exp(0.01*(u-CP)) + 316;%-> Time constant of
↪   recovery
            dw       = @(w1,u) (aerob(u)/tau(u))*(AWC-w1) - anaerob(u)*(u-CP);

            % Feasibility:
            for i = 1:N-1

                % Velocity:
                v0(i) = vss(u0(i),Theta(i));

                % Time:
                t0(i) = (distance(i+1) - distance(i))/v0(i);

                % Work capacity (simplified):
                w0(i+1) = w0(i) +
↪   t0(i)*dw(w0(i)+(t0(i)/2)*dw(w0(i),u0(i)),u0(i));

            end
        end
    end
end
```

A.3 Upper level test

```
close all


%% Loading parameters:
parameters;


%% Test track:
distance = [  0    5000   8125  11250   16412   21575   24700]; % Accumulative
↪   distance [m]
theta    = [-0.36  6.85  -6.85  0.35    -0.35   6.85];%    *        Inclination
↪   [%]

% distance  = [  0     1170   2150   3485   5000   6000    6550   6900    7400
↪   8000   8275    8875    9375    9725    10275   11275   12790   14125   15105
↪   16080   16730    17750   18730   20065   21580   22580   23130   23480
↪   23980   24660   24700];
% % elevation = [ 298    281    285    273    281     298     362    389     457
↪   494    494     457     389     362     298     281      273     285     281
↪   298     298      281     285     273     281     298     362     389     456
↪   494    494];
% theta     = [-1.45   0.41   -0.9   0.53   1.7    11.64   7.71   13.6    6.17
↪   0    -6.17   -13.6    -7.71   -11.64   -1.7   -0.53    0.9    -0.41   1.74
↪   0     -1.74     0.41   -0.9    0.53     1.7    11.64   7.71    13.6    6.17
↪   0];
```

```
%% Work/input bounds
%          ( Low       High  )
 bounds = [  1         AWC   % Work capacity
            CP-110     CP+110];  % Input power


%% Time trial:
UL1 = upperLevel(distance,theta,bounds,params);

%% Solving
% Options
options = optimoptions('fmincon',...
                    'Algorithm','active-set',...
                'MaxIterations', 1e8,...
        'MaxFunctionEvaluations', 1e8,...
           'OptimalityTolerance', 1e-8,...
           'ConstraintTolerance', 1e-10,...
             'FunctionTolerance', 1e-10,...
                 'StepTolerance', 1e-8);




% Init. cond.
[t0,v0,w0,u0] = upperLevel.initialGuess(distance,theta,params);
x0.t = t0; x0.v = v0; x0.w = w0; x0.u = u0;

% Solution
[sol,fval,eflag,output] = solve(UL1.problem,x0,'Options',options);

% Plot results
plotUL;
```

A.4 Plot results from upper level

```
%% Plotting solution

% Creating arrays
D = linspace(distance(1),distance(end),distance(end)+1);
Theta = pi.*(theta)./200; % Inclination [Rad]
V = zeros(length(D),1); V(1) = sol.v(1);
U = zeros(length(D),1); U(1) = sol.u(1);
E = zeros(length(D),1); E(1) = 0;
S = zeros(length(D),1); S(1) = 0;
S_int = zeros(length(distance),1);S_int(1) = 0;
E_int = zeros(length(distance),1);E_int(1) = 0;

seg = 1;
for i = 2:length(D)

    % Segments:
    if D(i) == distance(seg+1) && D(i) ~= distance(end)
        seg = seg + 1;
        E_int(seg) = E_int(seg-1) +
↪   (distance(seg)-distance(seg-1))*sin(Theta(seg-1));
```

```
        S_int(seg) = S_int(seg-1) +
↪   (distance(seg)-distance(seg-1))*cos(Theta(seg-1));
    elseif D(i) == distance(end)
        E_int(end) = E_int(end-1) +
↪   (distance(end)-distance(end-1))*sin(Theta(end));
        S_int(end) = S_int(end-1) +
↪   (distance(end)-distance(end-1))*cos(Theta(end));
    end

    % States
    V(i) = sol.v(seg);
    U(i) = sol.u(seg);

    % Elevation
    E(i) = E(i-1) + sin(Theta(seg));

    % Flat distance
    S(i) = S(i-1) + cos(Theta(seg));

end

figure(1)


% Making duration readable:
duration = sum(sol.t);
hour = floor(duration/(60*60));
if hour >= 1
    min = floor(rem(duration,60*60)/60);
    sec = ceil((rem(duration,60*60)/60-min)*60);
    dur = append('Total Duration: ', num2str(hour),' h ', num2str(min), ' min ',
↪   num2str(sec), ' sec');
else
    min = floor(duration/60);
    sec = ceil((duration/60-min)*60);
    dur = append('Total Duration: ',num2str(min), ' min ', num2str(sec), ' sec');
end

subplot(4,1,1)
plot(S,V, 'Linewidth',2)
title('Strategic Distribution','FontSize',17)
subtitle(dur)
for k = 1:length(distance)-1
    time = num2str(floor(sol.t(k)));
    text((distance(k+1)+distance(k))/2,sol.v(k)-2,time);
end
ylabel('Velocity [m/s]')
xlabel('Distance (flat) [m]')
grid on
hold on
yyaxis right
plot(S,E, 'Linewidth',2)
legend('Velocity (w/ time spent in seconds) [m/s]','Elevation [m]',
↪   'FontSize',10)

subplot(4,1,2)
plot(S_int,sol.w, 'Linewidth',2)
ylim([0 AWC+1000])
```

```
yline(AWC,'--','LineWidth',2)
ylabel('Work capacity [J]')
xlabel('Distance (flat) [m]')
grid on
hold on
yyaxis right
plot(S_int,E_int, 'Linewidth',2)
legend('Remaining anaerobic capacity [J]', 'Anaerobic Work Capacity
↪  [J]','Elevation [m]','FontSize',10)

subplot(4,1,3)
plot(S,U, 'Linewidth',2)
hold on
yline(CP,'--','Linewidth',2)
ylim([0 300])
ylabel('Input Power [W]')
xlabel('Distance (flat) [m]')
grid on
hold on
yyaxis right
plot(S,E, 'Linewidth',2)
legend('Input Power [W]','Critical Power (CP)','Elevation [m]','FontSize',10)

sol.w
```

A.5 Lower level optimisation

```
% Class definition for the local problem across a smaller segment of the
% track (an  uphill/downhill segment for instance).

classdef lowerLevel
    properties

        % Optimization problem:
        problem

        % Optimization variables:
        t
        v
        w
        u

    end
    methods
        function obj = lowerLevel(distance,theta,bounds,params,wInit,wTerm)

            % Track data:
            Theta = pi.*(theta)./200; % Inclination [Rad]

            % Number of points on track:
            N = length(distance);

            % Parameters:
            a     = params(1); b  = params(2);
            c     = params(3); d  = params(4);
            AWC   = params(5); CP = params(6);
            alpha = params(7);
```

```
            % u/w bounds:
            w_L = bounds(1,1); w_U = bounds(1,2);
            u_L = bounds(2,1); u_U = bounds(2,2);

            % Inclination term:
            B_t = @(inc) b.*sin(inc) + c.*cos(inc);

            % Steady-state velocity:
            vss = @(u,inc)
↪   (sqrt((abs(B_t(inc))/(3*d))^3+(a*u/(2*d))^2)+a*u/(2*d))^(1/3)...

↪   -B_t(inc)/(3*d*(sqrt((abs(B_t(inc))/(3*d))^3+(a*u/(2*d))^2)+a*u/(2*d))^(1/3));

            % Work dynamics:
            anaerob = @(u) 0.5 + tanh((u-CP-CP*0.005)/0.1)/2;%-----> Anaerobic
↪   activation
            aerob = @(u) 0.5 - tanh((u-CP+CP*0.1)/8)/2;%-----> Aerobic
↪   activation
            tau     = @(u) 546*exp(0.01*(u-CP)) + 316;%-> Time constant of
↪   recovery
            dw      = @(w1,u) (aerob(u)/tau(u))*(AWC-w1) - anaerob(u)*(u-CP);

            % Max/min segment distance [m]:
            Smin = min(diff(distance));
            Smax = max(diff(distance));

            % Max/min velocity [m/s]:
            v_L = vss(u_L,max(Theta));
            v_U = vss(u_U,min(Theta));

            % Max/min duration on a segment [s]:
            t_L = Smin/v_U;
            t_U = Smax/v_L;

            % Optimization variables:
            obj.t = optimvar('t',N-1,'LowerBound',t_L,'UpperBound',t_U);
            obj.v = optimvar('v',N,  'LowerBound',v_L,'UpperBound',v_U);
            obj.w = optimvar('w',N,  'LowerBound',w_L,'UpperBound',w_U);
            obj.u = optimvar('u',N-1,'LowerBound',u_L,'UpperBound',u_U);

            % Problem:
            obj.problem = optimproblem('ObjectiveSense','Minimize');

            % Objective function:
            % ITERATION 1:
            obj.problem.Objective = sum(obj.t);

            % ITERATION 2:
            obj.problem.Objective = sum(obj.t) + ((wInit-wTerm) -
↪   sum(obj.t(:).*anaerob(obj.u).*(obj.u-CP)))*((wInit-wTerm) -
↪   sum(obj.t(:).*anaerob(obj.u).*(obj.u-CP)));

            % Initializing constraints:
            tcons = optimconstr(N-1);
            vcons = optimconstr(N-1);
            wcons = optimconstr(N);
            ucons = optimconstr(N-1);
```

```
            % Initial condition for W':
            wcons(1)    = obj.w(1)    == wInit;

            % ITERATION 1:
            %wcons(end) = obj.w(end) == wTerm;

            % Velocity dynamics:
            %dv  = @(v1,u,th) a*(u/v1)-B_t(th)-d*v1^2;


            % States:
            for j = 1:N-1

                % Time:
                %tcons(j) = obj.t(j) == 2*(distance(j+1) -
↪   distance(j))/(obj.v(j+1) + obj.v(j));
                tcons(j) = obj.t(j) == (distance(j+1) - distance(j))/(obj.v(j));

                % Velocity:

                % ITERATION 1:
                vcons(j) = obj.v(j) == vss(obj.u(j),Theta(j));

                % ITERATION 2:
                %vcons(j+1) = obj.v(j+1) == obj.v(j) +
↪   obj.t(j)*dv(obj.v(j)+(obj.t(j)/2)*dv(obj.v(j),obj.u(j),Theta(j)),obj.u(j),Theta(j));


                % Work capacity (implicit midpoint rule):
                wcons(j+1) = obj.w(j+1) == obj.w(j) +
↪   obj.t(j)*dw(obj.w(j)+(obj.t(j)/2)*dw(obj.w(j),obj.u(j)),obj.u(j));

                % Input:
                % ITERATION 2:
                ucons(j) = obj.u(j) <= alpha*(obj.w(j) -
↪   obj.t(j)*(anaerob(obj.u(j))*(obj.u(j)-CP))) + CP;

                % ITERATION 1:
                %ucons(j) = obj.u(j) <= alpha*(obj.w(j+1)) + CP;

            end

            obj.problem.Constraints.timeCons  = tcons;
            obj.problem.Constraints.velCons   = vcons;
            obj.problem.Constraints.workCons  = wcons;
            obj.problem.Constraints.inputCons = ucons;

        end
    end
    methods (Static)
        % Generate feasible initial conditions for opt. var.:
        function [t0,v0,w0,u0] = initialGuess(distance,theta,params,wInit)

            % Track data:
            Theta = pi.*(theta)./200;  % Inclination [rad]

            % Number of points on track:
```

```
            N = length(distance);

            % Parameters:
            a   = params(1); b  = params(2);
            c   = params(3); d  = params(4);
            AWC = params(5); CP = params(6);

            % Inclination term:
            B_t = @(inc) b.*sin(inc) + c.*cos(inc);

            % Steady-state velocity:
            vss = @(u,inc)
↪   (sqrt((abs(B_t(inc))/(3*d))^3+(a*u/(2*d))^2)+a*u/(2*d))^(1/3)...

↪   -B_t(inc)/(3*d*(sqrt((abs(B_t(inc))/(3*d))^3+(a*u/(2*d))^2)+a*u/(2*d))^(1/3));

            % Initialising:
            t0 = zeros(N-1,1);
            v0 = zeros(N-1,1); %v0(1) = vInit; % Velocity of length N-1 for
↪   iteration 1
            w0 = zeros(N,1); w0(1) = wInit;
            u0 = CP.*ones(N-1,1);

            % Work dynamics:
            anaerob = @(u) 0.5 + tanh((u-CP-CP*0.005)/0.1)/2;%-----> Anaerobic
↪   activation
            aerob = @(u) 0.5 - tanh((u-CP+CP*0.1)/8)/2;%-----> Aerobic
↪   activation
            tau     = @(u) 546*exp(0.01*(u-CP)) + 316;%-> Time constant of
↪   recovery
            dw      = @(w1,u) (aerob(u)/tau(u))*(AWC-w1) - anaerob(u)*(u-CP);


            % Velocity dynamics:
            %dv  = @(v1,u,th) a*(u/v1)-B_t(th)-d*v1^2;

            % Feasibility:
            for i = 1:N-1

                % Velocity:
                % ITERATION 1:
                v0(i) = vss(u0(i),Theta(i));

                % ITERATION 2:
                %v0(i+1) = v0(i) +
↪   t0(i)*dv(v0(i)+(t0(i)/2)*dv(v0(i),u0(i),Theta(i)),u0(i),Theta(i));

                % Time:
                %t0(i) = 2*(distance(i+1) - distance(i))/(v0(i+1)+v0(i));
                t0(i) = (distance(i+1)-distance(i))/v0(i);

                % Work capacity (simplified):
                w0(i+1) = w0(i) +
↪   t0(i)*dw(w0(i)+(t0(i)/2)*dw(w0(i),u0(i)),u0(i));


            end
        end
```

```
    end
end
```

A.6 Lower level test

```
close all

%% Loading parameters:
parameters;


%distance = [  0     1170   2150   3485   5000   6000    6550   6900    7400
↪  8000   8275    8875   9375    9725    10275   11275   12790   14125   15105
↪  16080   16730    17750   18730   20065   21580   22580   23130   23480
↪  23980   24660   24700];
%theta    = [-1.45   0.41   -0.9   0.53   1.7    11.64   7.71    13.6   6.17    0
↪  -6.17   -13.6   -7.71   -11.64   -1.7   -0.53    0.9    -0.41   1.74     0
↪  1.74     -0.41    0.9    -0.53   -1.7   -11.64  -7.71   -13.6   -6.17
↪  0];

distance  = [  0     1170   2150   3485   5000   6000    6550   6900    7400
↪  8000];
elevation = [ 298    281    285    273     281    298    362     389     457
↪  494 ];
theta     = [-1.45   0.41   -0.9   0.53    1.7  11.64   7.71    13.6    6.17];


%% Work/input bounds
%         ( Low       High  )
 bounds = [  1         AWC       % Work capacity
            100        500];     % Input power

% Initial and terminal conditions:
w1 = AWC;
w2 = AWC;
w3 = 652;


%% Solving

% Options
options = optimoptions('fmincon',...
                       'Algorithm','sqp',...
                  'MaxIterations', 1e12 ,...
         'MaxFunctionEvaluations', 1e12,...
            'ConstraintTolerance', 1e-12,...
                  'StepTolerance', 1e-12);

% First problem:
LL1 = lowerLevel(distance(1:5),theta(1:4),bounds,params,w1,w2);
[t01,v01,w01,u01] = lowerLevel.initialGuess(distance(1:5),theta(1:4),params,w1);
x01.t = t01; x01.v = v01; x01.w = w01; x01.u = u01;
[sol1,fval1,eflag1,output1] = solve(LL1.problem,x01,'Options',options);
```

```
% Second problem:
LL2 = lowerLevel(distance(6:10),theta(6:9),bounds,params,sol1.w(end),w3);
[t02,v02,w02,u02] = lowerLevel.initialGuess(distance(6:10),theta(6:9),params,w2);
x02.t = t02; x02.v = v02; x02.w = w02; x02.u = u02;
[sol2,fval2,eflag2,output2] = solve(LL2.problem,x02,'Options',options);

plotLL;
```

A.7 Plot results from lower level

```
%% Plotting solution
% Making duration readable:
duration = sum(LL1sol.t)...
          +sum(LL2sol.t);
hour = floor(duration/(60*60));
if hour >= 1
    min = floor(rem(duration,60*60)/60);
    sec = ceil((rem(duration,60*60)/60-min)*60);
    dur = append('Total Duration: ', num2str(hour),' h ', num2str(min), ' min ',
↪   num2str(sec), ' sec');
else
    min = floor(duration/60);
    sec = ceil((duration/60-min)*60);
    dur = append('Total Duration: ',num2str(min), ' min ', num2str(sec), ' sec');
end

% Concatenating arrays from solutions:
V = zeros(length(distance),1);
W = zeros(length(distance),1);
U = zeros(length(distance)-1,1);

V(1:4)   = LL1sol.v;
V(5:9)   = LL2sol.v;

W(1:5)   = LL1sol.w;
W(6:10)  = LL2sol.w(2:end);


U(1:4)   = LL1sol.u;
U(5:9)   = LL2sol.u;



% Reshaping U-trajectory:
D = linspace(distance(1),distance(end),distance(end)+1);
E = zeros(length(D),1); E(1) = 0;
Theta = pi.*(theta)./200; % Inclination [Rad]
newU = zeros(length(D),1); newU(1) = LL1sol.u(1);
seg = 1;
for k = 2:length(D)
    if D(k) == distance(seg+1) && D(k) ~= distance(end)
        seg = seg + 1;
    end
```

```
    newU(k) =  U(seg);

    % Elevation
    E(k) = E(k-1) + sin(Theta(seg));

end




figure(1)
subplot(3,1,1)
plot(distance,V, 'Linewidth',2)
title('Short Lower Level Problem Solution')
subtitle(dur)
ylabel('Velocity [m/s]')
xlabel('Distance [m]')
grid on
hold on
yyaxis right
plot(distance,elevation, 'Linewidth',2)
legend('Velocity [m/s]','Elevation [m]','FontSize',10)

subplot(3,1,2)
plot(distance,W, 'Linewidth',2)
ylim([0 AWC+100])
yline(AWC,'--','LineWidth',2)
ylabel('Work capacity [J]')
xlabel('Distance [m]')
grid on
hold on
yyaxis right
plot(distance,elevation, 'Linewidth',2)
legend('Remaining Anerobic Work Capacity [m/s]','Anaerobic Work Capacity
↪  [J]','Elevation [m]', 'FontSize',10)

subplot(3,1,3)
plot(D,newU, 'Linewidth',2)
hold on
yline(CP,'--','Linewidth',2)
ylabel('Input Power [W]')
xlabel('Distance [m]')
grid on
hold on
yyaxis right
plot(distance,elevation, 'Linewidth',2)
legend('Input Power [W]','Critical Power (CP)','Elevation [m]','FontSize',10)
```

A.8 Sprint Problem

```
%% Trying one least method (velocity and work excluded from optimization
↪  variables, work possibly put back if necessary)
close all
% Parameters:
parameters;

% Simplified track (sprint):
% Distance  = [8000   8200   8400  ];
% Elevation = [ 494    494    488  ];
% Theta     = [   0    -3    ];

% Simplified Track (Second Ascent):
Distance  = [21600   22600   23100   23500   24000   24600];
Elevation = [ 281     298     362     389     456     494];
Theta     = [ 1.7    11.64   7.71    13.6    6.17];

% Smoothed
pelev  = csaps(Distance,Elevation,0.00001);
ptheta = csaps(Distance(1:end-1),Theta,0.00001);



% Resolution:
res = 200;
distance  = zeros((Distance(end)-Distance(1))/res,1);
elevation = zeros((Distance(end)-Distance(1))/res,1);
theta     = zeros((Distance(end)-Distance(1))/res,1);
distance(1)  = 8000; elevation(1) = 494;
for k = 1:(Distance(end)-Distance(1))/res
    distance(k+1)  = Distance(1) + k*res;
    elevation(k+1) = fnval(pelev,  distance(k+1));
    theta(k)     = fnval(ptheta, distance(k));
end

theta = pi.*(theta)/200;

%% OPTIMAL PROGRAM DESIGN:
% Bounds (sprint):
u_bounds = [ CP  PMAX];


% W' initial/terminal conditions [J] (sprint):
wInit = 11376; wTerm = 10000;
deltaW = wInit-wTerm;


% Work dynamics:
anaerob = @(u) 0.5 + tanh((u-CP-CP*0.005)/0.1)/2;%-----> Anaerobic activation
aerob   = @(u) 0.5 - tanh((u-CP+CP*0.1)/8)/2;%-----> Aerobic activation
tau     = @(u) 546*exp(0.01*(u-CP)) + 316;%-> Time constant of recovery
dw      = @(w1,u) (aerob(u)/tau(u))*(AWC-w1) - anaerob(u)*(u-CP);

% Velocity dynamics:
dv  = @(v1,u,th) a*(u/v1)-b*sin(th)-c*cos(th)-d*v1^2;

% Number of points on track:
```

```
N = length(distance);

% Max/min distance intervals
% Smax = max(distance);
% Smin = min(distance);

% Optimization variables:
t = optimvar('t',N-1,'LowerBound',0.01,'UpperBound',10);
v = optimvar('v',N,  'LowerBound',1,'UpperBound',30);
w = optimvar('w',N,  'LowerBound',1,'UpperBound',wInit);
u = optimvar('u',N-1,'LowerBound',u_bounds(1),'UpperBound',u_bounds(2));

% Problem:
problem = optimproblem('ObjectiveSense','Minimize');

% Objective function:
problem.Objective = 1e3*sum(t) + 1e1*(deltaW -
↪  sum(t(:).*anaerob(u).*(u-CP)))*(deltaW - sum(t(:).*anaerob(u).*(u-CP)));

% Initializing constraints:
tcons = optimconstr(N-1);
vcons = optimconstr(N);
wcons = optimconstr(N);
ucons = optimconstr(N-1);

% Initial Conditions for states:
vcons(1) = v(1) == 2.5;
wcons(1) = w(1) == wInit;

% States:
for j = 1:N-1

    % Time:
    tcons(j) = t(j) == 2*(distance(j+1)-distance(j))/(v(j+1) + v(j));

    % Velocity
    vcons(j+1) = v(j+1) == v(j) +
↪   t(j)*dv(v(j)+(t(j)/2)*dv(v(j),u(j),theta(j)),u(j),theta(j));

    % Work:
    wcons(j+1) = w(j+1) == w(j) + t(j)*dw(w(j)+(t(j)/2)*dw(w(j),u(j)),u(j));

    % Input:
    %ucons(j) = obj.u(j) <= alpha*(obj.w(j) -
↪   obj.t(j)*(anaerob(obj.u(j))*(obj.u(j)-CP))) + CP;
    ucons(j) = u(j) <= alpha*w(j) + CP;


end

problem.Constraints.tcons = tcons;
problem.Constraints.vcons = vcons;
problem.Constraints.wcons = wcons;
problem.Constraints.ucons = ucons;
```

```
%% INITIAL GUESS:

% Initialising:
t0 = zeros(N-1,1);
v0 = zeros(N,1); v0(1) = 2.5;
w0 = zeros(N,1); w0(1) = wInit;
u0 = CP.*ones(N-1,1);


% Feasibility:
for i = 1:N-1

    % Time:
    t0(i) = (distance(i+1)-distance(i))/v0(i);

    % Velocity:
    v0(i+1) = v0(i) +
↪   t0(i)*dv(v0(i)+(t0(i)/2)*dv(v0(i),u0(i),theta(i)),u0(i),theta(i));

    % Work:
    w0(i+1) = w0(i) + t0(i)*dw(w0(i)+(t0(i)/2)*dw(w0(i),u0(i)),u0(i));

end

x0.t = t0; x0.v = v0; x0.w = w0; x0.u = u0;


% Second ascent:
LLoptions  =  optimoptions('fmincon',...
                    'Algorithm','active-set',...
                'MaxIterations', 1e5,...
        'MaxFunctionEvaluations', 1e5,...
           'ConstraintTolerance', 1e-3,...
             'FunctionTolerance', 1e-3,...
           'OptimalityTolerance', 1e-2,...
                 'StepTolerance', 1e-2);


[ LLsol, LLfval, LLeflag, LLoutput ] = solve( problem, x0, 'Options', LLoptions);


% Making duration readable:
duration = sum(LLsol.t);
hour = floor(duration/(60*60));
if hour >= 1
    min = floor(rem(duration,60*60)/60);
    sec = ceil((rem(duration,60*60)/60-min)*60);
    dur = append('Total Duration: ', num2str(hour),' h ', num2str(min), ' min ',
↪   num2str(sec), ' sec');
else
    min = floor(duration/60);
    sec = ceil((duration/60-min)*60);
    dur = append('Total Duration: ',num2str(min), ' min ', num2str(sec), ' sec');
end

figure(1)
subplot(3,1,1)
plot(distance,LLsol.w,'r','LineWidth',2)
```

```
title('Optimal Solution to Sprint Prior to Descent','FontSize',17)
subtitle(dur)
ylabel('Work capacity [J]')
xlabel('Distance [m]')
grid on
hold on
ylim([0 AWC+500])
yline(AWC,'--','LineWidth',2)
hold on
yyaxis right
ax=gca;
ax.YColor = [0, 0, 1];
plot(distance,elevation, 'b','Linewidth',2)
legend('Detailed Distribution [J]','AWC [J]','Elevation [m]', 'FontSize',10)



subplot(3,1,2)
plot(distance,LLsol.v, 'r','Linewidth',2)
ylabel('Velocity [m/s]')
xlabel('Distance [m]')
grid on
hold on
yyaxis right
ax=gca;
ax.YColor = [0, 0, 1];
plot(distance,elevation, 'b','Linewidth',2)
legend('Velocity [m/s]','Elevation [m]','FontSize',10)

subplot(3,1,3)
LLsol.u(end+1) = LLsol.u(end);
plot(distance,LLsol.u, 'r','Linewidth',2)
hold on
yline(CP,'--','Linewidth',2)
ylabel('Input Power [W]')
xlabel('Distance [m]')
grid on
hold on
yyaxis right
ax=gca;
ax.YColor = [0, 0, 1];
plot(distance,elevation,'b', 'Linewidth',2)
legend('Input Power [W]','Critical Power (CP)','Elevation [m]','FontSize',10)
```

A.9 Total optimisation iteration 1

```
close all

%% Loading parameters:
parameters;


%% Track - Upper level:
ULdistance  = [  0    5000   8125  11250   16412   21575   24650];  %
↪  Accumulative distance [m]
```

```
ULelevation = [ 298    280    494    280     298     280     494];
ULtheta     = [-0.36  6.85  -6.85  0.35    -0.35   6.85];%    *
↪  Inclination [Degrees]

%% Track - Lower level (Iteration 1):
distance  = [  0     1170   2150   3485   5000   6000    6550   6900    7400
↪  8000   8275    8875    9375    9725    10275   11275   12790   14125   15105
↪  16080   16730    17750   18730   20065   21580   22580   23130   23480
↪  23980   24660   24650];
elevation = [ 298    281    285    273    281     298     362    389     457
↪  494    494     457     389     362     298     281      273     285     281
↪  298     298      281     285     273     281     298     362     389     456
↪  494    494];
theta     = [-1.45   0.41   -0.9   0.53   1.7    11.64   7.71   13.6    6.17    0
↪  -6.17   -13.6    -7.71   -11.64   -1.7   -0.53    0.9    -0.41   1.74      0
↪  -1.74     0.41   -0.9    0.53     1.7    11.64   7.71    13.6    6.17
↪  0];



%% Work/input bounds
%         ( Low       High  )
% Upper level:
ULbounds = [  1         AWC   % Work capacity
            CP-150  CP+20];  % Input power

% Lower level:
LLbounds = [  1         AWC    % Work capacity
             CP-120    500];  % Input power


%% Upper level:
UL1 = upperLevel(ULdistance,ULtheta,ULbounds,params);


%% Solving Upper level
% Options
ULoptions = optimoptions('fmincon',...
                    'Algorithm','active-set',...
                'MaxIterations', 1e10 ,...
        'MaxFunctionEvaluations', 1e10,...
           'ConstraintTolerance', 1e-10,...
                 'StepTolerance', 1e-10);

% Init. cond.
[t0_ul, v0_ul, w0_ul, u0_ul] =
↪  upperLevel.initialGuess(ULdistance,ULtheta,params);
x0UL.t = t0_ul; x0UL.v = v0_ul; x0UL.w = w0_ul; x0UL.u = u0_ul;

% Solution
[ULsol,ULfval,ULeflag,ULoutput] = solve(UL1.problem,x0UL,'Options',ULoptions);
energyDist = ULsol.w;

% Saving solution from upper level program:
% energyDist = (10^4).*[ 2.1970,...
%                        2.1964,...
%                        0.0641,...
%                        0.4420,...
```

```
%                       0.4464,...
%                       0.4503,...
%                       0.0128];
```

```
%% Solving Lower level:

% Options
LLoptions = optimoptions('fmincon',...
                    'Algorithm','active-set',...
                'MaxIterations', 1e4,...
        'MaxFunctionEvaluations', 1e6,...
           'ConstraintTolerance', 1e-7,...
             'FunctionTolerance', 1e-7,...
           'OptimalityTolerance', 1e-5,...
                 'StepTolerance', 1e-5);
```

```
% First segment:
LL1 = lowerLevel( distance(1:5),   theta(1:4),   LLbounds, params, energyDist(1),
↪  energyDist(2));
[t0_ll1, v0_ll1, w0_ll1, u0_ll1] = lowerLevel.initialGuess( distance(1:5),
↪  theta(1:4),  params, energyDist(1));
x0LL1.t = t0_ll1; x0LL1.v = v0_ll1; x0LL1.w = w0_ll1; x0LL1.u = u0_ll1;
[ LL1sol, LL1fval, LL1eflag, LL1output ] = solve( LL1.problem, x0LL1, 'Options',
↪  LLoptions);
```

```
% Second segment:
LL2 = lowerLevel( distance(5:11),  theta(5:10),   LLbounds, params,
↪  LL1sol.w(end), energyDist(3));
[t0_ll2, v0_ll2, w0_ll2, u0_ll2] = lowerLevel.initialGuess( distance(5:11),
↪  theta(5:10),  params, energyDist(2));
x0LL2.t = t0_ll2; x0LL2.v = v0_ll2; x0LL2.w = w0_ll2; x0LL2.u = u0_ll2;
[ LL2sol, LL2fval, LL2eflag, LL2output ] = solve( LL2.problem, x0LL2, 'Options',
↪  LLoptions);
```

```
% Third segment:
LL3 = lowerLevel( distance(11:16), theta(11:15), LLbounds, params, LL2sol.w(end),
↪  energyDist(4));
[t0_ll3, v0_ll3, w0_ll3, u0_ll3] = lowerLevel.initialGuess( distance(11:16),
↪  theta(11:15),params, energyDist(3));
x0LL3.t = t0_ll3; x0LL3.v = v0_ll3; x0LL3.w = w0_ll3; x0LL3.u = u0_ll3;
[ LL3sol, LL3fval, LL3eflag, LL3output ] = solve( LL3.problem, x0LL3, 'Options',
↪  LLoptions);
```

```
% Fourth segment:
```

```
LL4 = lowerLevel( distance(16:20), theta(16:19), LLbounds, params, LL3sol.w(end),
↪  energyDist(5));
[t0_ll4, v0_ll4, w0_ll4, u0_ll4] = lowerLevel.initialGuess( distance(16:20),
↪  theta(16:19),params, energyDist(4));
x0LL4.t = t0_ll4; x0LL4.v = v0_ll4; x0LL4.w = w0_ll4; x0LL4.u = u0_ll4;
[ LL4sol, LL4fval, LL4eflag, LL4output ] = solve( LL4.problem, x0LL4, 'Options',
↪  LLoptions);


% Fifth segment:
LL5 = lowerLevel( distance(20:25), theta(20:24), LLbounds, params, LL4sol.w(end),
↪  energyDist(6));
[t0_ll5, v0_ll5, w0_ll5, u0_ll5] = lowerLevel.initialGuess( distance(20:25),
↪  theta(20:24),params, energyDist(5));
x0LL5.t = t0_ll5; x0LL5.v = v0_ll5; x0LL5.w = w0_ll5; x0LL5.u = u0_ll5;
[ LL5sol, LL5fval, LL5eflag, LL5output ] = solve( LL5.problem, x0LL5, 'Options',
↪  LLoptions);


% Sixth segment:
LL6 = lowerLevel( distance(25:31), theta(25:30), LLbounds, params, LL5sol.w(end),
↪  energyDist(7));
[t0_ll6, v0_ll6, w0_ll6, u0_ll6] = lowerLevel.initialGuess( distance(25:31),
↪  theta(25:30),params, energyDist(6));
x0LL6.t = t0_ll6; x0LL6.v = v0_ll6; x0LL6.w = w0_ll6; x0LL6.u = u0_ll6;
[ LL6sol, LL6fval, LL6eflag, LL6output ] = solve( LL6.problem, x0LL6, 'Options',
↪  LLoptions);



% Results:
plotTimeTrial;
```

A.10 Plot results from total optimisation iteration 1

```
%% Plotting Time Trial results

% Making duration readable:
duration = sum(LL1sol.t)...
          +sum(LL2sol.t)...
          +sum(LL3sol.t)...
          +sum(LL4sol.t)...
          +sum(LL5sol.t)...
          +sum(LL6sol.t);

hour = floor(duration/(60*60));
if hour >= 1
    min = floor(rem(duration,60*60)/60);
    sec = ceil((rem(duration,60*60)/60-min)*60);
    dur = append('Total Duration: ', num2str(hour),' h ', num2str(min), ' min ',
↪  num2str(sec), ' sec');
else
    min = floor(duration/60);
    sec = ceil((duration/60-min)*60);
    dur = append('Total Duration: ',num2str(min), ' min ', num2str(sec), ' sec');
```

```
end

% Concatenating arrays from solutions:
V = zeros(length(distance),1);
W = zeros(length(distance),1);
U = zeros(length(distance)-1,1);

% ITERATION 1:
% V(1:4)   = LL1sol.v;
% V(5:10)  = LL2sol.v;
% V(11:15) = LL3sol.v;
% V(16:19) = LL4sol.v;
% V(20:24) = LL5sol.v;
% V(25:30) = LL6sol.v;
%
% W(1:5)   = LL1sol.w;
% W(6:11)  = LL2sol.w(2:end);
% W(12:16) = LL3sol.w(2:end);
% W(17:20) = LL4sol.w(2:end);
% W(21:25) = LL5sol.w(2:end);
% W(26:31) = LL6sol.w(2:end);
%
% U(1:4)   = LL1sol.u;
% U(5:10)  = LL2sol.u;
% U(11:15) = LL3sol.u;
% U(16:19) = LL4sol.u;
% U(20:24) = LL5sol.u;
% U(25:30) = LL6sol.u;

% ITERATION 2:
V(1:5)   = LL1sol.v;
V(6:10)  = LL2sol.v(2:end);
V(11:18) = LL3sol.v(2:end);
V(19:22) = LL4sol.v(2:end);
V(23:27) = LL5sol.v(2:end);
V(28:33) = LL6sol.v(2:end);

W(1:5)   = LL1sol.w;
W(6:10)  = LL2sol.w(2:end);
W(11:18) = LL3sol.w(2:end);
W(19:22) = LL4sol.w(2:end);
W(23:27) = LL5sol.w(2:end);
W(28:33) = LL6sol.w(2:end);

U(1:4)   = LL1sol.u;
U(5:9)   = LL2sol.u;
U(10:17) = LL3sol.u;
U(18:21) = LL4sol.u;
U(22:26) = LL5sol.u;
U(27:32) = LL6sol.u;


% Reshaping U-trajectory:
D = linspace(distance(1),distance(end),distance(end)+1);
E = zeros(length(D),1); E(1) = 0;
Theta = pi.*(theta)./200; % Inclination [Rad]
newU = zeros(length(D),1); newU(1) = LL1sol.u(1);
newV = zeros(length(D),1); newV(1) = LL1sol.v(1);
```

```
seg = 1;
for k = 2:length(D)
    if D(k) == distance(seg+1) && D(k) ~= distance(end)
        seg = seg + 1;
    end

    % States
    newU(k) = U(seg);
    newV(k) = V(seg);

    % Elevation
    E(k) = E(k-1) + sin(Theta(seg));

end



subplot(4,1,1)
plot(ULdistance,energyDist, 'k','Linewidth',2)
title('Optimal Solution to Time Trial','FontSize',17)
subtitle(dur)
ylabel('Work capacity [J]')
xlabel('Distance [m]')
hold on
plot(distance,W,'r','LineWidth',2)
grid on
hold on
ylim([0 AWC+500])
yline(AWC,'--','LineWidth',2)
hold on
yyaxis right
ax=gca;
ax.YColor = [0, 0, 1];
plot(distance,elevation, 'b','Linewidth',2)
legend('Strategic Distribution [m/s]','Detailed Distribution [J]','AWC
↪  [J]','Elevation [m]', 'FontSize',10)

subplot(4,1,2)
plot(D,newV, 'r','Linewidth',2)
ylabel('Velocity [m/s]')
xlabel('Distance [m]')
grid on
hold on
yyaxis right
ax=gca;
ax.YColor = [0, 0, 1];
plot(distance,elevation, 'b','Linewidth',2)
legend('Velocity [m/s]','Elevation [m]','FontSize',10)

subplot(4,1,3)
plot(D,newU, 'r','Linewidth',2)
hold on
yline(CP,'--','Linewidth',2)
ylabel('Input Power [W]')
xlabel('Distance [m]')
grid on
hold on
yyaxis right
```

```
ax=gca;
ax.YColor = [0, 0, 1];
plot(distance,elevation,'b', 'Linewidth',2)
legend('Input Power [W]','Critical Power (CP)','Elevation [m]','FontSize',10)
```